Distribution agreement

In presenting this thesis or dissertation as a partial fulfillment of the requirements for an advanced degree from Emory University, I hereby grant to Emory University and its agents the non-exclusive license to archive, make accessible, and display my thesis or dissertation in whole or in part in all forms of media, now or hereafter known, including display on the world wide web. I understand that I may select some access restrictions as part of the online submission of this thesis or dissertation. I retain all ownership rights to the copyright of the thesis or dissertation. I also retain the right to use in future works (such as articles or books) all or part of this thesis or dissertation.

Signature:

_____ _____

Justus M. Huelse Date

Approval page

MERTK inhibition selectively activates a DC – T-cell axis to provide anti-leukemia immunity

By

Justus M. Huelse
Doctor of Philosophy

Graduate Division of Biological and Biomedical Science
Cancer Biology

Douglas K. Graham, MD, PhD

Advisor

Curtis J. Henry, PhD

Committee Member

Gregory B. Lesinski, PhD, MPH

Committee Member

Haydn T. Kissick, PhD

Committee Member

Nicki Panoskaltsis, MD, PhD, FRCP

Committee Member

Accepted:

Kimberly Jacob Arriola, PhD, MPH

Dean of the James T. Laney School of Graduate Studies Date

Date

MERTK inhibition selectively activates a DC – T-cell axis to provide anti-leukemia immunity

By

Justus M. Huelse
B.Sc. University of Konstanz, Germany, 2011
M.Sc. University of Copenhagen, Denmark, 2014

Advisor: Douglas K. Graham, MD PhD

An abstract of
A dissertation submitted to the Faculty of the
James T. Laney School of Graduate Studies of Emory University
in partial fulfillment of the requirements for the degree of
Doctor of Philosophy
in
Graduate Division of Biological and Biomedical Sciences
Cancer Biology
2023

Abstract

MERTK inhibition selectively activates a DC – T-cell axis to provide anti-leukemia immunity

By Justus M. Huelse

TAM-family tyrosine kinases (TYRO3, AXL and MERTK) are potential cancer therapeutic targets in a wide range of human cancers. In previous studies, MERTK inhibition in the immune microenvironment was therapeutically effective in a B-cell acute leukemia (B-ALL) model. Here, we probed anti-leukemia immune mechanisms and evaluated roles for TYRO3 and AXL in the leukemia microenvironment. Host *Mertk* knockout or MERTK inhibitor MRX-2843 increased CD8α^{+} dendritic cells (DCs) with enhanced antigen-presentation capacity in the leukemia microenvironment and inhibited leukemogenesis. High *MERTK* or low DC gene expression were associated with poor prognosis in pediatric patients with ALL, indicating the clinical relevance of these findings. MRX-2843 also decreased potentially exhausted TOX$^{[HIGH]}$ CD8^{+} T-cells, implicating a DC – T-cell axis. Indeed, combined depletion of CD8α^{+} DCs and CD8^{+} T-cells was required to abrogate anti-leukemia immunity in *Mertk*$^{-/-}$ mice. *Tyro3*$^{-/-}$ mice were also protected against B-ALL, implicating TYRO3 as an immunotherapeutic target. In contrast to *Mertk*$^{-/-}$ mice, *Tyro3*$^{-/-}$ did not impact CD8α^{+} DC frequency or antigen-presentation capacity and therapeutic activity was less dependent on DCs, indicating a different immune mechanism.

In contrast to *Mertk*$^{-/-}$ or *Tyro3*$^{-/-}$, host *Axl* deletion did not impact B-ALL leukemogenesis. Moreover, host knockout of all three TAM-family kinases prolonged survival in an MML-AF9 AML model, while only *Mertk* ablation provided immunity in a second AML model, suggesting context-dependent roles of individual TAM-family kinases in anti-leukemia immunity.

These data demonstrate differential roles for TAM-family kinases in the leukemia microenvironment and provide rationale for the development of MERTK and/or TYRO3-targeted B-ALL immunotherapies.

MERTK inhibition selectively activates a DC – T-cell axis to provide anti-leukemia immunity

By

Justus M. Huelse
B.Sc. University of Konstanz, Germany, 2011
M.Sc. University of Copenhagen, Denmark, 2014

Advisor: Douglas K. Graham, MD PhD

A dissertation submitted to the Faculty of the
James T. Laney School of Graduate Studies of Emory University
in partial fulfillment of the requirements for the degree of
Doctor of Philosophy
in
Graduate Division of Biological and Biomedical Sciences
Cancer Biology
2023

Acknowledgements

I would like to express my deepest gratitude to the following individuals and institutions who have played a pivotal role in the successful completion of my doctoral journey:

First and foremost, I extend my profound appreciation to my advisor, Dr. Douglas Graham, for his mentorship, encouragement, and dedication to my academic growth. Your enthusiasm and leadership has been instrumental in shaping my research path.

I am immensely thankful to my thesis committee members: Dr. Curtis Henry, Dr. Haydn Kissick, Dr. Gregory Lesinski, and Dr. Nicki Panoskaltsis. Your guidance, expertise, and invaluable feedback have greatly enriched the quality of my research and thesis.

I am also grateful to Dr. Deborah DeRyckere and Dr. H. Shelton Earp for their many insightful contributions to my research endeavors.

This dissertation represents the collective effort and support of many, and I am truly grateful for all the contributions that have shaped this work. Firstly, I want to thank Dr. Swati Bhasin and Dr. Manoj Bhasin for the fantastic collaboration on the single-cell RNA-sequencing experiments. Dr. Swati Bhasin performed the bioinformatic analysis of the dataset and helped interpret the results in many scientific discussions, as did Juhye Yim. Dr. Beena Thomas prepared the single-cell RNA-sequencing libraries. Dr. Kristen Jacobsen performed the initial survival studies in TAM knockout mice. Madison Chimenti and Travon Baxter crucially helped with the many mouse studies. Dr. Xiaodong Wang and Dr. Stephen Frye provided important reagents. Rebecca Parker set up the initial survival studies with the C1498 AML model. Thank you all for your invaluable contributions.

A special thanks goes out to all present and former members of our research laboratory. Your collaboration and camaraderie have made this journey both intellectually stimulating and enjoyable.

I would like to acknowledge the Graduate School for providing an excellent academic environment that fostered my intellectual development. The resources and opportunities offered by the Graduate School have been instrumental in my academic growth.

Likewise, I extend my appreciation to the Cancer Biology program leadership for their continuous support and guidance throughout my doctoral studies.

Lastly, I am indebted to my beloved wife for her unwavering support, understanding, and patience throughout this academic pursuit. My family's love and encouragement have been my constant motivation.

Table of contents

List of abbreviations

ABL	Abelson tyrosine kinase
ADC	antibody-drug conjugate
ALL	acute lymphoblastic leukemia
AML	acute myeloid leukemia
APC	antigen-presenting cell
ARG-1/2	arginase-1/2
BATF3	basic leucine zipper ATF-like transcription factor
BCL2	B cell lymphoma 2
BCR	breakpoint cluster region
BET	bromodomain and extra-terminal motif
BiTE	bispecific T cell engager
BMDC	bone marrow-derived dendritic cell
CAR T cell	chimeric antigen receptor-T cell
ccRCC	clear cell renal cell carcinoma
CD	cluster of differentiation
cDC1	classical type 1 dendritic cell
cDC2	classical type 2 dendritic cell
CDC42	cell division control protein 42 homolog

CNS	central nervous system
CRK-II	CT10 regulator of kinase-II
CRLF2	Cytokine receptor-like factor 2
Csf1r	colony stimulating factor 1 receptor
CTLA4	cytotoxic T-lymphocyte-associated protein 4
DAG	diacylglycerol
DC	dendritic cell
DOCK180	dedicator of cytokinesis 180
EGFR	epidermal growth factor receptor
ELMO	engulfment and cell motility protein
ERK	extracellular signal-regulated kinase
ETV	translocation-Ets-leukemia virus
FAK	focal adhesion kinase 1
Fc	fragment crystallizable (region)
FLT3	fms like tyrosine kinase 3
FLT3-ITD	FLT3 internal tandem duplication
FNIII	fibronectin III
GAS6	growth arrest-specific 6
HER2	human epidermal growth factor receptor 2
HGF	hepatocyte growth factor

HLA-I/II	human leukocyte antigen - class I/II
HNSCC	head and neck squamous cell carcinoma
HSCT	hematopoietic stem cell transplantation
HSPCs	hematopoietic stem and progenitor cells
IFN-α/β/γ	interferon-α/β/γ
Ig-like	immunoglobulin-like
IKK	IκB kinase complex
IL	interleukin
ILK	integrin-linked protein kinase
IP3	inositol trisphosphate
IκB	inhibitor of κB
JAK	Janus kinase
KMT2A	lysine methyltransferase 2A
LGALS3	Galectin-3
LXR	liver X receptor
MAPK	mitogen-activated protein kinase
MDSC	myeloid-derived suppressor cell
MEK	mitogen-activated extracellular signal-regulated kinase
MHC-I/II	major histocompatibility complex - class I/II
MLL	mixed lineage leukemia gene

MRD	minimal residual disease
mTOR	mammalian target of rapamycin
MyD88	myeloid differentiation primary response 88
NK cell	natural killer cell
NKT cell	natural killer T cell
NO	nitric oxide
NOTCH	Neurogenic locus notch homolog protein
NSCLC	non-small cell lung cancer
OT-I	OVA-specific T cell receptor transgenic line – MHC-I-restricted
OVA	ovalbumin
p38	ribonuclease P protein subunit p38
PBX1	pre-B-cell leukemia transcription factor 1
PD-1	programmed cell death protein 1
pDC	plasmacytoid dendritic cell
PD-L1/2	programmed cell death 1 ligand 1/2
PDX	patient-derived xenograft
Ph	Philadelphia chromosome
PI3K	Phosphoinositide 3-kinase
PIP2	phosphatidylinositol 4,5-bisphosphate
PLC-γ2	phospholipase C-γ2

PROS1	vitamin K-dependent protein S
PtdSer	phosphatidylserine
PTP18	tyrosine-protein phosphatase 18
RAC	Ras-related C3 botulinum toxin substrate
RAC1	Ras-related C3 botulinum toxin substrate 1
RAS	rat sarcoma virus
RHOA	Ras homolog family member A
RNA	ribonucleic acid
RTK	receptor tyrosine kinase
RUNX1	runt-related transcription factor 1
scRNA-seq	single cell RNA sequencing
SRC	sarcoma
STAT	signal transducer and activator of transcription
TAM (family kinases)	TYRO3, AXL, MERTK
TCF3	transcription factor 3
TCR	T cell receptor
TGF-β	transforming growth factor-β
TKI	tyrosine kinase inhibitor
TLR	Toll-like receptor
TNF-α	Tumor necrosis factor-α

TRAF3/6	TNF receptor-associated factor3/6
T_{reg} cell	regulatory T cell
TRIF	TIR-domain-containing adapter-inducing interferon-β
TULP-1	tubby-like protein 1
Twist1/2	Twist-related protein 1/2
WT	wild-type

List of figures

Chapter 1: Introduction

1.1 Acute leukemia

Acute leukemias, including acute lymphoblastic leukemia (ALL) and acute myeloid leukemia (AML), are the most common type of pediatric cancers and despite remarkable improvements in therapeutic outcomes they remain the second leading cause of cancer-related death in children (1-3). The current cytotoxic chemotherapies are associated with severe late effects or secondary malignancies in pediatric patients (3-6) and often fail in refractory or relapsed disease (7). Additionally, many elderly acute leukemia patients struggle to tolerate these treatments, leading to survival rates below 40% (3, 8). Hence, there is a significant need for novel treatment options with reduced toxicities, such as targeted therapies and immunotherapies, but more research is needed to identify potential targets and understand the underlying mechanisms.

1.1.1 Pathobiology of acute leukemia

Acute leukemias are characterized by rapid proliferation and expansion of malignant hematopoietic precursor cells (blasts) in the bone marrow, leading to impaired normal hematopoiesis. Acute leukemia blasts can eventually exit the bone marrow, reach other major organs, and disrupt their functions as well (9). Malignant blasts can originate from either the lymphoid or the myeloid lineage of hematologic cells, leading to the classification of acute leukemia into two main types: acute lymphoblastic leukemia (ALL), and acute myeloid leukemia (AML). While ALL is the most common acute leukemia in children, the prevalence of AML increases with age and it is the predominant subtype in adult patients (10-12). Both, ALL and AML, are a heterogenous malignancies and various genomic alterations and post-translational modifications can drive or contribute to their development (13, 14).

ALL can be further divided into B cell ALL (B-ALL) and T cell ALL (T-ALL), depending on the lymphoid cell type affected (15), while AML is typically stratified into clinically relevant subgroups

based on morphological, molecular, cytochemical, cytogenic, and immunophenotypic attributes of the blasts (11, 16). At the time of diagnosis, acute leukemia blasts are typically characterized by maturation arrest and high proliferative capacities, and this phenotype can be driven by various genetic alterations. In ALL, these commonly include fusion genes, such as *BCR-ABL, TCF3-PBX1*, or *ETV-RUNX1*, as well as *CRLF2* rearrangements (17, 18), while AML patients often carry FLT3 mutations, such as internal tandem duplications (FLT3-ITD) (19). Moreover, fusions of *KMT2A/MLL* with one of several known partners occur frequently in both, ALL and AML, and are associated with particularly poor survival outcomes and resistance to the current standard chemotherapies (11, 13, 17, 20).

1.1.2 Current standard of care in pediatric patients

Treatment outcomes for pediatric acute leukemia have greatly improved over the past decades, owing to basic and clinical research-driven improvements of conventional chemotherapy regimens, risk stratification, supportive care, and central nervous system prophylaxis (21-23). The current standard of care for acute leukemia are combinations of cytotoxic chemotherapies. Pediatric B-ALL and T-ALL patients are generally treated in three successive phases: remission induction, consolidation, and maintenance (24). Each phase consists of different chemotherapeutic combinations, treatment durations, and intensities, that are determined based on risk stratification. The goal of the initial phase is to induce complete remission (cancer becomes undetectable), which is achieved in over 90% of pediatric ALL patients (25). The chemotherapeutics applied typically include vincristine, asparaginase, or corticosteroids, as well as doxorubicin or daunorubicin for higher-risk patient (26). Allogeneic bone marrow transplant may be performed for patients in which induction fails. The following consolidation phase aims to eradicate any residual disease remaining following complete remission, and usually includes chemotherapeutics not applied during remission induction, such as cyclophosphamide, etoposide, and methotrexate (24, 27). The final maintenance phase generally consists of less

intensive treatment regimens and has the goal to further consolidate and maintain remission. Pediatric ALL patients in this phase are typically treated with mercaptopurine and methotrexate, which may be intensified with vincristine and steroids (24).

The standard of care for pediatric AML patients also consists of chemotherapeutic combinations, such as cytarabine with daunorubicin or mitoxantrone, with intensities determined based on risk-stratification (22). The treatment regimens are typically given in a remission induction phase and subsequent consolidation or intensification phases. In contrast to ALL treatment, maintenance therapy is not standard of care but may be added if needed. High-risk AML patients may furthermore receive allogeneic hematopoietic stem cell transplantation (HSCT) with the goal of eliciting anti-leukemia activity by donor-derived immune cells (graft-versus-leukemia response (28)).

Acute leukemia, especially in the case of ALL, can penetrate the central nervous system (CNS). Hence, CNS prophylaxis is an important part of ALL therapy since most pediatric and adult patients are at risk of developing CNS relapse. Treatment options include CNS-direct radiation, systemic administration of chemotherapeutics that can cross the blood-brain barrier, or direct intrathecal administration of chemotherapies, such as methotrexate, cytarabine, or hydrocortisone (29, 30).

1.1.3 Challenges of current cytotoxic chemotherapies

Despite improved treatment results for pediatric acute leukemia patients, several challenges remain that warrant the research and development of novel treatment options. Children with relapsed or refractory ALL or AML face poor outcomes, with long-term survival rates of only 40-50% (31-34). Notably, about 20-25% of pediatric ALL patients experience relapse, as do 25 – 30% of AML patients (33, 34). Relapsed or refractory children receive salvage or reinduction therapy, typically consisting of several blocks of chemotherapeutic combinations followed by HSCT (35, 36). While outcomes remain poor for relapsed or refractory patients, graft-versus-leukemia

responses following allogeneic HSCT in some patients highlight the potential for immunotherapeutic strategies in acute leukemia (37).

Additionally, the current cytotoxic chemotherapy regimens are associated with severe late effects and secondary malignancies (3-6). Methotrexate, mercaptopurine, and vincristine are components of standard pediatric ALL therapy and several side effects have been directly linked to these compounds: High doses of methotrexate are associated with neuronal impairments (38), while high doses of mercaptopurine increase the risk of secondary myeloid malignancies (39), and may also increase the risk of liver injury or relapse in some patients (40). Vincristine is associated with acute peripheral neuropathy leading to impaired motor-, nerve-, and muscle functions and reduced quality of life (41, 42). Other severe side effects associated with chemotherapeutic ALL treatment include osteoporosis and osteonecrosis, pancreatitis, thrombosis, neurocognitive impairments, infertility, secondary malignancies, and an increased risk for early mortality in survivors (42-46). Moreover, prophylactic CNS-directed radiation can have severe, long-lasting effects, such as neurocognitive decline, endocrine abnormalities, and brain necrosis (30). Treatment outcomes for pediatric T-ALL patients are generally worse than for B-ALL patients, and treatment-associated mortality or late effects are more common (45, 46).

Late effects in pediatric AML patients associated with standard chemotherapeutic treatment include cardiomyopathy, neurocognitive impairments, physical function impairments, and secondary malignancies (47). In addition, infections, intracerebral hemorrhage, or multiple organ failure may also lead to chemotherapy-related mortality (48).

Given the poor outcomes in relapsed or refractory patients, as well as the severe late effects and secondary malignancies, there is a significant need for novel pediatric acute leukemia treatment options. Such a need also exists in adult patients, who generally tolerate cytotoxic chemotherapies less, resulting in survival rates below 75% for ALL, below 35% for AML, and below 15% for patients older than 60 years with either disease (3, 8, 49, 50).

1.2 Novel treatment approaches for acute leukemia

Novel non-chemotherapeutic treatment options for acute leukemias, including targeted therapies and immunotherapies, are under development with the aim of reducing toxicities and late effects, as well as improving treatment outcomes.

1.2.1 Targeted therapies in acute leukemia

Targeted therapies act specifically on well-defined targets or pathways to inhibit their oncogenic functions, and a significant number of these targeted therapeutic agents are tyrosine kinase inhibitors (TKIs) (51). The small-molecule TKI imatinib, which targets the tyrosine kinase ABL, has revolutionized the treatment of ALL patients expressing the BRC-ABL fusion protein (52). BCR-ABL expression is found in 1-5% of pediatric and 11-30% of adult ALL patients and is associated with poor prognosis if treated with chemotherapy alone (53). The chimeric protein is a result of translocation of chromosome 9 and 22 (t9;22), also known as Philadelphia chromosome (Ph), and leads to constitutive activation of the ABL kinase function, thereby driving leukemia blast proliferation. The clinical use of imatinib and other BCR-ABL TKIs has dramatically improved the 5-year event free survival rates in pediatric Ph^+ ALL patients from 34% to 70%, and greatly reduced the need for HSCT in these patients (54). Unfortunately, resistance occurs in some patients, often caused by point mutations in the BRC-ABL kinase domain (52). Second generation inhibitors are being developed and these aim to overcome resistance by targeting the structural stability of the fusion protein, downstream signaling pathways, or by inhibiting multiple kinases in addition to BCR-ABL. Furthermore, various other targeted agents are being developed for B-ALL or T-ALL treatment in preclinical studies or clinical trials, including BCL-2 family inhibitors, BET family inhibitors, cell cycle inhibitors, MDM2 inhibitors, p53 reactivators, and inhibitors of oncogenic signaling pathways, such as JAK-STAT, PI3K-AKT-mTOR, MAPK-RAS, or NOTCH signaling (46, 55).

Targeted therapies in clinical use for AML include TKIs targeting common FLT3 mutants, and hypomethylating agents, but most patients eventually relapse or develop resistance (56, 57). Moreover, venetoclax, a BCL-2 inhibitor, shows promising results in elderly AML patients or patients unfit for intense chemotherapy when combined with low doses of the chemotherapeutic cytarabine, or a hypomethylating agent (58).

1.2.2 The acute leukemia immune microenvironment

Immunotherapies aim to activate the patient's immune system to fight cancer cells and have shown remarkable success in some cancers (59). Cancer cells can avoid immune surveillance or suppress the immune system through several mechanism, ultimately allowing them to escape anti-cancer immunity. The relatively low mutational rate in acute leukemia results in low availability of tumor-specific antigens, the detection of which is a crucial part of anti-cancer immune surveillance (60, 61). These antigens can be taken up by antigen-presenting cells (APCs), such as macrophages or dendritic cells (DCs), and presented on MHC class II (MHC-II) molecules to $CD4^+$ T cells (62, 63). Stimulated $CD4^+$ T cells subsequently help orchestrate the immune response and activate cytotoxic $CD8^+$ T cells, which have the ability to eliminate cancer cells. Some specialized APCs, in particular $CD103^+$ DCs are capable of cross-presenting antigens directly to cytotoxic $CD8^+$ T cells (64). Moreover, $CD8^+$ T cells can recognize tumor-specific mutant antigens presented on MHC-I molecules on the surface of cancer cells (62, 63). Downregulation of MHC-I molecules has been detected in some relapsed acute leukemia patients, which may provide a mechanism of avoiding immune surveillance (65). Complete activation of T cells also requires the binding of co-stimulatory proteins expressed on APCs, such as CD80, the expression of which is low in the tumor microenvironment (TME) of acute leukemia (66). Acute leukemias may also impair the cytotoxic functions and IFN-γ production of natural killer (NK) cells, which are cytotoxic lymphocytes that can recognize and eliminate cancer cells in the absence of MHC molecules (67, 68). Moreover, malignant leukemia blasts no longer develop into normal immune

cells and prior chemotherapy treatment may also impair immune cell functions, resulting in additional factors that can contribute to an insufficient immune surveillance and/or response (61, 69).

Another important mechanism of cancer-induced immunosuppression is the upregulation of immune checkpoint proteins, such as PD-L1 (programmed cell death 1 ligand 1) or PD-L2 (programmed cell death 1 ligand 2). Cancer cells can overexpress these proteins on their cell surface or induce their expression on other cells in the TME, such as macrophages, DCs, or epithelial cells. Together with the receptor protein PD-1 (programmed cell death protein 1), these immune-inhibitory proteins physiologically function as built-in "brakes" of the immune system to prevent chronic inflammation and auto-immune reactions. PD-1 is predominantly expressed on activated T cells (70) and binding of PD-L1 and PD-L2 to PD-1 inhibits T cell activation and induces exhaustion, a state broadly characterized by a decreased ability to proliferate and/or kill target cells (71-74). Immune checkpoint inhibitors targeting PD-1 or PD-L1 to overcome T cell exhaustion are in clinical use for various cancer types and have delivered dramatic results in some patients (75). Clinical data show PD-L1 expression on leukemic blasts from de novo AML and ALL patients (76-78), and increased PD-L1 expression levels in relapsed patients (77, 78), indicating a role for the PD-1 axis in suppressing anti-acute leukemia immunity. Another immune checkpoint protein with increased expression in acute leukemia patients is CTLA-4, a T cell receptor protein that inhibits T cell activation when bound to CD80, or CD86 expressed by APCs (79, 80).

Cancers can furthermore induce immunosuppressive conditions in the TME by changing the balance between pro- and anti-inflammatory cytokines. Pediatric ALL patients display changes in the levels of several cytokines compared to healthy children (81) and an altered cytokine balance at birth may contribute to later disease development (82). Moreover, decreased levels of the pro-inflammatory cytokine IFN-γ are associated with high risk in pediatric ALL patients (83, 84), while high levels of the receptor for the pro-inflammatory IL-15 correlated with improved survival

outcomes (85). These data point toward an important role for the TME cytokine composition in acute leukemia progression.

Acute leukemias can also increase the presence of immunosuppressive immune cells in the TME, such as regulatory T cells (T_{regs} cells) and myeloid-derive suppressor cells (MDSCs) (81, 86, 87). T_{regs} cells possess immunosuppressive functions that play important physiologic roles in self-tolerance and immune homeostasis, but cancer cells can increase their recruitment to the TME thereby leading to suppressed anti-cancer immunity (81). MDCSs are a heterogenous group of immature myeloid cells that can also contribute to cancer progression through potent immunosuppressive capacities (88).

Furthermore, cancers often manipulate macrophages by inducing an immunosuppressive M2 phenotype, characterized by anti-inflammatory gene expression, cytokine profiles, and functions (89). Macrophage phenotypes can be broadly categorized as pro-inflammatory M1 or anti-inflammatory M2, although the transition is fluid with many different stages. Adult T-ALL/lymphoma patients display increased expression of M2 markers by macrophages of the TME, and this was associated with poor prognosis (90). Moreover, M2-like macrophages are increased in the bone marrow of AML patients (91).

Based on the implication of the immune system for acute leukemia progression, and the promising results of graft-versus-leukemia responses following allogeneic HSCT in some patients (37), several immunotherapeutic treatment modalities have been developed or are being tested for the treatment of acute leukemia.

1.2.3 Immunotherapies in acute leukemia

Acute leukemia immunotherapies have made the most promising advances in B-ALL and several agents are in clinical use, including chimeric antigen receptor (CAR) T cells, bispecific T cell engagers (BiTEs), and antibody-drug conjugates (ADCs) (9, 92, 93). These therapies capitalize on

the expression of surface antigens that are highly expressed by B-ALL blasts, such as CD19, CD20, and CD22 (93, 94). Although these targets allow for relatively specific leukemia cell targeting, they are also expressed by normal B cells, and patients need to be monitored for adverse effects related to B cell-ablation, such as hypogammaglobulinemia (93).

CAR T cells are patient-derived T cells that have been engineered to express chimeric antigen receptors (CAR) targeting cancer-cell specific antigens (95). CARs are additionally engineered to express T cell co-stimulatory domains and binding to the cancer antigen induces proliferation and cytolytic activity of the CAR T cell, without requiring antigen-presentation on MHC molecules. The CD19-targeted CAR T cell tisagenlecleucel is approved for refractory or relapsed patients up to 25 years of age and has achieved remarkable results (9, 93, 96, 97). However, a considerable portion of patients develop resistance and severe side effects, such as cytokine release syndrome, neurotoxicity, or an increased risk for infections are common.

The BiTE blinatumomab is a fusion protein consisting of two single-chain variable antibody fragments, one of which binds to CD19 on B-ALL cells, while the other binds to CD3 on T cells, thereby in inducing T cell-mediated killing of $CD19^+$ leukemia cells (98). The BiTE-mediated adherence between T cell and leukemia cell is sufficient to activate T cells, requiring no antigen-presentation on MHC molecules (99). Blinatumomab is approved in pediatric and adult refractory or relapsed B-ALL patients, as well as B-ALL patient with minimal residual disease (MRD) (93). Promisingly, clinical studies indicated that treatment with the BiTE has benefits compared to intensive consolidation chemotherapy (100, 101). However, resistance and severe adverse effects, including cytokine release syndrome and neurotoxicity, can occur (93).

The ADC inotuzumab ozogamicin is an anti-CD22 antibody linked to a cytotoxic anti-tumor antibiotic and is currently approved for use in adult patients with relapsed or refractory B-ALL (93), while a phase-I clinical trial found promising results in relapsed or refractory children (102).

A major side effect and limitation of inotuzumab ozogamicin treatment is sinusoidal obstruction syndrome, especially in patients that have or will receive HSCT (93).

Despite the increased PD-L1 levels observed in acute leukemia patients (76-78), immune checkpoint blockade targeting PD-1 or PD-L1 as ALL monotherapy did not deliver promising results in clinical trials, although combinations therapies with chemotherapy or other agents may prove more effective (61).

The clinical development of T-ALL immunotherapies has been complicated by the fact that most antigen markers expressed by T-ALL blasts are shared with normal T cells, resulting in a risk of severe immunodeficiency through elimination of the latter (46). Nonetheless, pre-clinical trials showed efficacy for several immunotherapeutic modalities, including anti-CD38 antibodies, as well as CAR T cells targeting CD1a, CD2, CD5, or CD6, and phase-1 clinical trials have been initiated for some agents (46, 93).

AML blasts display a great diversity in surface antigens and the resulting difficulty of selecting specific antigens is a major challenge for the development of AML immunotherapies (69, 103). Furthermore, the relatively low frequency of AML among children limits the potential to evaluate immunotherapies in clinical trials (104). Nonetheless, several immunotherapeutic agents are being investigated for the use in AML patients, including CAR T cells, BiTEs, ADCs, and immune checkpoint inhibitors (69, 103).

Targeted and immunotherapeutic agents have delivered promising – and in some patients remarkable - results, particularly in B-ALL. However, not all patients are eligible, or respond well, and others may develop resistance. Hence, more research is needed to identify new targets and provide additional treatment options. TYRO3, AXL and MERTK are receptor tyrosine kinases (RTKs) that have been indicated as promising cancer therapeutic targets in a range of malignancies (105). In this work, we investigate their potential as immunotherapeutic targets in

acute leukemia with the overall aim to contribute to the development of novel treatment strategies.

1.3 TAM family RTKs as therapeutic cancer targets

The receptor tyrosine kinases (RTKs) of the TAM (TYRO3, AXL and MERTK) family are aberrantly expressed and associated with poor prognosis in a wide range of human cancers, including acute leukemia (105-107). Within cancer cells, they play important roles that promote tumor establishment, survival, progression, and treatment resistance. Additionally, TAM RTKs expressed by immune cells of the tumor microenvironment (TME) can exert immunosuppressive functions to inhibit anti-cancer immunity. Hence, TAM RTKs represent promising therapeutic targets for both, direct anti-cancer cell-, as well as immune-oncologic therapies.

1.3.1 Introduction to TAM RTKs

Physiologically, TAM RTKs are expressed by epithelial cells, platelets, as well as various immune cells, and play crucial roles in tissue homeostasis and immunoregulation (106). The three TAM RTKs share a common structure comprising two immunoglobulin-like and two fibronectin III domains at the extracellular N-terminal end, a single pass transmembrane domain, and a cytoplasmic tail with a kinase domain that is characterized by a highly conserved KWIAIES sequence (106, 108-111). TAM RTK activation by ligand binding induces receptor homodimerization, autophosphorylation and kinase activation, thereby regulating a variety of downstream signaling pathways (Fig. 1.1 *A*). The two best-studied TAM ligands are the secreted proteins GAS6 (growth arrest-specific 6) and PROS1 (vitamin K-dependent protein S). In most cases, TAM activation by these ligands requires creation of a unique ternary complex by additional binding of membrane-bound phosphatidylserine (PtdSer), typically expressed on the surface of an adjacent cell, such as apoptotic cells (Fig. 1.1 *B*) (112-118). GAS6 has the highest affinity for AXL but binds and activates all three TAM kinases, while PROS1 only activates TYRO3 and MERTK (Fig. 1.1 *B*) (112, 116, 117, 119). Further TAM ligands include the MERTK-selective tubby (120, 121), tubby-like protein 1 (TULP-1), which interacts with all three TAM kinases (120) and

Galectin-3 (LGALS3), which activates TYRO3 and MERTK (122-125). Of note, tubby and TULP-1 bridge to apoptotic cells through PtdSer-independent mechanism (120).

TAM kinases may also be activated through heterodimerization and/or cross-phosphorylation with other kinases, including family members (126, 127) and unrelated kinases, such as EGFR (128-133) or HER2 (134) (Fig. 1.1 *B*). Additionally, they can be constitutively activated (for example, in cancer (126, 135)), possibly mediated by impaired receptor degradation following activation (136), or through feed-forward mechanisms resulting in amplified TAM signaling (137) (Fig. 1.1 *C*).

TAM RTK activation can be attenuated through TAM cleavage by metalloproteases (138-142), for example following kinase activation (118), and the cleaved extracellular domains can be shed off the cell surface and act as soluble forms that sequester ligands (139, 140, 143-146) (Fig. 1.1 *D*). Additionally, splice isoforms of all three TAM kinases have been described and secreted isoforms may also function as decoy receptors (108, 110, 147-150).

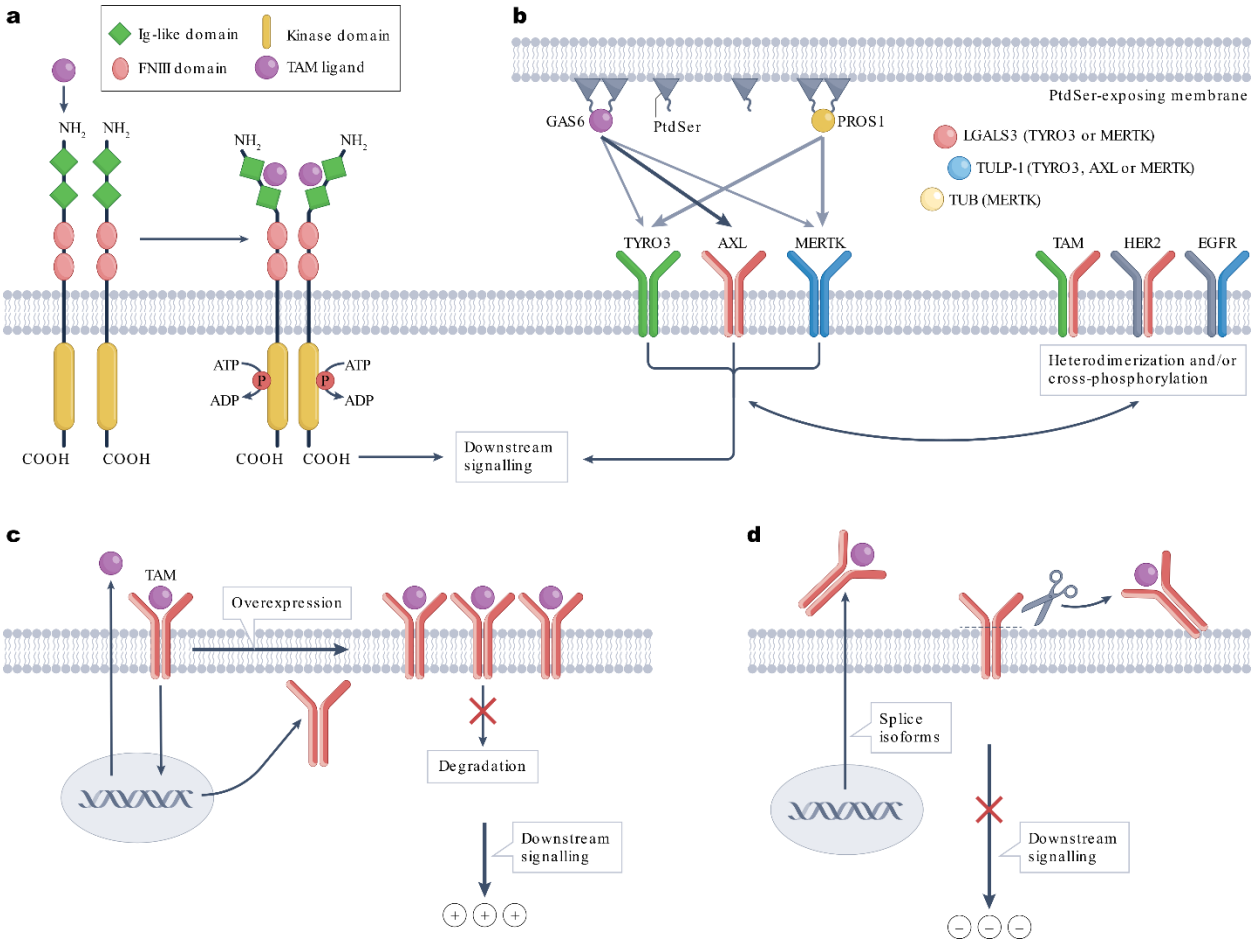

Fig. 1.1: TAM structure and activation mechanisms.
(First published in: *DeRyckere & Huelse et al., Nat Rev Clin Oncol., 2023 Sep 4. doi: 10.1038/s41571-023-00813-7. Online ahead of print,* by *Springer Nature*. Reproduced with permission from *Springer Nature*.)

A) The three TAM receptor tyrosine kinases (RTKs), TYRO3, AXL and MERTK, share a common structure comprising two immunoglobulin-like (Ig-like) and two fibronectin III (FNIII) domains in their extracellular *N*-terminal region, a single-pass transmembrane domain, and a cytoplasmic *C*-terminal region with a kinase domain characterized by a unique and highly conserved KWIAIES sequence (106, 108-111). Activation by ligand binding results in TAM RTK homodimerization, autophosphorylation and subsequent downstream signaling.

B) In most cases, activation by growth arrest-specific 6 (GAS6) or vitamin K-dependent protein S (PROS1) requires additional binding of these secreted ligands to phosphatidylserine (PtdSer) presented on the surface of an adjacent cell (112-118). Furthermore, increased presence of PtdSer can maximize TAM RTK activation. GAS6 can bind to and activate all three TAM kinases but has the highest affinity for AXL, whereas PROS1 only binds to and activates TYRO3 and MERTK (the thickness of the arrows provides a rough indication of relative binding affinity) (112, 116, 117, 119). Additional TAM ligands include galectin-3 (LGALS3), tubby-like protein 1 (TULP-1) and tubby (TUB), the known selectivities of which are indicated in parentheses within the figure (120-125).

TAM RTKs can also be activated through heterodimerization and/or cross-phosphorylation by other TAM family members or unrelated RTKs, such as HER2 or EGFR (126-134).

C) TAM RTKs can be constitutively activated (for example, in cancer) via feed-forward mechanisms that amplify TAM signaling, (through increased ligand production or TAM RTK expression), impaired receptor degradation following activation, overexpression, and in rare cases gene amplification (106, 126, 135-137).

D) Attenuated TAM RTK activation can occur through TAM cleavage by metalloproteases and shedding from the cell surface as soluble factors that can sequester ligands (138-146). Alternatively spliced TAM isoforms have been described (108, 110, 147-149) and secreted isoforms may also act as decoy receptors (150).

1.3.2 Physiologic TAM RTK functions

Physiologically, TAM RTKs play important roles in the regulation of tissue homeostasis and repair, platelet aggregation, and immune control. Often, these roles are linked to their function as essential mediators of efferocytosis, the clearance of apoptotic cells by phagocytotic immune or epithelial cells. Apoptotic cells expose PtdSer on their surface and ligand complexation and activation of TAM RTKs expressed on phagocytotic cells is required for efferocytosis (106). Subsequent downstream signaling induces cytoskeletal and cell shape changes necessary for engulfment of apoptotic cells (151) (detailed in Fig. 1.2 *A*). TAM knockout mice develop enlarged organs as they age due to accumulating apoptotic cells, indicating the importance of this process for tissue homeostasis and repair (152, 153). Indeed, TAM RTK-mediated efferocytosis is crucial for the clearance of dead germ cells in the testis (154), of apoptotic material during weaning-induced involution (155), of renal glomerulus podocytes following nephrotoxic injury (156), and of apoptotic material shed by rods and cones in the retina (115, 157). Moreover, MERTK-dependent efferocytosis is important during adult neurogenesis (121, 158-160), and the clearance of myelin debris in the brain (161).

TAM RTKs are also involved in regulating the aggregation of platelets. Platelets externalize PtdSer and produce GAS6 during the initial phase of aggregation, and all three TAM RTKs are required

to promote integrin signaling, fibrinogen adherence, platelet spreading, and production of aggregation-promoting factors (162-165).

In addition, TAM RTKs are expressed by cells of the immune systems, in which they play crucial homeostatic and immunoregulatory roles. TAM signaling in immune cells mainly results in immunosuppressive functions that are physiologically important as control mechanisms to prevent tissue damage, chronic inflammation and auto-immunity and to allow for tissue repair following the resolution of an inflammatory response (152, 166-172). Consequently, wound healing and the resolution of inflammation are impaired in TAM RTK knockout mice, which can result in increased production of pro-inflammatory cytokines (152, 156, 170), endotoxic shock in response to lipopolysaccharides (152), persistent liver injury and inflammation in a model of acute liver damage (173), chronic hepatitis (174), increased susceptibility to ischemic injury (175, 176), accelerated atherosclerosis (177), and inflammatory brain damage (178). Additionally, deletion of any of the three TAM RTKs leads to autoimmune effects, such as hyperactivation of antigen-presenting cells and increased autoantibody production (153, 179-181). Notably, autoimmunity is more severe in triple-knockout mice, which additionally display splenomegaly and increased B- and T cell proliferation (153). Moreover, TAM RTK knockout increases susceptibility to autoimmune disorders in murine models of multiple sclerosis (182, 183), diabetes mellitus (184, 185), rheumatoid arthritis (186, 187), lupus erythematosus (153, 180, 188, 189), antibody-mediated glomerulonephritis (156), and pemphigus vulgaris(153).

Several immune cell types express TAM RTKs, including macrophages, dendritic cells (DCs), natural killer (NK) and natural killer T (NKT) cells. In macrophages, MERTK signaling can induce an immunosuppressive and wound-healing M2 phenotype, as characterized by increased expression of anti-inflammatory cytokines, such as IL-10, TGF-β, and HGF (171, 190-192), and decreased production of pro-inflammatory cytokines such as TNF-α, IL-1, and IL-6 (152, 190, 193) (detailed in Fig. 1.2 *B*). This is often associated with MERTK-mediated clearance of apoptotic

material (194, 195). Interestingly, downregulation of inflammation in macrophages with a classically-activated, pro-inflammatory phenotype primarily depends on MERTK and TYRO3 (172), although AXL may mediate this function in certain macrophage subsets (196, 197). TAM RTKs also suppress inflammatory functions of DCs (detailed in Fig. 1.2 *C*), where they can inhibit the expression of pro-inflammatory cytokines, MHC class I/II (MHC I/II) molecules and co-stimulatory proteins, such as CD80 and CD86 (168-170, 198, 199). Moreover, TAM signaling mediates inhibition of Toll-like receptor (TLR) signaling in DCs and DCs from TAM-knockout mice are unable to downregulate pro-inflammatory cytokines induced by TLR activation (170). Additionally, TAM RTK signaling inhibits proliferation and pro-inflammatory functions of natural killer (NK) cells, including IFN-γ production and degranulation (200, 201).

Through indirect, non-cell autonomous mechanisms, TAM RTKs can also suppress activation and pro-inflammatory functions of T cells. For example, proliferation of wild-type T cells was increased following adoptive transfer into TAM triple-knockout mice compared with wild-type recipients (153). *In vitro* activated wild-type T cells also displayed decreased motility in pancreatic islets following transfer into *Mertk*$^{-/-}$ mice and treatment with a MERTK inhibitor increased T cell activation in murine diabetes and melanoma models by strengthening and prolonging the interaction with professional antigen-presenting cells (APCs) (185). Furthermore, TAM RTKs can inhibit pro-inflammatory T cell functions through upregulation of the immune checkpoint ligands PD-L1 or PD-L2 on macrophages, DCs, or epithelial cells. Ectopic expression of any of the three TAM RTKs induces PD-L1 and/or PD-L2 expression in epithelial cells (116, 202-204) and *Axl*$^{-/-}$ DCs showed reduced PD-L1 upregulation following antigen uptake compared to wild-type DCs in a murine lung cancer model (205). Likewise, murine macrophages upregulate PD-L1 expression following efferocytosis in a *Mertk*-dependent manner (204) and host *Mertk* deletion or pharmacologic inhibition reduced PD-L1 and PD-L2 expression by CD11b^{+} myeloid cells in an acute leukemia model (206).

While it was long believed that T cells do not express TAM RTKs, more recent studies found that subsets of human T cells upregulate MERTK following activation (207-209). In these subsets, MERTK appears to play immunosuppressive roles: Sequestration of MERTK ligands using a MERTK–Fc decoy receptor fusion protein suppressed the *ex vivo* activation of naïve $CD4^+$ T cells and antigen-specific response of memory $CD4^+$ T cells (207). Similarly, PROS1 induced $CD8^+$ T cell proliferation and activation *in vitro*, and this was overcome by knockdown or pharmacologic inhibition of MERTK, or by treatment with a PROS1-blocking antibody (208). The differential roles for MERTK in human T cell subsets and other (innate) immune cells suggest a tightly regulated system in which the immunomodulatory consequences are context dependent.

Similar to its role in T cells, MERTK was found to have pro-inflammatory functions in B cell subsets and NKT cells. B cell subsets upregulate MERTK expression following activation (209, 210) and B cells from *Mertk*$^{-/-}$ mice have a reduced capability to produce autoantibodies (210) or to activate memory T cells (211) in models of graft-versus-host disease. Likewise, *Mertk*$^{-/-}$ NKT cells have a decreased ability to produce cytokines following antigen stimulation (166).

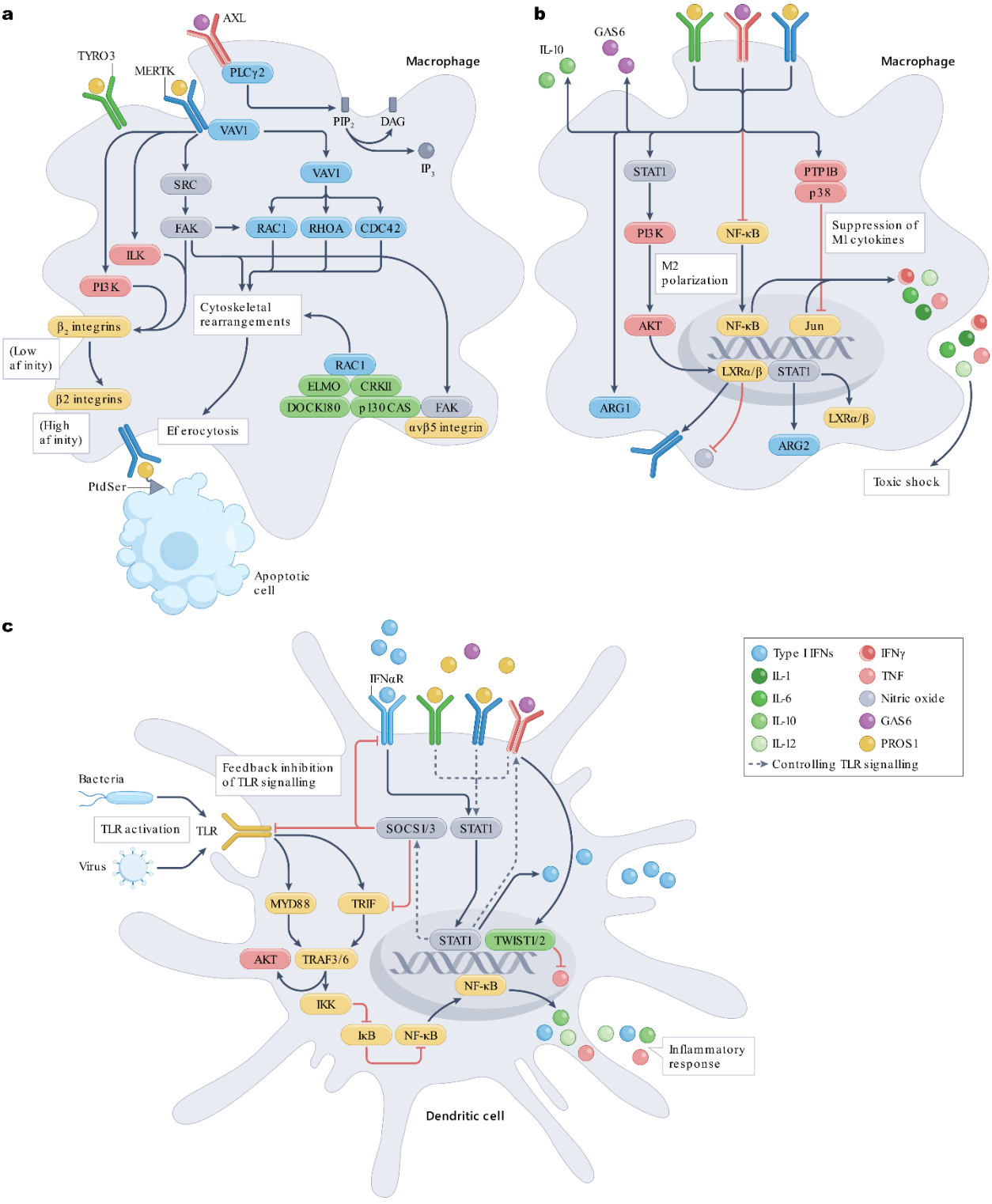

Fig. 1.2 Physiologic TAM signaling in immune cells.

(First published in: *DeRyckere & Huelse et al., Nat Rev Clin Oncol., 2023 Sep 4. doi: 10.1038/s41571-023-00813-7. Online ahead of print,* by *Springer Nature*. Reproduced with permission from *Springer Nature*.)

A) Activation of the TYRO3, AXL and MERTK (TAM) receptor tyrosine kinases (RTKs) by ligands complexed to phosphatidylserine (PtdSer) exposed on the surface of apoptotic cells is required for engulfment and clearance (efferocytosis) of these cells by macrophages (106). TAM activation during efferocytosis promotes downstream signaling through PLCγ2 and VAV1–RHOA, as well as activation of RAC1 downstream of SRC, FAK and αVβ5 integrin through a p130CAS/CRKII/DOCK180/ELMO-mediated mechanism to induce the cytoskeletal reorganization and cell shape changes required for engulfment of the target apoptotic cell (151). Emerging data also identify MERTK as part of a large, multi-protein signaling complex on the macrophage surface that undergoes further aggregation upon MERTK-mediated activation of co-clustered β2 integrin via a PI3K–SRC–FAK–ILK-dependent mechanism, forming an efferocytic synapse that facilitates cell engulfment (212).

B) TAM signaling promotes macrophage polarization to an immunosuppressive M2 phenotype. In particular, MERTK activation leads to inhibition of NF-κB and thereby promotes a wound-healing M2 phenotype characterized by expression of anti-inflammatory mediators and tissue-repair factors, including TAM ligands, with concomitant suppression of pro-inflammatory M1 mediators (152, 171, 191, 195). Suppression of M1 cytokines is also mediated in part by formation of a MERTK–PTP1B–p38α complex, whereby MERTK activation inhibits p38α and ultimately alters the binding of activating and inhibitory Jun transcription factor complexes at target promoters to decrease expression of M1 cytokines (172). MERTK can also mediate PI3K–AKT–STAT1-dependent activation of LXR transcription factors to promote expression of M2 markers and reduce nitric oxide (NO) levels (213).

C) TAM RTKs also mediate suppressor of cytokine signalling (SOCS)-dependent inhibition of Toll-like receptor (TLR) signaling in dendritic cells (170, 214). Upon recognition of pathogen-associated molecular patterns, TLR signaling activates NF-κB and downstream expression of pro-inflammatory cytokines, including IFNα. In turn, IFNα induces expression of AXL via STAT1, and AXL interacts with and co-opts IFNα/β receptor (IFNαR)–STAT1 signaling to drive expression of SOCS1 and SOCS3, which provide feedback inhibition of TLR signaling and inflammatory cytokine production via multiple mechanisms (feedback loop indicated by dashed arrows).

1.3.3 Targeting TAM RTKs in cancer cells

A continuously growing body of research indicate TAM RTKs as promising therapeutic targets in cancer cells. TAM RTKs, as well as their ligands, are aberrantly expressed in a wide range of human cancers, including hematologic malignancies, and this is often associated with poor prognosis, metastasis, and treatment resistance (105-107). Blasts from AML patients have been found to overexpress AXL, MERTK, or *TYRO3* mRNA (215, 216), and expression of AXL, GAS6 or *TYRO3* mRNA is associated with unfavorable survival outcomes in this cancer (215, 217).

Moreover, MERTK is frequently overexpressed in B-ALL, T-ALL and myeloma (218-220). MERTK and TYRO3 overexpression has also been found in patients with lymphoma subtypes (221, 222) and high levels of *AXL* mRNA expression correlate with poor survival outcomes in Burkitt's lymphoma patients (223). Additionally, aberrant TAM RTKs and/or association with poor prognosis can be found in patient samples from many solid tumor types, including non-small cell lung cancer (NSCLC), lung squamous cell carcinoma, uterine cancer, ovarian cancer, breast cancer, pancreatic ductal adenocarcinoma, clear cell renal cell carcinoma (ccRCC), and melanoma (105, 106).

Cancer cell-intrinsic roles of TAM RTKs include pro-survival signaling and suppression of apoptosis, evasion of senescence, promotion of stemness, and downregulation of growth suppressors (105, 106). Moreover, TAM RTKs expressed by cancer cells can promote angiogenesis, metastasis, and treatment resistance. Hence, TAM RTKs crucially contribute to tumor establishment, maintenance and progression. Activation of TAM RTKs expressed by cancer cells can lead to signaling through several canonical oncogenic pathways, including PI3K–AKT and MEK–ERK signaling, ultimately resulting in the pro-tumorigenic functions listed above, and outlined in Fig. 1.3 (105, 106). Additionally, AXL (224), MERTK (225, 226) or cleaved intracellular TAM domains (227, 228) have been found to localize to the nucleus of cancer cells, where they may possess additional non-canonical roles.

Importantly, genetic silencing of TAM RTKs or ligands, or pharmacological inhibition of TAM signaling in cancer cells, inhibited the oncogenic potential in a wide range of preclinical cancer models (105, 106). The results included decreased tumor growth and prolonged survival in various murine xenograft models, indicating TAM RTKs as promising therapeutic targets in cancer cells. Moreover, metastasis and resistance to chemotherapies or targeted agents were inhibited by TAM RTK knockdown or pharmacological inhibition in a range of cancer models (105, 106). Notably, gene mutations or amplifications of TAM RTKs in cancers are rare and unlike

classical oncogenic drivers, TAM RTKs often do not function as strong growth factors but promote cell survival rather than proliferation (106). As such, effects of TAM RTK inhibition are often more pronounced under conditions that induce cell stress, including serum-starvation and anchorage-independent growth (229-232). However, overexpression of TAM RTKs can be transforming in some contexts (233-235) and mice with transgenic MERTK expression by hematopoietic cells have been found to develop leukemia (236).

In summary, aberrantly expressed TAM RTKs provide cancer cells with crucial survival advantages and pre-clinical studies have identified them as promising cancer cell-intrinsic targets for therapies in a wide range of cancers.

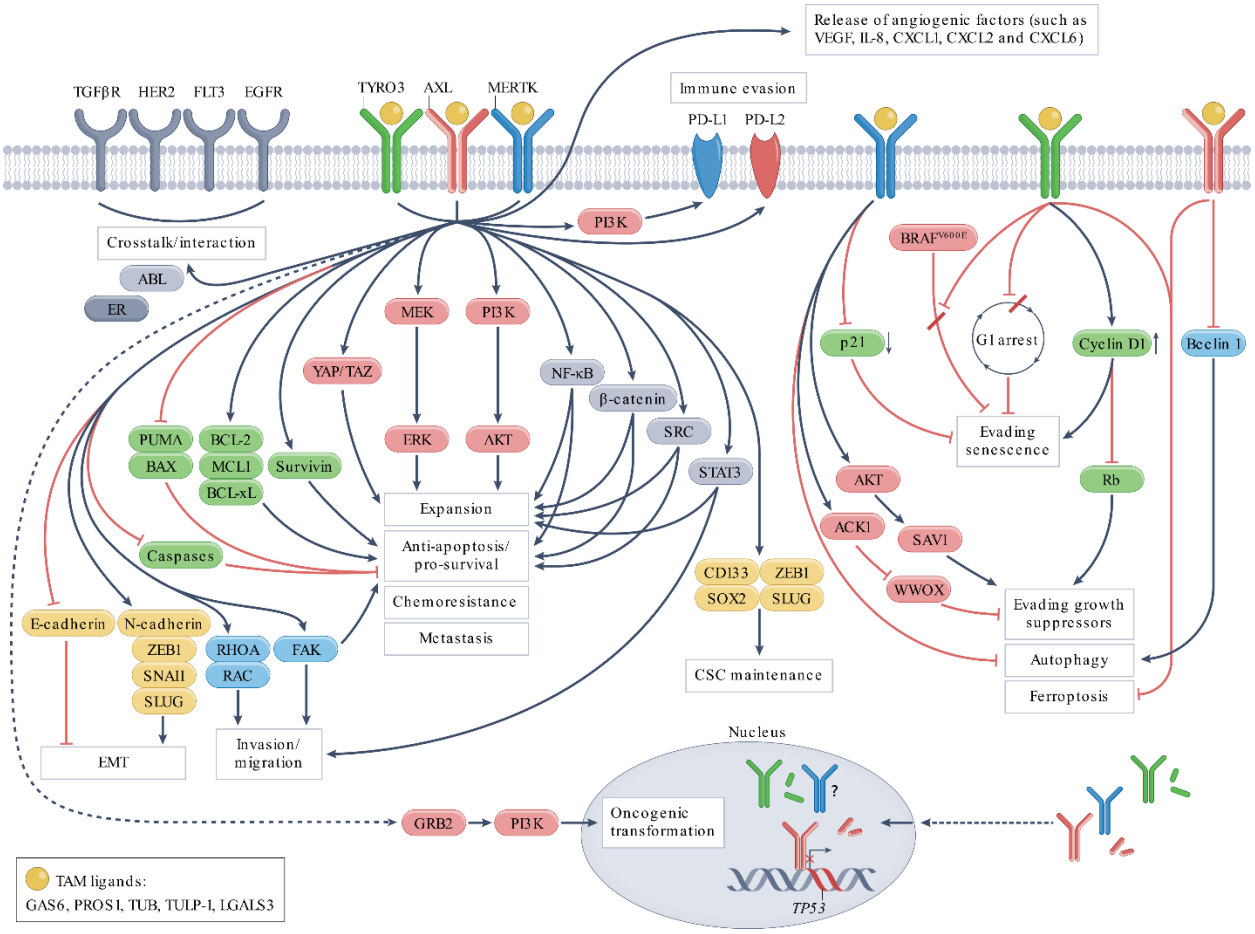

Fig. 1.3 TAM RTK signaling and functions in cancer cells.

(First published in: *DeRyckere & Huelse et al., Nat Rev Clin Oncol., 2023 Sep 4. doi: 10.1038/s41571-023-00813-7. Online ahead of print,* by *Springer Nature*. Reproduced with permission from *Springer Nature*.)

TYRO3, AXL and MERTK (TAM) receptor tyrosine kinase (RTK) signaling regulates a variety of oncogenic pathways and functions, depending on the kinase(s) and ligand(s) involved, the cancer type, and/or context (105). Signaling pathways and proteins and downstream functions depicted on the left side of the figure have been reported to be mediated by at least two of the three TAM RTKs. By contrast, the pathways depicted on the right side have been identified downstream of individual TAM family members, as specifically indicated. TAM RTKs or cleavage products derived from their intracellular regions have also been identified in the nucleus, although the functions of these nuclear forms remain unclear. Additionally, crosstalk and interaction with a variety of other receptor tyrosine kinases and other potential oncogenic mediators, such as ER and ABL, has been reported, as indicated on the far left of the figure.

1.3.4 Pathologic roles for TAM RTKs of the TME in suppressing anti-cancer immunity

In addition to directly target cancer cells, TAM RTK inhibition may also increase anti-cancer immunity. While TAM RTK signaling in immune cells is physiologically important for immune homeostasis, cancer cells can subvert and exploit these immunosuppressive functions to evade anti-cancer immunity and create a TME that favors tumor growth. Pathologic TAM RTK roles in the TME include a range of immunosuppressive mechanisms, such as the induction of anti-inflammatory macrophage polarization, upregulation of immune checkpoint proteins, inhibition of pro-inflammatory DC functions, recruitment and promotion of myeloid-derived suppressor cells (MDSCs) or regulatory T cells (T_{regs} cells), as well as the suppression of $CD8^+$ T cell anti-cancer responses (Fig. 1.4) (105).

Conversely, TAM RTK inhibition increased anti-cancer immunity in a variety of murine cancer models, implicating these RTKs as promising immunotherapeutic targets. Compared to wild-type mice, tumor growth and progression was decreased in mice with deletion of host TAM RTKs in immunocompetent models of breast cancer, colon cancer, lung cancer, melanoma, and pancreatic cancer (237-241). Likewise, treatment with TAM-selective tyrosine kinase inhibitors (TKIs) reduced tumor growth and/or disease progression in immunocompetent models of breast cancer,

bladder cancer, colon cancer, melanoma, and osteosarcoma (204, 242-245), as did administration of an antagonistic anti-MERTK antibody in a colon cancer model (246). Deletion of host *Axl* or *Mertk* or pharmacologic TAM RTK inhibition also reduced disease progression and/or improved survival in syngeneic leukemia models (206, 247, 248). In many cases, the anti-cancer effects of TAM RTK inhibition were abrogated in immunocompromised mice (206, 245, 247, 248), or sufficiently induced by transfer of *Mertk*$^{-/-}$ bone marrow or immune cells into wild-type mice, confirming an immune-mediated mechanism (238, 239).

Cancer cells may increase immunosuppressive TAM RTK signaling in the TME through the release of TAM ligands (106), or the induction of TAM ligand production by immune cells, stromal cells, or endothelial cells (201, 247, 249). For example, GAS6 is expressed by AML and ALL cell lines (250) and PROS1 in AML cell lines (251). Moreover, leukemia cells from ALL or AML patients induced *GAS6* mRNA expression in healthy human monocytes *ex vivo* and high *GAS6* levels are associated with significantly decreased overall survival of patients with either disease (247, 253). Similarly, high bone marrow *LGALS3* (Galectin-3) expression is associated with poor outcomes in AML (254), and Galectin-3 expression is increased in the bone marrow of ALL patients (252). TAM RTK signaling may additionally be increased by elevated PtdSer levels in the TME, caused by cancer cell-derived PtdSer-coated tumor exosomes (255), generally increased apoptosis, and increased PtdSer exposure on tumor-associated endothelial cells (256).

Several immune cell types can contribute to TAM-mediated suppression of anti-cancer immunity. As described in chapter 1.3.2, TAM RTK signaling can polarize macrophages towards an immunosuppressive M2 phenotype, which has been associated with poor outcomes for patients in a broad range of cancers (257). In murine models of breast cancer, host *Mertk* deletion led to an intertumoral decrease in M2 markers and anti-inflammatory cytokines, while pro-inflammatory cytokines were increased compared to wild-type mice (239, 258). Similar effects were achieved in wild-type mice treated with TAM-targeting TKIs in models of breast cancer,

ovarian cancer; colon cancer; and bladder cancer (242-244, 258), or following treatment with an anti-MERTK antibody in a colon cancer model (246). Moreover, deletion of the TAM ligand *Pros1* in melanoma cells resulted in increased expression of pro-inflammatory M1 gene markers in response to TLR activation (172).

TAM RTKs signaling can also affect cytokine production by cancer cells, and deletion of *Axl* in breast cancer cells altered their cytokine and chemokine expression profile, correlating with decreased *in vivo* tumor growth and increased radiosensitivity in immunocompetent but not immunodeficient mice (259). Cytokines and chemokines mediate the recruitment of immune cells and accordingly, TAM-induced changes in their production are associated with altered presence of various immune cell populations in the TME (237-239, 242, 243, 245, 246, 260-262). Consequently, anti-cancer immunity following TAM inhibition is often associated with changes in the TME composition, which can include increased DCs and $CD8^+$ T-cells, as well as altered macrophage numbers and polarization, even though the specific effects appear to be context dependent (237-240, 242, 243, 245-247, 258, 260-263) .

TAM RTK inhibition can also increase tumor antigen presentation to T cells in the TME. In breast cancer models, pharmacological inhibition of MERTK and/or AXL induced expression of T cell co-stimulatory molecules on DCs and increased the number and activation of tumor-associated $CD103^+$ DCs (242). These cells play crucial roles in anti-tumor immunity (264, 265) and are specialized to transport antigens to draining lymph nodes for cross-presentation to $CD8^+$ T cells (64). Moreover, a small molecule inhibitor targeting MERTK, AXL and CSF1R increased cancer cell expression of MHC-I and $CD8^+$ T cell populations in the TME (260). Likewise, MERTK inhibition increased tumor antigen cross-presentation capabilities by tumor-associated macrophages in a colon cancer models (246). Inhibited efferocytosis following TAM RTK inhibition can also increase the presence of apoptotic tumor cells, thereby increasing the availability of tumor antigens in the TME (246, 262).

Enhanced antigen presentation capacities by APCs may lead to efficient anti-cancer immunity through increased activation of cytotoxic T cell functions. Indeed, depletion studies found that anti-cancer immunity in mice with *Mertk* or *Axl* ablation was dependent on $CD8^+$ T cells in several models (239, 242, 247). Additionally, proliferation of splenic lymphocytes in a melanoma model was increased in *Mertk*$^{-/-}$ compared to wild-type mice (239), and treatment with an AXL TKI increased proliferation, activation and effector function of infiltrating $CD4^+$ and $CD8^+$ T cells in an ovarian cancer model (242). Likewise, *Mertk* ablation or pharmacological inhibition increased the activation of $CD4^+$ and $CD8^+$ T cells in a co-culture system with leukemia cells (206).

Inhibition of TAM RTKs can also promote T cell-mediated anti-cancer activity by modulating expression of immune checkpoint proteins in the TME. As discussed in chapter 1.3.2, TAM RTK signaling can increase expression levels of PD-L1 and PD-L2 on APCs and epithelial cells. Likewise, TAM RTKs can induce these immunosuppressive checkpoint proteins on cancer cells. For example, AXL expression levels correlate with PD-L1 expression in breast cancer cell lines (116) and PD-L1 expression was increased in cervical and breast cancer cell lines following treatment with GAS6 and PtdSer (116, 202). Accordingly, knockdown of *AXL* or *MERTK*, or pharmacologic TAM RTK inhibition reduced PD-L1 and/or PD-L2 expression in cell lines of various cancers, including breast cancer (116, 202, 263), head and neck squamous cell carcinoma (HNSCC) (203), NSCLC (266) and osteosarcoma (204). Additionally, host *Mertk* deletion or pharmacologic inhibition decreased PD-L1 and PD-L2 expression by $CD11b^+$ myeloid cells or tumor associated macrophages in leukemia models (206, 248). AXL expression also correlates with PD-L1 and/or PD-L2 expression levels in tumor samples from patients with ccRCC (267), NSCLC (266), or HNSCC (203). Furthermore, high *MERTK* expression is associated with PD-L1 expression signaling in pediatric osteosarcoma patients (204), while *TYRO3* expression correlated with poor survival outcomes and treatment resistance in melanoma patients receiving anti-PD-1 therapeutics (268). Together, these data implicate TAM RTK inhibition as a potential therapeutic strategy to improve outcomes of immune checkpoint inhibitors. Indeed, TAM RTK

knockout or pharmacological inhibition increased the therapeutic activity of immune checkpoint inhibitors in murine models of triple-negative breast cancer (240, 242, 244-246, 260, 263, 268, 269), melanoma (238, 270), colon cancer (243, 245), NSCLC (271-274), ovarian cancer (242) or leukemia (247).

TAM RTK inhibition may also increase anti-cancer activity of NK cells. Treatment with a pan-TAM inhibitor increased the presence of NK cells in melanoma and breast cancer models, which was accompanied by decreased growth of the primary tumor and decreased metastasis (201). Moreover, adoptive transfer of TAM TKI-pretreated NK cells was sufficient to inhibit metastasis in the melanoma model. Importantly, the anti-cancer activity following TAM RTK inhibition was overcome by NK cell depletion in this and other cancer models (201, 247).

TAM RTKs can also promote the recruitment and immunosuppressive functions of MDSCs and T_{reg} cells. *Axl* ablation in myeloid cells and pharmacologic MERTK and/or AXL inhibition decreased the presence of MDSCs in the TME of a leukemia model (247) and tumors from pancreatic cancer and breast cancer models (260, 262). Additionally, host knockout of any of the three TAM RTKs reduces the immunosuppressive functions of MDSCs in a melanoma model and treatment with a pan-TAM TKI reduced tumor growth in wild-type mice in a MDSC-dependent manner (238). Tumor growth was also inhibited in wild-type mice when melanoma cells were co-transplanted with TAM RTK knockout MDSCs compared to wild-type MDSCs. Similarly, host *Mertk* or *Axl* deletion or treatment with a MERTK inhibitor reduced T_{reg} cell presence in the leukemia TME (206, 247). T_{reg} cells have also been shown to express AXL and MERTK (209, 275), and treatment with antagonistic antibodies against these kinases reduced GAS6-induced T cell-suppressive functions of T_{reg} cells (275). Moreover, *Pros1* knockout in melanoma cells reduced tumor infiltration by T_{reg} cells *in vivo* (172).

In summary, TAM RTKs suppressed anti-cancer immunity through various mechanism in preclinical models of a variety of cancers, which was overcome by genetic deletion or pharmacologic targeting, implicating them as promising immunotherapeutic targets.

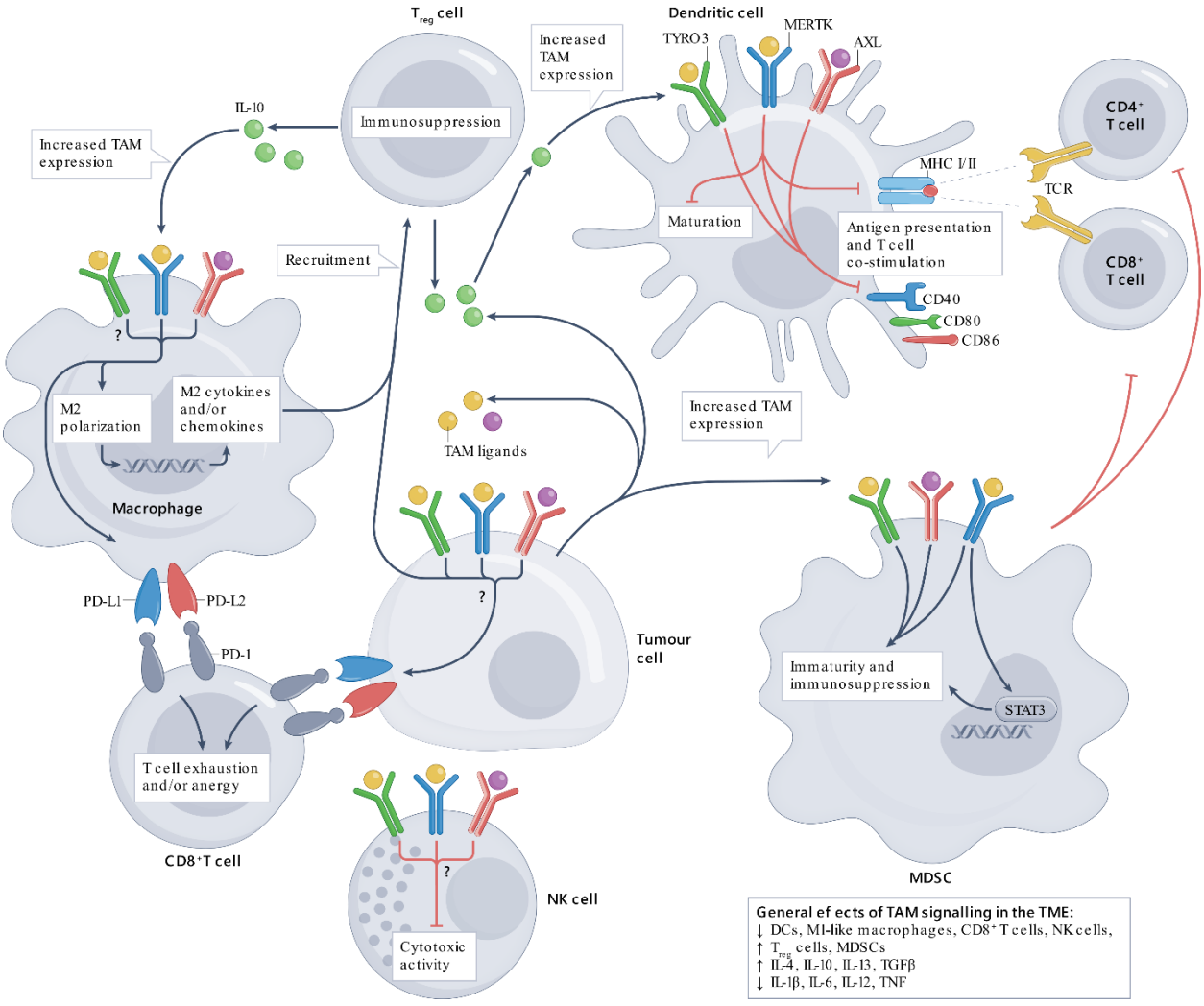

Fig. 1.4 Functions of TAM RTKs in the TME.
(First published in: *DeRyckere & Huelse et al., Nat Rev Clin Oncol., 2023 Sep 4. doi: 10.1038/s41571-023-00813-7. Online ahead of print,* by *Springer Nature*. Reproduced with permission from *Springer Nature*.)

The TAM receptor tyrosine kinases (RTKs) — TYRO3, AXL and MERTK — and their ligands are often enriched in the tumor microenvironment (TME), where they have crucial immunosuppressive roles through a variety of mechanisms. In macrophages, TAM signaling induces an M2 phenotype characterized by reduced expression of pro-inflammatory cytokines

and/or chemokines, such as TNF, and increased expression of immunosuppressive cytokines, such as TGFβ (239, 258). Moreover, M2 chemokines produce by macrophages can attract immunosuppressive regulatory T (T_{reg}) cells to the TME (206, 247). Additionally, TAM signaling in macrophages as well as cancers cells upregulates expression of the immune-checkpoint ligands PD-L1 and PD-L2 (206, 248), which can induce $CD8^+$ T cell anergy and/or exhaustion through binding to PD-1. In dendritic cells (DCs), TAM signaling inhibits functional maturation, downregulates MHC class I and II (MHC I/II)-mediated antigen presentation to T cells and decreases expression of the co-stimulatory molecules CD40, CD80 and CD86 (242). Regarding myeloid-derived suppressor cells (MDSCs), TAM RTK have key roles in the recruitment of these cells and promote an immature MDSC differentiation state and immunosuppressive functions. STAT3 is an essential downstream mediator of MERTK signaling in MDSCs (238). As noted above, TAM kinase signaling in the TME promotes T_{reg} cell recruitment and immunosuppressive activity. In turn, T_{reg} cell-derived IL-10 can increase TAM expression on innate immune cells, including macrophages and DCs (171, 275). TAM signaling might result in impaired cytotoxic activity by NK cells and has been associated with a reduced abundance of NK cells in the TME (201, 247).

1.3.5 TAM RTKs as immunotherapeutic targets in acute leukemia

As discussed above, preclinical studies using murine cancer models have implicated TAM RTKs as promising immunotherapeutic targets in multiple solid cancers. Additionally, recent publications indicate TAM RTKs as potential immunotherapeutic targets in acute leukemia. Host deletion of *Mertk*, or *Gas6* decreased tumor burden and/or prolonged survival in immunocompetent and syngeneic mouse models of AML and ALL, as did *Axl* knockout selectively in cells expressing the colony stimulating factor 1 receptor (*Csf1r*$^+$, including monocytes, macrophages and DCs) (206, 247, 248). Moreover, treatment with TKIs targeting MERTK or AXL recapitulated the extended survival in wild-type mice in these models. Importantly, the leukemia cells themselves were shown to not express the targeted TAM RTK, indicating that the therapeutic activity was caused by immune-mediated effects and not direct leukemia cell killing. Additionally, the anti-leukemia effects of TAM RTK inhibition were abrogated in immunocompromised mice (206, 247, 248).

Macrophages and other myeloid cells may play an important role in the underlying anti-leukemia immune mechanisms: Immunity induced by genetic *Mertk* deletion in AML (248) or *Axl* deletion in AML and B-ALL (247) was mainly driven by ablating the respective TAM RTK in myeloid cells and macrophages. Similarly, MERTK inhibition in AML (248) and *Csf1r*-specific *Axl* knockout in B-ALL (247) shifted macrophage polarization toward a pro-inflammatory phenotype. Nonetheless, the exact mechanisms underlying anti-leukemia immunity may differ depending on the model and/or the TAM RTK inhibited: Immunity induced by *Csf1r*-specific *Axl* deletion was dependent on $NK1.1^+$ cells in AML and B-ALL, while $CD8^+$ T cells were only required for anti-B-ALL immunity (247). In contrast, the optimal anti-AML immune response induced by MERTK inhibition was dependent on conventional α/β T cells, which comprise $CD8^+$ T cells in addition to $CD4^+$ T cells (248). Nonetheless, MERTK inhibition still significantly prolonged survival compared to saline-treated groups in mice lacking α/β T cells, indicating that AML can be cleared even in the absence of these cells.

MERTK was also shown to play a crucial role in regulating expression of PD-1, PD-L1 and PD-L2 in the acute leukemia microenvironment. Host *Mertk* knockout or pharmacologic inhibition reduced expression levels of PD-L1 and PD-L2 on leukemia associated macrophages in an AML model (248), as well as on $CD11b^+$ myeloid cells in a B-ALL model (206) and reduced T cell exhaustion in these leukemias *in vivo* and in *ex vivo* co-culture systems (206, 248). Notably, *in vitro* co-culture experiments with human immune cells derived from peripheral blood mononuclear cells (PBMCs) and human AML cell lines, suggested that MERTK inhibition can also induce pro-inflammatory changes in macrophages and decreased T cell exhaustion in human patients (248).

In this work, we sought to investigate the immune mechanism induced by MERTK inhibition in the B-ALL microenvironment in more detail and additionally evaluated roles for the other TAM kinases, TYRO3 and AXL, in immune-mediated B-ALL clearance.

1.4 Aims and approach

The overarching aim of this dissertation research was to understand how inhibition of individual TAM RTKs can contribute to anti-cancer immunity in acute leukemia, the most common and the 2nd most deadly cancer in children (1-3).

MERTK inhibition in the immune-microenvironment of a syngeneic B-ALL mouse model was previously shown to significantly prolong survival, implicating MERTK as a promising immunotherapeutic target (206). Chapter 2 aims to investigate the underlying immune mechanism and to test potential roles for the other TAM kinases, TYRO3 and AXL, in immune-mediated B-ALL clearance. Survival experiments in immunocompromised *Mertk*$^{-/-}$ mice confirmed an immune-mediated mechanism driving prolonged survival following *Mertk* ablation. To determine the potential roles of TYRO3 or AXL, additional survival experiments in knockout mice were performed. Furthermore, we conducted single cell RNA sequencing (scRNA-seq) experiments with the goal of identifying differences in the quantity and quality of bone marrow immune cell populations following host TAM RTK ablation or pharmacologic MERTK inhibition. Flow cytometry was used to test whether scRNA-seq findings could be confirmed on a protein expression level. Together, these experiments suggested an important role for CD8α^{+} DCs and CD8^{+} T-cells for anti-leukemia immunity in *Mertk*$^{-/-}$ mice, while *Tyro3*$^{-/-}$ mice were protected against B-ALL through a mechanism less dependent on CD8α^{+} DCs. Indeed, *in vivo* immune cell depletion experiments further substantiated this observation. Lastly, analysis of publicly available and relapse-enriched pediatric B-ALL patient data was performed to generate evidence for MERTK as a translationally-relevant therapeutic target.

Given that MERTK and TYRO3 are potential immunotherapeutic targets in B-ALL, Chapter 3 aims to probe the roles of individual TAM RTKs in the anti-AML immune response. Survival experiments in knockout mice, inoculated with two different syngeneic AML models, highlighted context-dependent roles for TYRO3, AXL and MERTK in acute leukemia immunity.

Ultimately, I hope that this work will aid the development of novel therapeutic agents for acute leukemia patients that reduce side effects and improve treatment outcomes.

Chapter 2. MERTK inhibition selectively activates a DC – T-cell axis to provide anti-leukemia immunity in B cell acute leukemia

2.1 Introduction

Despite remarkable improvements in therapeutic outcomes, acute leukemias remain the 2nd leading cause of cancer-related death in children (1-3). Current cytotoxic chemotherapies often cause severe long-term side effects or secondary malignancies in pediatric patients (3, 4), are ineffective in many cases (7) and are not well tolerated in elderly patients, resulting in survival rates below 40% (3, 8). Anti-leukemia immunotherapies provide novel and less toxic treatment options (92), but more research is needed to identify potential targets and understand the underlying mechanisms.

The TAM (TYRO3, AXL, MERTK) family receptor tyrosine kinases are frequently overexpressed and associated with poor prognosis in a variety of cancers, including acute leukemia (106, 107), and AXL and MERTK have been implicated as promising immunotherapeutic targets in multiple solid tumors (239, 240, 263). Under physiologic conditions, TAM kinases play important and predominantly inhibitory roles in the immune system. In macrophages and dendritic cells (DCs), the main antigen-presenting cells of the innate immune system, they provide regulatory feedback mechanisms to prevent chronic inflammation and auto-immunity (152, 168-170, 172). Similarly, TAM kinases suppress pro-inflammatory functions in natural killer (NK) cells (200, 201).

Cancer cells can exploit TAM kinase functions to create an immuno-suppressive microenvironment that promotes disease progression, for example by expressing TAM ligands (172). Conversely, AXL, MERTK or pan-TAM inhibition increased anti-cancer immunity in a variety of models, often accompanied by a compositional shift in the immune microenvironment, including increased DCs and $CD8^+$ T-cells, altered macrophage numbers and polarization, increased pro-inflammatory cytokines and enhanced immune cell activation (239, 240, 242, 246,

247, 258, 263). Roles for TYRO3 as a therapeutic target in the microenvironment are less understood.

We previously demonstrated prolonged survival in response to MERTK inhibition in the immune-microenvironment in a syngeneic B-cell ALL (B-ALL) model, implicating MERTK as a promising immuno-oncology target in acute leukemia (206). Here, we investigated the underlying immune mechanisms and probed roles for the other TAM kinases in immune-mediated B-ALL clearance.

2.2 Materials and methods

2.2.1 Cell culture

GFP$^+$ *Arf*$^{-/-}$ *BCR-ABL* p185$^+$ B-ALL cells (276) were cultured in RPMI 1640 medium (Gibco™ #11835030) with 10% FBS (Atlanta Biologicals #S11550), 1x penicillin/streptomycin (Gibco™ #15140122), and 0.55 μM 2-Mercaptoethanol (Gibco™ #21985023).

2.2.2 Murine B-cell ALL model

Mertk$^{-/-}$ (B6;129-*Mertk*^{tm1Grl}/J) (152), *Axl*$^{-/-}$ and *Tyro3*$^{-/-}$ (277) mice were backcrossed with WT C57BL/6J mice (Jackson Laboratory #000664) for at least 10 generations (206). C57BL/6 *scid* mice (Jackson Laboratory #001913) were crossed with C57Bl/6 *Mertk*$^{-/-}$ mice to generate *Mertk*$^{-/-}$ *scid* mice. *Batf3*$^{-/-}$ mice were purchased from Jackson Laboratory (#013755). Male and female mice were used for experiments at 8-16 weeks of age (180). p185$^+$ B-ALL cells (0.3 – 0.56 x 10^6 cells/kg) were injected into the tail vein. Within each cohort, all mice were injected with the same cell dose. MRX-2843 or saline were administered via oral gavage. Mice with advanced leukemia (> 20% weight loss, tachypnea, hind-limb paralysis, minimal activity) were euthanized. Animal studies were conducted in accordance with relevant regulatory standards and approved by the Emory University IACUC (PROTO201700276).

2.2.3 Immune cell depletion

InVivoMab depletion antibodies (Bio X cell) were administered at 200 ug/mouse via intraperitoneal injection starting 1-2 days before B-ALL inoculation. Anti-mouse NK1.1 (#BE0036) or mouse IgG2a isotype control (#BE0085) were administered every 6 days and anti-mouse CD8α (#BE0061), rat IgG2b isotype control (# BE0090), anti-mouse CD8β (#BE0223) or rat IgG1 isotype control (#BE0088) were administered every 7 days.

2.2.4 Murine tissue collection

Bone marrow was flushed from femurs and tibia in PBS (Corning Life Science #21-040-CV) supplemented with 2% FBS (Atlanta Biologicals #S11550), 1 µM $MgCl_2$ (Sigma-Aldrich #M2393-100G) and 2 U/mL DNase I (Sigma-Aldrich #D4263). Spleens were diced into 1-2 mm^3 pieces and incubated in 2 mg/mL collagenase A (Millipore Sigma #10103586001) with 1 µM $MgCl_2$ and 50 U/mL DNase I in PBS for 30 min at 37°C. EDTA was added to spleen and bone marrow suspensions at a final concentration of 10mM and samples were incubated for an additional 5min at room temperature, then passed through a 40µM cell strainer.

Bone marrow and spleens were dissected, and single cell suspensions were generated. For scRNA-seq, mononuclear cells were separated by density centrifugation using Ficoll® Paque Plus (Cytiva #17-1440-03) and SepMate tubes (STEMCELL Technologies #85450). For flow cytometry, red blood cells were lysed using Gey's solution (8.3 g/L NH4Cl (Sigma Aldrich #A9434-500G), 1.0 g/L KHCO3 (Sigma Aldrich #237205-500G) in ddH2O). See supplemental methods for more detail.

2.2.5 Single cell RNA sequencing and data processing

Freshly prepared single cell bone marrow suspensions were processed for scRNA-seq. Single cells were captured in droplets together with uniquely barcoded primer beads in the Chromium Controller (10x Genomics, 110211) and libraries were generated using the 10X Genomics Chromium single cell 3'V3 kit. Sequencing was performed on the NovaseqS4 platform with > 20 000 reads per cell. The data was aligned with CellRanger 3.1.0 to mm10 mouse reference genome and counts were generated to measure the expression of 1 000-3 000 genes per cell. Quality filtering of scRNA-seq data was performed using multiple filtering parameters including filtering out cells with > 25% mitochondrial genes and/or expression of < 200 genes captured and filtering out genes expressed in < 5 cells in the dataset. For analysis, different sets of samples were grouped and merged, as indicated in the results section, and count data were normalized using

SCTransform function in Seurat v3.0 Bioconductor package (278). Unsupervised analysis using principal component analysis (PCA) was performed on variable genes to identify principal components with significant variation. PCs with significant variations were used as input for UMAP analysis to determine the overall relationship among the cells (279).

Cells with similar transcriptome profiles clustered together and were annotated as different cell types based on the expression of specific well-established genes – i.e. T-cells (*Cd3e*$^{+}$, *Tcf7*$^{+}$, *Trbc2*$^{+}$, *Cd8a*$^{+}$ or *Cd4*$^{+}$), NK cells (*Klrb1c*$^{+}$, *Gzma*$^{+}$, *Klrk1*$^{+}$, *Cd3d*$^{-}$), NKT cells (*Klrb1c*$^{+}$, *Gzma*$^{+}$, *Klrk1*$^{+}$, *Cd3d*$^{+}$), B cells (*Cd19*$^{+}$, *Igkc*$^{+}$, *Iglc2*$^{+}$), monocytes (*Cd68*$^{+}$, *Adgre1*$^{+}$, *Fcgr2b*$^{+}$, *Ccr2*$^{+}$, *Apoe*$^{+}$), macrophages (monocyte gene markers + *Cd74*$^{+}$. *H2-Ab1*$^{+}$, *H2-Eb1*$^{+}$ *C1qa*$^{+}$, *C1qb*$^{+}$), DCs (*Cd74*$^{+}$. *H2-Ab1*$^{+}$, *H2-Eb1*$^{+}$, *Ly6d*$^{+}$, *Itgax*$^{+}$, *Cadm1*$^{+}$, *Siglech*$^{+}$, *Ccr9*$^{+}$), neutrophils/granulocytes (*S100a9*$^{+}$, *Mmp8*$^{+}$, *Ly6g*$^{+}$), and other immune cells. Putative B-ALL cell clusters were annotated based on co-expression of the *Bcr* and *Abl1* genes and absence of markers for canonical stromal and immune cells. Split UMAPs were generated and analyzed to assess differences in the abundance of cells between groups.

To determine changes in cell state or activation under various conditions, a comparative analysis of specific cell type marker genes was performed using dot plot function (278). In an unbiased approach, cell type and subtype signatures were generated by comparing the expression profile of the target cell type with the rest of the cells using the non-parametric Wilcoxon rank test ($P < .01$) and fold change > 1.2. Cell populations with differences in enrichment were further evaluated in the sub-clustering analysis by subsetting out specific groups of cells. For comparative analysis of populations, cells were counted based on expression of marker gene(s) in individual samples/conditions. In the sub-clustering analysis, PCs with significant variation were selected from the top 3,000 variable genes for clustering analysis to determine the overall relationship among cells based on transcriptome profile.

2.2.6 Pathway and systems biology analysis

To precisely characterize cell types/subtypes, pathways enrichment and systems biology analyses were performed using the Ingenuity Pathway Analysis software package (IPA 9.0) (Qiagen), which calculates a P-value for each pathway according to the fit of the user's data to the IPA database using the one-tailed Fisher exact test. Pathways with raw P-values < 0.05 were considered significantly affected. IPA also calculates Z score indicating directional effects on pathways with a Z-score > 2 considered as significantly activated and Z-score < -2 defined as significant inhibition.

Systems biology analysis was performed using the upstream regulators enrichment approach to identify upstream transcriptional regulators predicted by the observed transcriptome changes. Regulatory analysis was conducted to assist with identification of significantly activated or inhibited transcriptional regulators based on upregulation or downregulation of their target genes. Significantly activated/inhibited transcriptional regulators were determined using the one-tailed Fisher's Exact test. Regulators with $P < .05$ and an absolute Z-score of 2 were considered statistically significant. Pathways and upstream regulators are shown as interactive networks generated in the IPA tool based on the overlap of genes between pathways and key upstream regulators.

2.2.7 Flow cytometry

Single cell suspensions were stained in PBS with a fixable viability dye (Zombie NIR™ Fixable Viability Dye (BioLegend #423106), or LIVE/DEAD™ Fixable Red Dead Cell Dye (Thermo Fisher Scientific #L34971)). Cells were fixed and permeabilized prior to staining with antibodies to detect intracellular TOX, Ki-67, iNOS, or Cathepsin-E.

The following antibodies were used to phenotype T, NK and NKT cells: CD3ε (145-2C11)-BV421 (BioLegend #100341); CD4 (GK1.5)-AF532 (Novus Biologicals #NBP2-25191AF532); CD8α (53-6.7)-PE-Cy7 (BioLegend #100721), or -PE (BioLegend #100708); NK1.1 (PK136)-BV605

(BioLegend #108739), or -AF488 (BioLegend #108718); CD69 (H1.2F3)-BUV737 (BD Biosciences #612793), or -PE-Cy7 (Biolegend #104511); PD-1 (29F.1A12)-BV785 (BioLegend #135225); TOX (REA473)-PE (Miltenyi Biotec #130-120-785); GZMB (GB11)-APC (Thermo Fisher Scientific #GRB05); Ki-67 (B56)-BV650 (BD Biosciences #563757); CD44 (IM7) -BV510 (BioLegend #103043); CD19 (6D5)-AF700 (BioLegend #115528); CD11b (M1/70)-AF700 (BioLegend #101222); CD11c (N418)-AF700 (BioLegend #117320)

The following antibodies were used to phenotype dendritic cells: CD11c (N418)-BV421 (BioLegend #117343), or -BB515 (BD Biosciences #565586); MHC-II (I-A/I-E) (M5/114.15.2)-BV785 (BioLegend #105043), or -BV711 (BioLegend #107643); CD8α (53-6.7)-BV510 (BioLegend #100751); CD11b (M1/70)-BV650 (BioLegend #101259), or -BV421 (BioLegend #101235); iNOS (CXNFT)-PE-Cy7 (Thermo Fisher Scientific #25-5920-82); CD103 (2E7)-APC-Cy7 (BioLegend #121431); CD80 (16-10A1)-PE-Cy5 (BioLegend #104711), or -PE-Cy7 (BioLegend #104733); CD86 (GL-1)-BV605 (BioLegend #105037), or -APC-Cy7 (BioLegend #105029); CD40 (1C10)-PE (Thermo Fisher Scientific #12-0401-82); CD3 (17A2)-AF700 (BioLegend), or -BV650 (BioLegend #100229), or BV605 (BioLegend #100237); CD19 (6D5)-AF700 (BioLegend #115528), or -BV650 (BioLegend #115541), or -BV605 (BioLegend #115539); XCR1 (ZET)-BV650 (BioLegend #148220); PDCA1 (927)-BV711 (BioLegend #127039); MERTK (2B10C42)-BV711 (BioLegend #151515); TYRO3 (109646)-PE (R&D Systems #FAB759P). The unconjugated antibodies against CADM1 (clone #30, MBL International #CM004-3) and CTSE (polyclonal, R&D System #AF1130) were detected using the secondary AF488-tagged rabbit anti-chicken IgY antibody (polyclonal, Jackson ImmunoResearch #303-545-003) and PE-tagged donkey anti-goat IgG antibody (polyclonal, R&D Systems #F0107), respectively.

The following antibodies were used to determine *in vivo* depletion of T-cells and DCs following treatment with anti-CD8α and anti-CD8β antibodies: CD3 (17A2) -APC (BioLegend #100236); CD11c (N418)-BV711 (BioLegend #117349); CD8α (53-6.7)-PE (BioLegend #100708); CD11b

(M1/70)-BV421 (BioLegend #101235); CD4 (GK1.5)-AF532 (Novus Biologicals NBP2-25191AF532); CD19 (6D5) -PE-Cy7 (BioLegend #115519).

Flow data were acquired on a Cytek Aurora flow cytometer (Cytek Biosciences) and analyzed using FlowJo software (version 10.8).

2.2.8 TARGET survival data

The publicly available TARGET-ALL-P2 data set was analyzed using the *Survival Genie* webtool (https://bbisr.shinyapps.winship.emory.edu/SurvivalGenie/ (280)). High or low *MERTK* expression was defined using the Cutp (cutpoint) method. The DC gene set was pre-defined in *Survival Genie*.

2.2.9 Statistics

Statistical analyses were performed using GraphPad Prism software (version 9.3.1).

Differences in survival were determined by log-rank test. Differences between groups were determined using 2-tailed t test (2 groups), 1-way ANOVA with Tukey's post-test (3 or more groups), or 2-way ANOVA with Šidák post-test (2 different categorical variables). P values < 0.05 were considered significant. Data from individual cohorts were normalized to account for varying baselines due to potential differences in sample processing on different days. See 2.2.5 and 2.2.6 for scRNA-seq statistics.

2.3 Results

2.3.1 MERTK inhibitor MRX-2843 increases immune cells in the leukemia microenvironment and promotes anti-leukemia immunity.

In previous work, *Mertk* knockout or treatment with the MERTK-selective inhibitor MRX-2843 significantly prolonged survival in an immune-competent, syngeneic and MERTK-negative GFP$^+$ *Arf*$^{-/-}$ p185(*BCR-ABL*)$^+$ B-ALL model (p185$^+$ B-ALL) (206). To further characterize the role of MERTK, *Mertk*$^{-/-}$ or immunocompromised *Mertk*$^{-/-}$ *scid* mice were inoculated with p185$^+$ B-ALL cells. While *Mertk*$^{-/-}$ mice were protected against B-ALL, this survival advantage was lost in *Mertk*$^{-/-}$ *scid* mice, indicating an immune-mediated mechanism (Fig. 2.1 *A*). Of note, *scid* mice have compromised dendritic cell (DC) function and lack mature B- and T-cells (281).

To investigate immune mechanisms, single cell RNA sequencing (scRNA-seq) profiles were determined in bone marrow from wild-type (WT) leukemic mice treated with MRX-2843 (282, 283) (*MRX-2843 study,* Fig. 2.1 *B*). Treatment was initiated 19 days after inoculation of leukemia, when mice had ~50 - 70% GFP$^+$ leukemic blasts in bone marrow (Fig. 2.2 *A*). Mice received 60 mg/kg MRX-2843 daily, a regimen that significantly prolonged survival in previous studies (206), or saline. Bone marrow aspirates were collected without treatment on day 0 (Pre-Rx) and after 3 or 6 days of treatment, then subjected to scRNA-seq. Unsupervised analysis identified 16 transcriptionally distinct cell clusters (Fig. 2.1 *C*). Immune cell clusters were annotated using canonical gene markers and B-ALL cell clusters were identified by *Bcr* and *Abl1* (ABL) co-expression (Fig. 2.1 *D* + Fig. 2.2 *D*).

Treatment with MRX-2843 decreased B-ALL cell clusters (Fig. 2.1 *E*) and flow cytometry confirmed decreased leukemic blasts (Fig. 2.2 *A*). Thus, MRX-2843 was therapeutically effective, even in the context of robustly established disease. Conversely, *Ptprc*$^+$ (CD45$^+$) immune cell clusters increased with treatment (Fig. 2.1 *E*). Additionally, treatment with MRX-2843 for 6 days

increased DCs (Fig. 2.1 *F* + Fig. 2.2 *C*), which play critical roles in anti-cancer immune responses including recruitment and activation of T and NK cells and tumor antigen presentation to T-cells (264). T/NK/NKT cell clusters also increased after MRX-2843 treatment compared to saline controls. Frequencies of other immune cell types are summarized in Fig. 2.2 *C*. In summary, these data demonstrate immune-mediated anti-leukemia activity in mice treated with MRX-2843 and suggest a role for DCs and/or T, NK, or NKT cells.

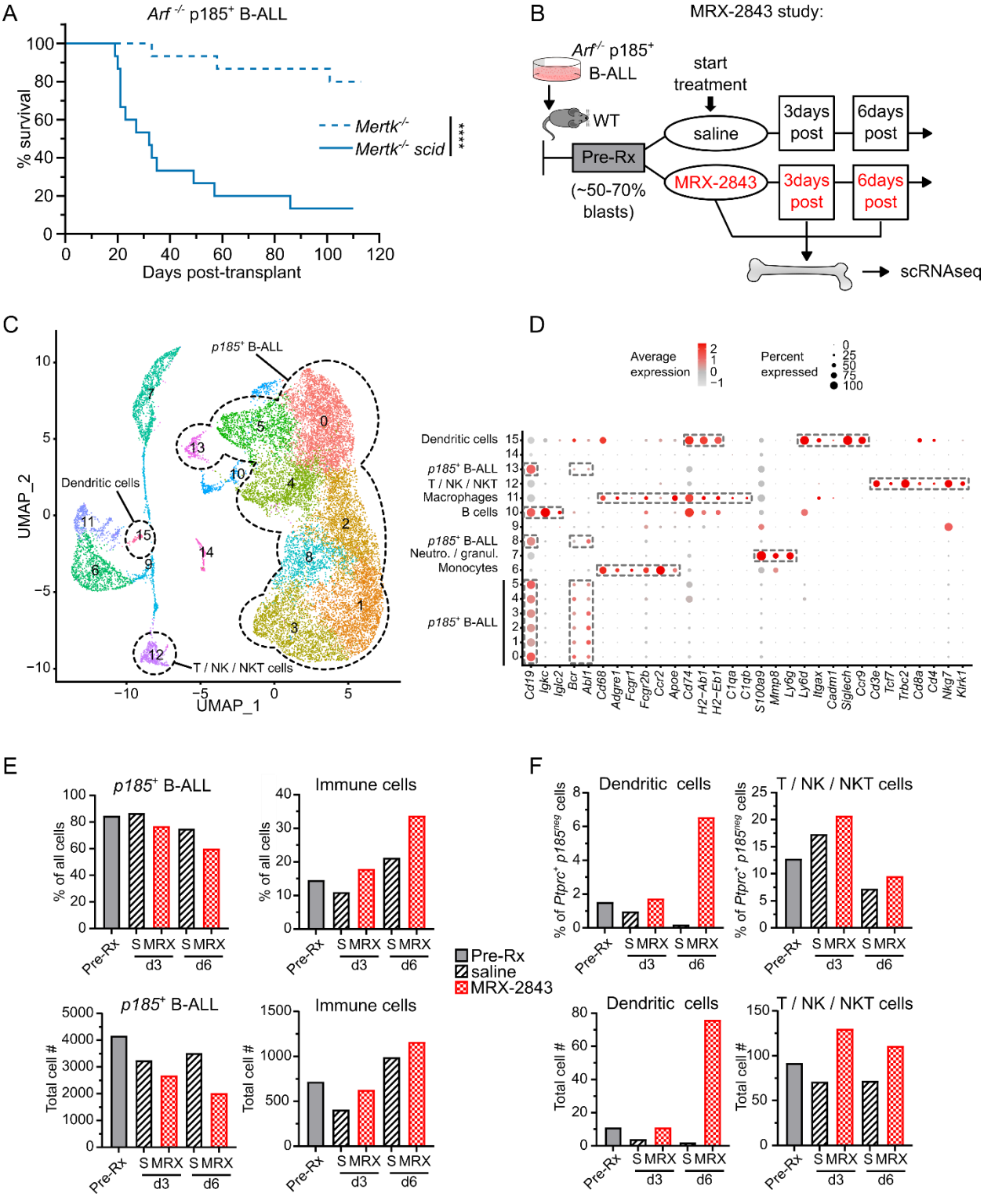

Fig. 2.1: MERTK Inhibitor MRX-2843 increases immune cells and decreases disease burden in leukemic bone marrow in a murine B-ALL model.

A) Kaplan-Meier survival curves from *Mertk*$^{-/-}$ or *Mertk*$^{-/-}$ *scid* mice inoculated with syngeneic *Arf*$^{-/-}$ p185^{+} B-ALL cells. B-ALL cells were injected into the tail vein (n=15 per group in 2 independent cohorts, ****$P < 0.0001$).

B) *MRX-2843 study* design: WT C57Bl/6 mice were injected with syngeneic MERTK-negative, GFP-expressing *Arf*$^{-/-}$ p185^{+} B-ALL cells, and leukemia was established for 19 days (~50 - 70% GFP^{+} blasts in bone marrow) before daily treatment with saline or 60 mg/Kg MRX-2843 was initiated. Whole bone marrow aspirates were collected from cohorts of mice prior to treatment initiation on day 19 (Pre-Rx) and after 3 or 6 days of treatment, and scRNA-seq libraries were prepared using the 10X Genomics platform.

C) UMAP visualization of unsupervised clustering of 20 281 individual cells pooled from control and MRX-2843-treated conditions (combined object of cells from all 5 conditions, 3 430 – 4 921 cells per condition).

D) Dot plot of canonical gene markers used to identify cell populations. For an extended list, see Suppl. Fig 1D. Neutro/granul = neutrophils/granulocytes.

E,F) Frequency (top panels) and total numbers (bottom panels) of B-ALL cells and *Prtpc*$^{+}$ (CD45^{+}) immune cells in the bone marrow (E) or dendritic cells and T/NK/NKT cells in immune cell populations, excluding B-ALL cells (F), as determined by scRNA-seq analysis, prior to treatment initiation (Pre-Rx) and after 3 or 6 days of treatment with saline (S) or 60 mg/Kg MRX-2843 (MRX).

Pre-Rx = prior to treatment initiation, d = day S = saline, MRX = MRX-2843

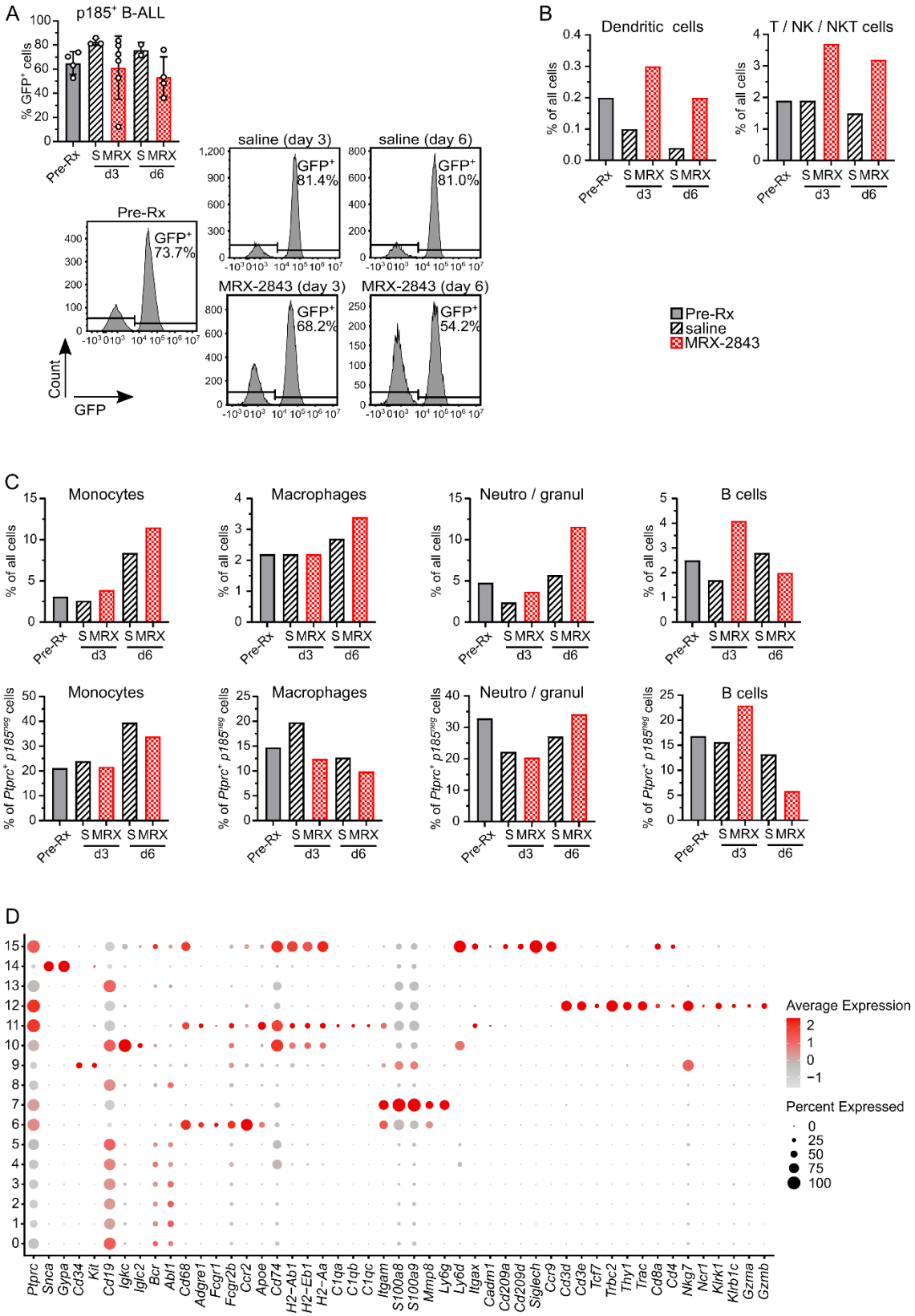

Fig. 2.2: Treatment with MRX-2843 increases immune cell presence in leukemic bone marrow.

A) TOP: Percentage of GFP$^+$ B-ALL cells in bone marrow collected prior to treatment initiation (Pre-Rx) and after 3 or 6 days of treatment with saline (S) or 60 mg/Kg MRX-2843 (MRX) determined by flow cytometry. BOTTOM: Representative flow cytometry plots.

B) Frequency of dendritic cells and T/NK/NKT cells among all cells in the bone marrow.

C) Frequency of other immune cells among all cells in the bone marrow and among non-B-ALL cells.

D) Dot plots of extended canonical gene markers used to identify cell populations.

Data were derived from the scRNA-seq experiment shown in Fig. 1 (*MRX-2843 study*). Pre-Rx = prior to treatment initiation, d = day S = saline, MRX = MRX-2843, Neutro / granul = neutrophils/granulocytes.

2.3.2 TAM-family kinases have differential roles in the leukemia microenvironment.

TAM kinases often have redundant functions (106). To determine whether TYRO3 and/or AXL also suppress anti-leukemia immunity, knockout mice were inoculated with p185$^+$ B-ALL cells. Strikingly, *Tyro3*$^{-/-}$ mice were protected against B-ALL, comparable to *Mertk*$^{-/-}$, while survival of *Axl*$^{-/-}$ mice was not different from WT mice (Fig. 2.3 *A*). These data implicate TYRO3 as a novel immuno-oncology target in acute leukemia.

To investigate and compare the immune mechanisms underlying protection from B-ALL in *Mertk* and *Tyro3* knockout mice, scRNA-seq profiles were derived from bone marrow collected from WT, *Mertk*$^{-/-}$, *Tyro3*$^{-/-}$, or *Axl*$^{-/-}$ mice without B-ALL (naïve mice, day 0) and 3, 6 or 9 days after inoculation of leukemia cells (*KO study*, Fig. 2.3 *B*). Unsupervised analysis identified 27 cell clusters (Fig. 2.3 *C*) and immune cell types were annotated based on expression of established marker genes (Fig. 2.3 *D* + Fig. 2.4 *C*). The incidence of *Ptprc*$^+$ immune cells did not differ between genotypes or over time (Fig. 2.4 *A*), but an increase in DCs and T/NK/NKT cells was observed in naïve *Mertk*$^{-/-}$ mice, similar to MRX-2843-treated WT mice (Fig. 2.3 *E*). Other compositional changes between *Mertk*$^{-/-}$ and WT mice (Fig. 2.3 *E* + Fig. 2.4 *B*) differed from those observed in

MRX-2843-treated WT mice with advanced disease. Hence, the changes described in Fig. 2.2 *C* might be more relevant in the context of fully established B-ALL.

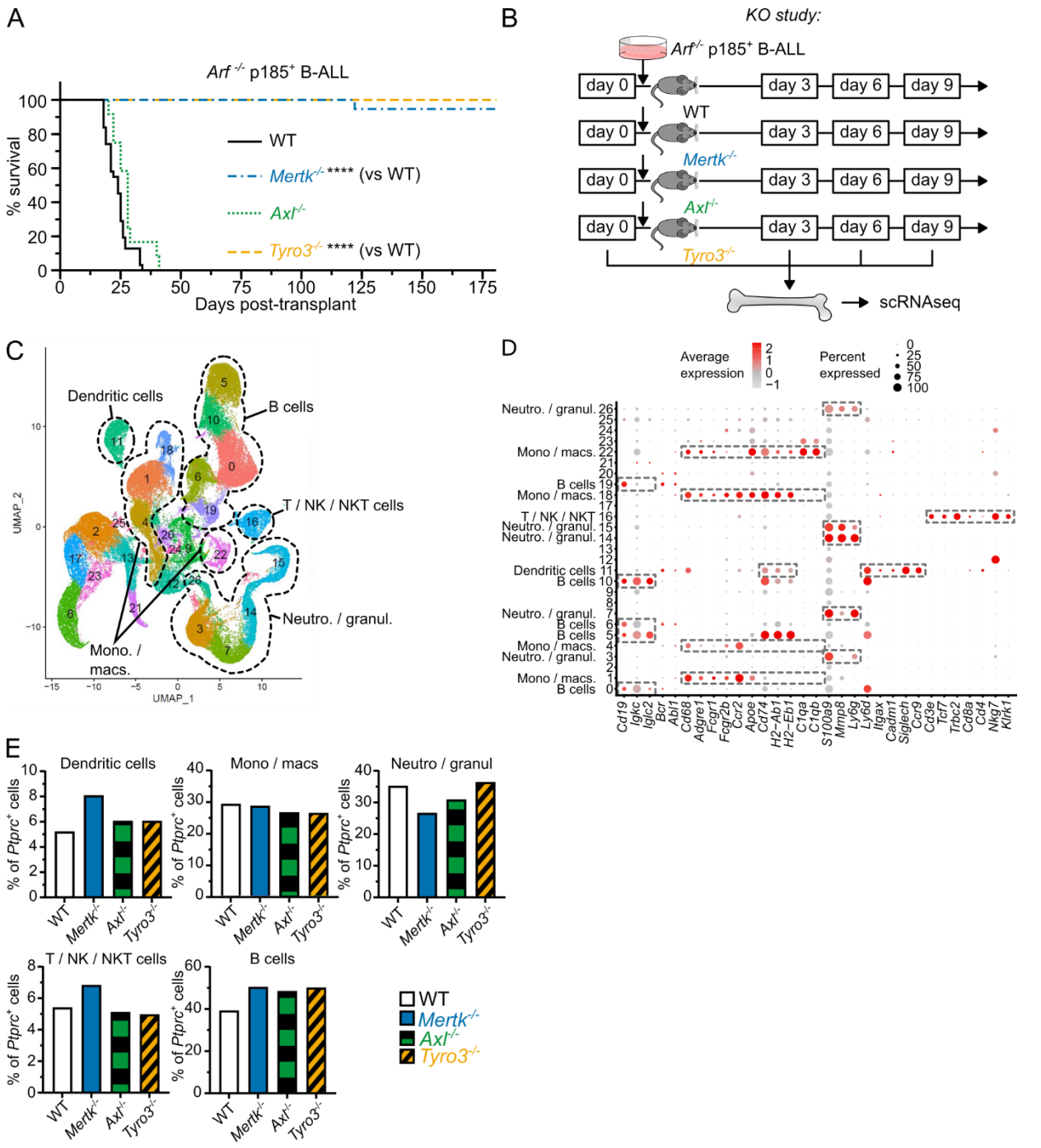

Fig. 2.3: TAM-family kinases have differential roles in the B-ALL immune microenvironment.

A) Kaplan-Meier survival curves derived from wild-type (WT), *Tyro3*$^{-/-}$, *Axl*$^{-/-}$ or *Mertk*$^{-/-}$mice inoculated with syngeneic, GFP-expressing *Arf*$^{-/-}$ p185^{+} B-ALL cells by tail vein injection.

Statistically significant differences were determined using Mantel-Cox log-rank test (WT n=31, *Tyro3*$^{-/-}$ *n=16, Axl*$^{-/-}$ *n=12, Mertk*$^{-/-}$ *n=19* in 3 independent cohorts, ****P < 0.0001).

B) *KO study* design: Bone marrow aspirates were collected from WT, *Mertk*$^{-/-}$, *Tyro3*$^{-/-}$, or *Axl*$^{-/-}$ mice without leukemia (day 0) and 3, 6 or 9 days after inoculation of B-ALL cells. Samples were pooled from 2 mice for each condition and scRNA-seq libraries were prepared using the 10X Genomics platform.

C) UMAP visualization showing unsupervised clustering of 97 522 individual cells pooled from all conditions (4 839 – 7 446 cells per condition).

D) Dot plots of canonical gene markers used to identify cell populations. For an extended list, see Fig S1B.

E) Frequency of immune cell types among *Ptprc*$^{+}$ (CD45^{+}) cells in day 0 samples. Mono/macs = monocytes/macrophages, Neutro/granul = neutrophils/granulocytes.

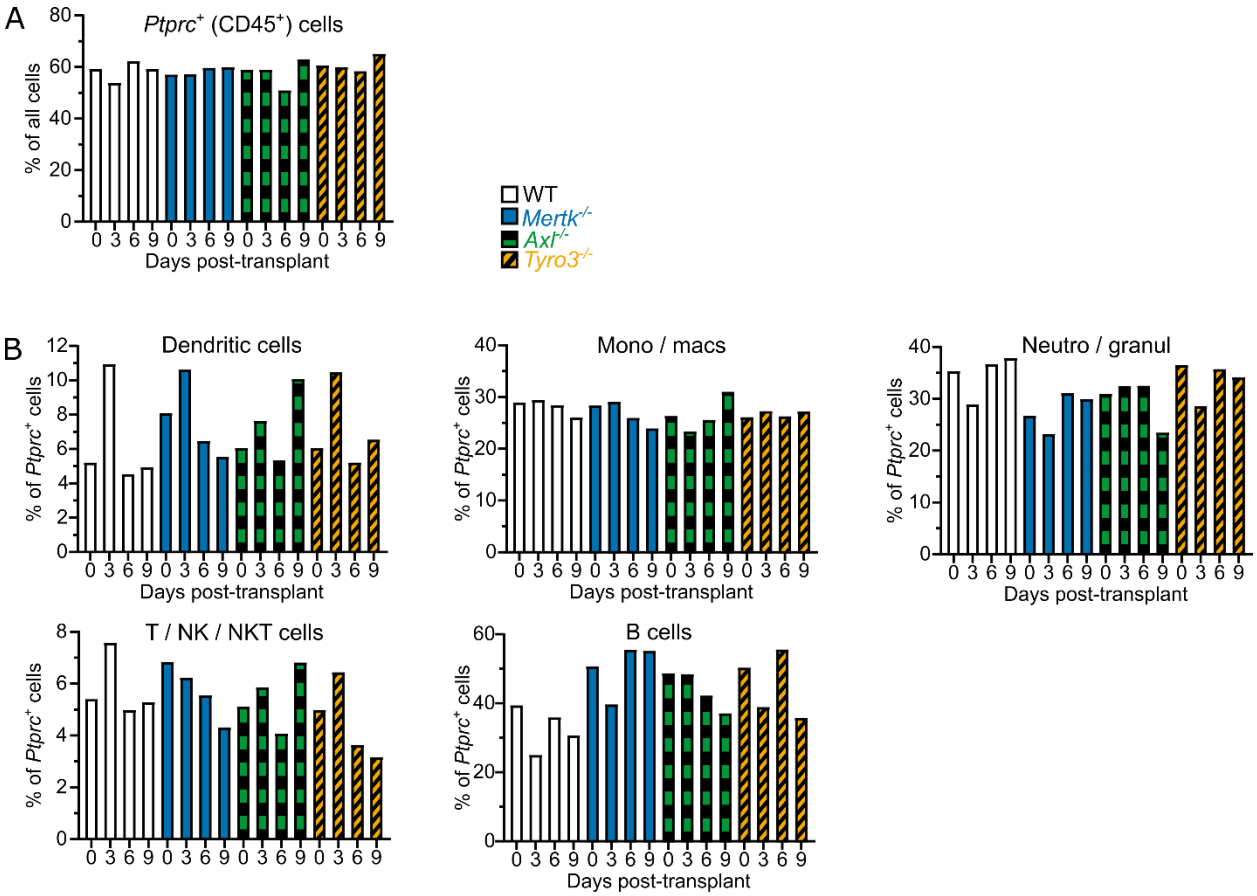

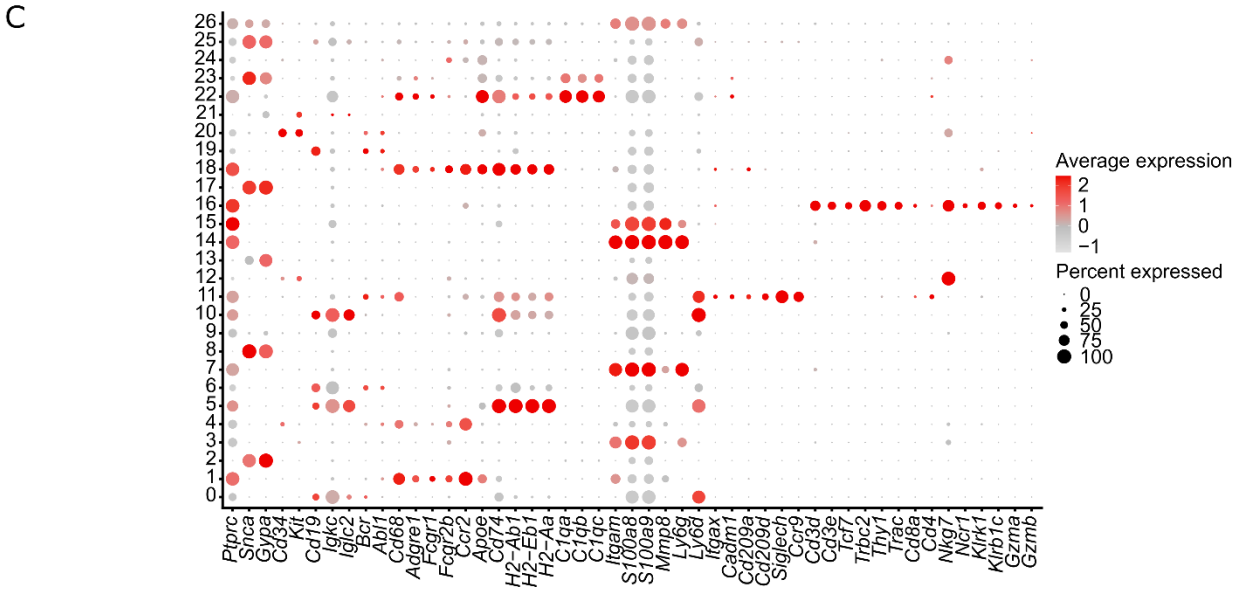

Fig. 2.4: TAM-family kinases differentially impact immune cell composition in the leukemia microenvironment.

A) Frequency of *Ptprc*$^{+}$ (CD45^{+}) immune cells in bone marrow from wild-type (WT), *Mertk*$^{-/-}$, *Tyro3*$^{-/-}$ and *Axl*$^{-/-}$ mice at day 0 (without leukemia) and on days 3, 6 and 9 after leukemia inoculation.

B) Frequency of immune cell subsets among *Ptprc*$^{+}$ (CD45^{+}) cells in C57Bl/6 WT, *Mertk*$^{-/-}$, *Tyro3*$^{-/-}$ and *Axl*$^{-/-}$ mice at day 0 (without leukemia) and on days 3, 6 and 9 after leukemia inoculation.

C) Dot plot of extended canonical gene markers used to identify cell populations.

Data were derived from the scRNA-seq experiment shown in Fig. 2 (*KO study*).

2.3.3 Mertk$^{-/-}$ *or MRX-2843 but not Tyro3*$^{-/-}$ *increases CD8α*$^{+}$ *DCs with markers indicating increased antigen-presenting capacity.*

To characterize DCs as potential players in anti-B-ALL immunity mediated by MERTK inhibition in more detail, the *MRX-2843 study* and *KO study* scRNAseq objects were combined into a single object (Fig. 2.5 *A*, LEFT) and DC clusters were subjected to unsupervised sub-clustering (Fig. 2.5 *A*, RIGHT). Subcluster #0, derived from the *KO study*, was increased in *Mertk*$^{-/-}$ mice compared to WT mice at all timepoints (Fig. 2.5 *C*), and subcluster #12, derived from the *MRX-2843 study*, was increased in mice treated with the drug (Fig. 2.5 *D*). Both subclusters were characterized by *Cd8a* expression (Fig. 2.5 *B*) and antigen-presentation gene signatures: subcluster #0 (*Cd74*, *H2-Ab1*, *H2-Aa*, *Klk1*, *H2-Eb1*, *Iglc3*, *Ctsl*, *Cd209d*, *Ptlp*, *Ly6a*) and subcluster #12 (*Ubc*, *Klf2*, *CD74*, *H2-Aa*, *H2-Eb1*, *Ly6a*) (Fig. 2.5C+D). Subcluster #12 was further characterized by proliferation-related genes (*Fos*, *Fosb*, *Jun*, *Jund)* (Fig. 2.5 *D*). Analyses of pathways and upstream regulators revealed activation of pro-inflammatory pathways and cytokines in both subclusters, including (*"Th1 pathway"*, "*immune response of antigen presenting cells* (#0) / *of cells* (#12)", MHC-II genes (#0) and *Ciita* (a coactivator regulating transcription of MHC-I and MHC-II genes (284), (#12)). (Fig. 2.5 *E*+*F*). These data demonstrate induction of pro-inflammatory *Cd8a*$^{+}$ DCs with high antigen-presenting capacity in response to both genetic and pharmacologic MERTK inhibition. Importantly, subcluster #0 was also increased in *Mertk*$^{-/-}$ compared to *Tyro3*$^{-/-}$ mice,

indicating a selective role for MERTK in this context. Changes in other DC subsets are summarized in Fig 2.6.

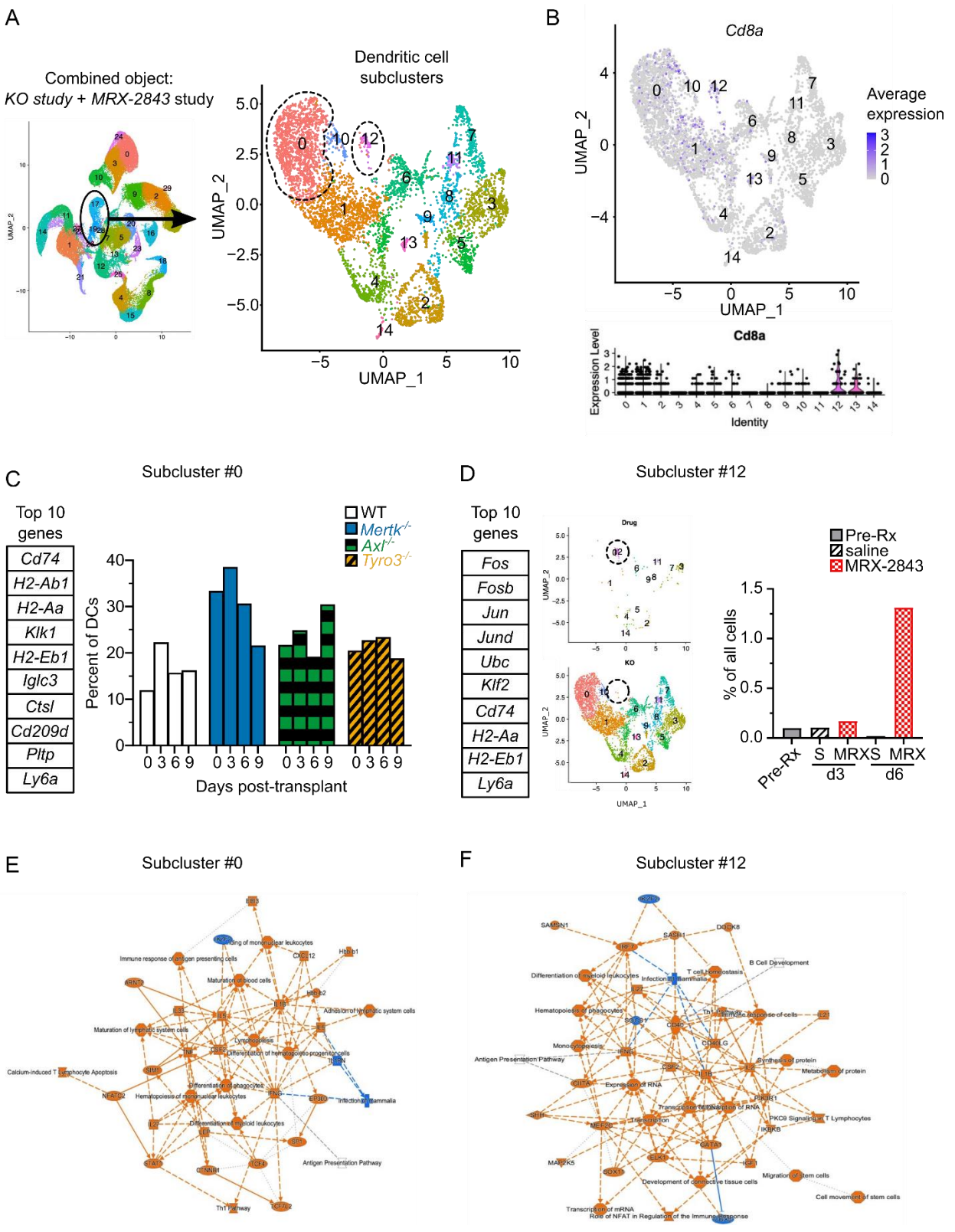

Fig. 2.5: *Mertk*$^{-/-}$ or MRX-2843 but not *Tyro3*$^{-/-}$ increases CD8a-expressing DCs with markers indicating increased antigen-presenting capacity.

A) LEFT: UMAP visualization of the scRNA-seq object derived from combined data from the *MRX-2843* (Fig 1A, B) and *KO* (Fig 2C, D) studies (117 803 cells combined from all conditions, 3 430 – 7 446 cells per condition). RIGHT: UMAP visualization of unsupervised sub-clustering of cells from the main DC cell clusters (#17, #19) in the combined data on the left (5737 individual cells combined from all conditions, 13 – 571 cells per condition). The analysis identified 14 DC sub-clusters.

B) Feature plot (top panel) and violin plot (bottom panel) showing *Cd8a* expression in dendritic cell subclusters.

C) LEFT: Top 10 differentially expressed genes (DEGs) in subcluster #0 relative to all other subclusters. RIGHT: Percentage of subcluster #0 among all dendritic cells in bone marrow from wild-type (WT), *Mertk*$^{-/-}$, *Axl*$^{-/-}$ or *Tyro3*$^{-/-}$ mice without B-ALL (0) and 3, 6 or 9 days after inoculation of leukemia.

D) LEFT: Top 10 DEGs in subcluster #12 relative to all other subclusters. CENTER: Split UMAP showing DC sub-clusters derived from *MRX-2843 study* (top) or *KO study* (bottom). RIGHT: Percentage of subcluster #12 among all bone marrow dendritic cells in leukemic WT mice prior to treatment initiation (Pre-Rx) and after 3 or 6 days of treatment with saline (S) or 60 mg/kg MRX-2843 (MRX).

E,F) The pathways and upstream regulators that are significantly activated (*P* value < 0.05, abs Z-Score > 2) in subcluster #0 (E) or subcluster #12 (F) determined by Ingenuity Pathway Analysis of differentially expressed genes. Significantly upregulated (orange) or downregulated (blue) genes and pathways are shown.

DCs = dendritic cells, Pre-Rx = prior to treatment initiation, d = day S = saline, MRX = MRX-2843

A

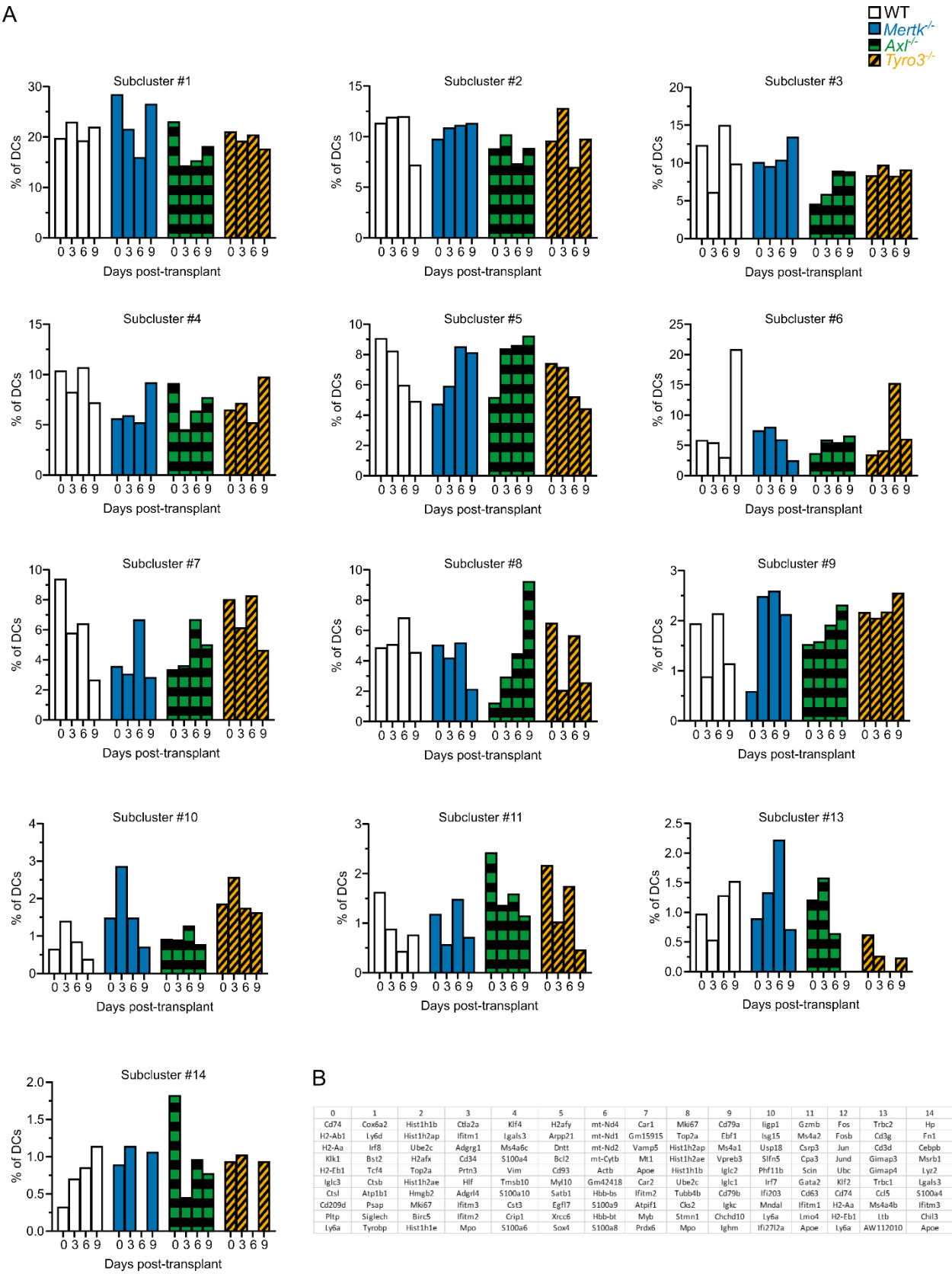

B

0	1	2	3	4	5	6	7	8	9	10	11	12	13	14
Cd74	Cox6a2	Hist1h1b	Ctla2a	Klf4	H2afy	mt-Nd4	Car1	Mki67	Cd79a	Iigp1	Gzmb	Fos	Trbc2	Hp
H2-Ab1	Ly6d	Hist1h2ap	Ifitm1	Lgals3	Arpp21	mt-Nd1	Gm15915	Top2a	Ebf1	Isg15	Ms4a2	Fosb	Cd3g	Fn1
H2-Aa	Irf8	Ube2c	Adgrg1	Ms4a6c	Dntt	mt-Nd2	Vamp5	Hist1h2ap	Ms4a1	Usp18	Csrp3	Jun	Cd3d	Cebpb
Klk1	Bst2	H2afx	Cd34	S100a4	Bcl2	mt-Cytb	Mt1	Hist1h2ae	Vpreb3	Slfn5	Cpa3	Jund	Gimap3	Msrb1
H2-Eb1	Tcf4	Top2a	Prtn3	Vim	Cd93	Actb	Apoe	Hist1h1b	Iglc2	Phf11b	Scin	Ubc	Gimap4	Lyz2
Iglc3	Ctsb	Hist1h2ae	Hlf	Tmsb10	Myl10	Gm42418	Car2	Ube2c	Iglc1	Irf7	Gata2	Klf2	Trbc1	Lgals3
Ctsl	Atp1b1	Hmgb2	Adgrl4	S100a10	Satb1	Hbb-bs	Ifitm2	Tubb4b	Cd79b	Ifi203	Cd63	Cd74	Ccl5	S100a4
Cd209d	Psap	Mki67	Ifitm3	Cst3	Egfl7	S100a9	Atpif1	Cks2	Igkc	Mndal	Ifitm1	H2-Aa	Ms4a4b	Ifitm3
Pltp	Siglech	Birc5	Ifitm2	Crip1	Xrcc6	Hbb-bt	Myb	Stmn1	Chchd10	Ly6a	Lmo4	H2-Eb1	Ltb	Chil3
Ly6a	Tyrobp	Hist1h1e	Mpo	S100a6	Sox4	S100a8	Prdx6	Mpo	Ighm	Ifi27l2a	Apoe	Ly6a	AW112010	Apoe

Fig. 2.6: Changes in DC subpopulations in TAM knockout mice.

A) Percentages of dendritic cell (DC) subclusters among all DCs in bone marrow from WT, *Mertk*$^{-/-}$, *Axl*$^{-/-}$ or *Tyro3*$^{-/-}$ mice without leukemia (Day 0) and 3, 6 or 9 days after leukemia inoculation. Data were derived from the scRNA-seq object shown in Fig 3A.

B) Top 10 genes differentially expressed in each cluster relative to all other clusters.

Similar changes were observed when bone marrow DCs (Fig. 2.8 *A*) from naïve WT, *Mertk*$^{-/-}$ and *Tyro3*$^{-/-}$ mice were analyzed by flow cytometry. While CD8α^{+} DC numbers were comparable in all genotypes (Fig. 2.8 *B*), there was a trend towards increased percentage of CD8α^{+} DCs expressing high levels of MHC-II (MHC-II$^{(HIGH)}$) in *Mertk*$^{-/-}$ mice compared to WT (P = 0.165) (Fig. 2.7 *A*+*B*, left panel). The median fluorescence intensity (MFI) of MHC-II was significantly increased on CD8α^{+} MHC-II$^{(HIGH)}$ DCs in *Mertk*$^{-/-}$ mice compared to WT or *Tyro3*$^{-/-}$, indicating higher per cell expression (Fig. 2.7 *A*+*B*, right panel). Additionally, the fraction of CD8α^{+} bone marrow DCs expressing activation and maturation markers was increased in naïve *Mertk*$^{-/-}$ *and* *Tyro3*$^{-/-}$ mice compared to WT (Fig. 2.7 *C*+*D*, no significant differences in MFI: Fig. 2.8 *C*). Notably, CD8α^{+} DCs expressing CD103, a marker of highly-efficient antigen-presentation, cross-presentation, and priming of CD8^{+} T-cell anti-tumor activity (264, 265), were significantly increased in *Mertk*$^{-/-}$ mice compared to WT, but not in *Tyro3*$^{-/-}$ mice. 6-day MRX-2843 treatment confirmed a trend towards increased CD103 expression in non-leukemic (Fig. 2.8 *D*) and leukemic WT mice (Fig. 2.7 *E*). Subset analysis by scRNA-seq (Fig. 2.8E) and flow cytometry (Fig. 2.7 *F* + Fig. 2.8 *F*) revealed that bone marrow CD8α^{+} DCs contained XCR1^{+} cDC1 DCs, as well as DCs displaying cDC2-like, and pDCs-like characteristics, which may include activated DCs that upregulated various markers (285, 286). MRX-2843 induced CD103 specifically in the cDC1 subset and no increase was observed in cDC1-deficient *Batf3*$^{-/-}$ mice (287) (Fig. 2.7 *E*+*G*+*H*).

These data confirm that MERTK inhibition selectively increases the incidence of CD8α^{+} DCs with increased antigen-presenting capacity.

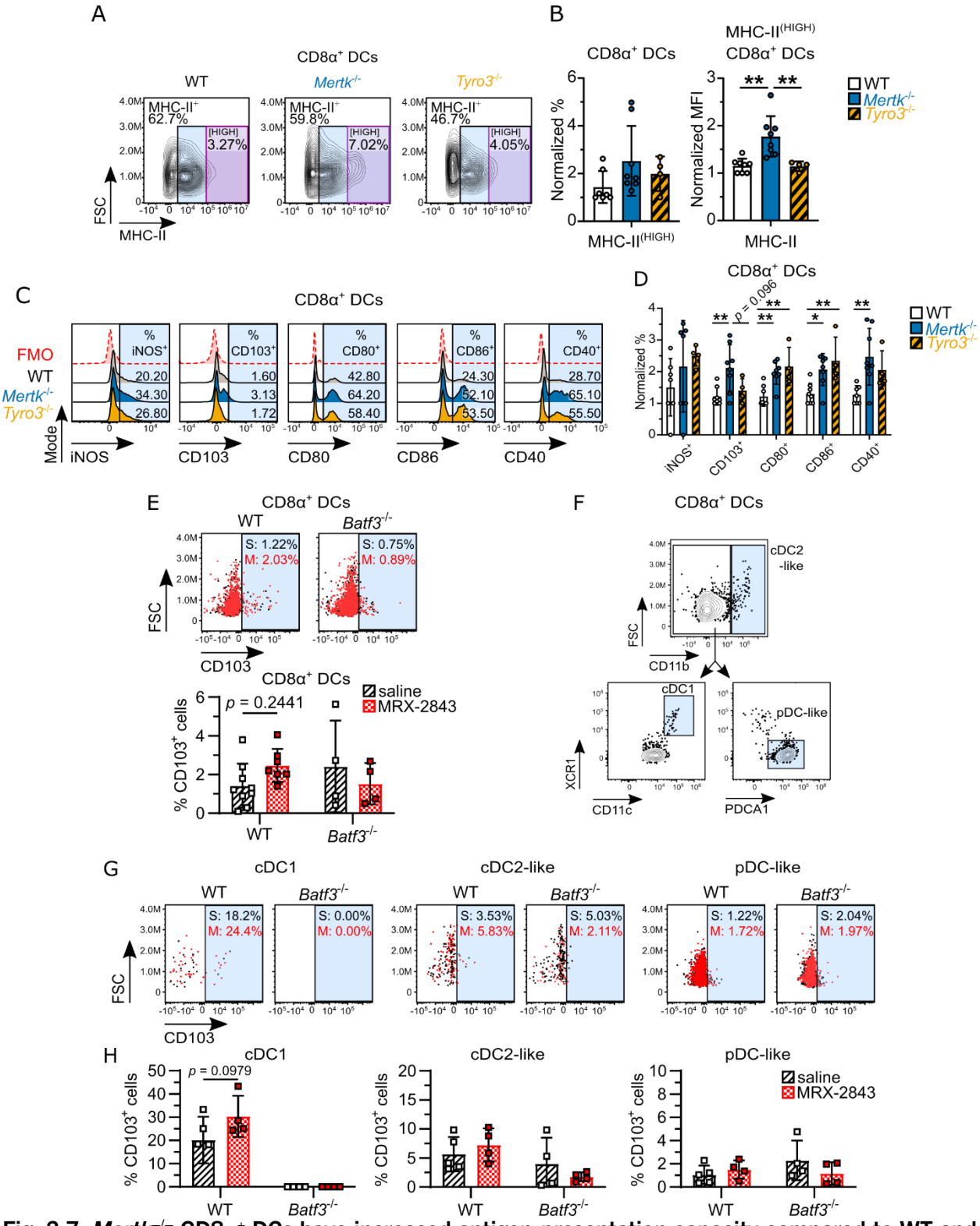

Fig. 2.7: *Mertk*$^{-/-}$ CD8α^{+} DCs have increased antigen-presentation capacity compared to WT and *Tyro3*$^{-/-}$, and *Mertk*$^{-/-}$ or MRX-2843 increases CD103 expression.

A) Representative flow plots showing expression of MHC-II on CD8α^{+} DCs (CD3^{-} CD19^{-} NK1.1^{-} CD11c^{+} CD8α^{+}).

B) LEFT: Frequency of CD8α$^+$ dendritic cells (DCs, CD3$^-$ CD19$^-$ NK1.1$^-$ CD11c$^+$ CD8α$^+$ MHC-II$^+$) expressing high levels of MHC-II (MHC$^{(HIGH)}$) in bone marrow from naïve wild-type (WT), *Mertk*$^{-/-}$ and *Tyro3*$^{-/-}$mice determined by flow cytometry. RIGHT: Median fluorescence intensity of MHC-II on MHC$^{(HIGH)}$ CD8α$^+$ DCs in bone marrow from naïve WT, *Mertk*$^{-/-}$, or *Tyro3*$^{-/-}$ mice determined by flow cytometry. Data from individual cohorts were normalized to account for varying baselines due to potential differences in sample processing on different days. Mean values and standard deviations from 1-3 independent cohorts are shown (n = 4–7, $^{**}P < 0.01$; 1-way ANOVA).

C) Representative flow plots showing expression of activation and maturation markers on CD8α$^+$ DCs. FMO = Fluorescence Minus One control, Mode = normalized to mode.

D) Percentage of CD8α$^+$ DCs (CD3$^-$ CD19$^-$ NK1.1$^-$ CD11c$^+$ CD8α$^+$ MHC-II$^+$) expressing iNOS, CD103, CD80, CD86 and CD40 in bone marrow from naïve WT, *Mertk*$^{-/-}$ and *Tyro3*$^{-/-}$ mice determined by flow cytometry. Data from individual cohorts were normalized to account for varying baselines due to potential differences in sample processing on different days. Mean values and standard deviations from 1-3 independent cohorts are shown (n = 4–7, $^{*}P < 0.05$, $^{**}P < 0.01$; 1-way ANOVA).

E) CD103 expression on CD8α$^+$ DCs (CD3$^-$ CD19$^-$ NK1.1$^-$ CD11c$^+$ CD8α$^+$ MHC-II$^+$) from leukemic WT or *Batf3*$^{-/-}$ mice treated with saline or MRX-2843 for 6 days (treatment initiated at day 12 post B-ALL inoculation). TOP: Representative flow plots. BOTTOM: Quantification showing mean values and standard deviations from 2-3 independent cohorts (n = 4–9, 2-way ANOVA).

F) Gating strategy to identify classical type 1 (cDC1) DCs, classical type 2 (cDC2)-like, and plasmacytoid (pDC)-like DCs among bone marrow CD8α$^+$ DCs.

G) Representative flow plots showing CD103 expression on CD8α$^+$ DC subsets from leukemic WT or *Batf3*$^{-/-}$ mice treated with saline or MRX-2843 for 6 days (treatment initiated at day 12 post B-ALL inoculation). LEFT: cDC1 DCs (CD11b$^-$ CD11c$^{[HIGH]}$ XCR1$^+$), CENTER: cDC2-like DCs (CD11b$^+$), RIGHT: pDC-like DCs (CD11b$^-$ XCR$^-$ PDCA1$^+$).

H) Percentage of CD103 expression on CD8α$^+$ DC subsets from leukemic WT or *Batf3*$^{-/-}$ mice treated with saline or MRX-2843 for 6 days (treatment initiated at day 12 B-ALL post inoculation). LEFT: cDC1 DCs (CD11b$^-$ CD11c$^{[HIGH]}$ XCR1$^+$), CENTER: cDC2-like DCs (CD11b$^+$), RIGHT: pDC-like DCs (CD11b$^-$ XCR$^-$ PDCA1$^+$). Mean values and standard deviations from 2 independent cohorts are shown (n = 6, 2-way ANOVA).

S = saline, MRX / M = MRX-2843

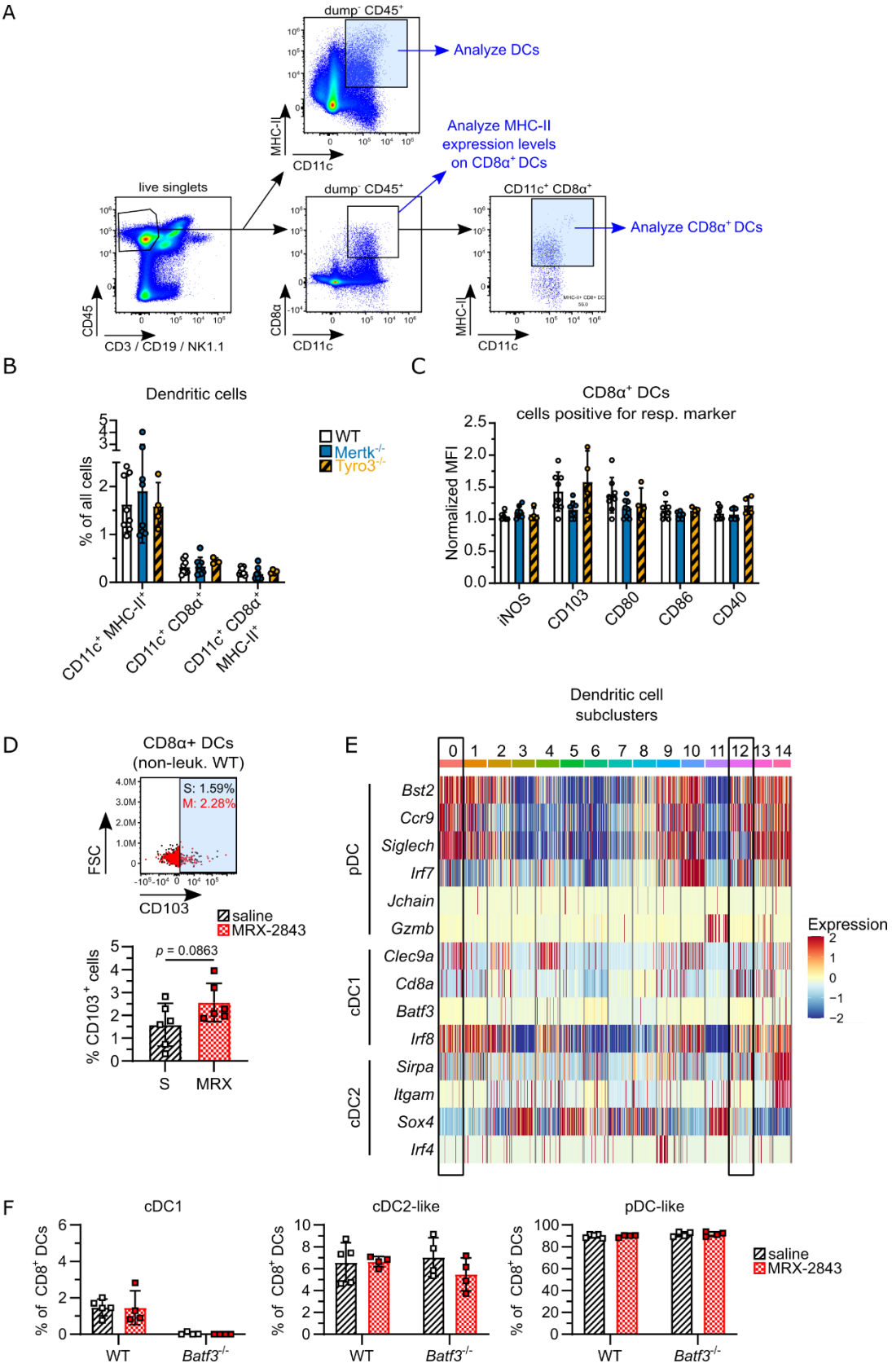

Fig. 2.8: Analysis of bone marrow (CD8α⁺) DCs in WT, *Mertk*$^{-/-}$ *Tyro3*$^{-/-}$, and MRX-2843-treated mice.

A) Gating strategy for analysis of dendritic cells (DCs) and CD8α$^+$ DCs.

B) Frequency of CD11c$^+$ MHC-II$^+$, CD11c$^+$ CD8α$^+$, and CD11c$^+$ CD8α$^+$ MHC-II$^+$ DCs (all gated as CD3$^-$ CD19$^-$ NK1.1$^-$) in bone marrow from naïve wild-type (WT), *Mertk*$^{-/-}$, or *Tyro3*$^{-/-}$mice determined by flow cytometry. Mean values and standard deviations from 1-3 independent cohorts are shown (n = 4–7).

C) Normalized median fluorescence intensity (MFI) of activation and maturation markers on CD8α$^+$ DCs (CD3$^-$ CD19$^-$ NK1.1$^-$ CD11c$^+$ CD8α$^+$ MHC-II$^+$) positive for the respective marker in bone marrow from naïve WT, *Mertk*$^{-/-}$, or *Tyro3*$^{-/-}$mice determined by flow cytometry. Data from individual cohorts were normalized to account for varying baselines due to potential differences in sample processing on different days. Mean values and standard deviations from 1-3 independent cohorts are shown (n = 4–7).

D) CD103 expression on non-leukemic WT CD8α$^+$ DCs (CD3$^-$ CD19$^-$ NK1.1$^-$ CD11c$^+$ CD8α$^+$ MHC-II$^+$) treated with saline (S) or MRX-2843 (MRX, M) for 6 days. TOP: Representative flow plots. BOTTOM: Quantification showing mean values and standard deviations from 2 independent cohorts (n = 6, 1-way ANOVA).).

E) Heatmap showing expression of canonical gene markers for plasmacytoid DCs (pDCs), classical type 1 DCs (cDC1s), and classical type 2 DCs (cDC2s) in the DC subclusters identified in Fig. 3A. Cell number in each subcluster was randomly downsampled to 47 cells to improve comparability.

F) Frequency of cDC1 (CD11b$^-$ CD11c$^{[HIGH]}$ XCR1$^+$), cDC2-like (CD11b$^+$), and pDC-like (CD11b$^-$ XCR$^-$ PDCA1$^+$) DCs among CD8α$^+$ DCs in bone marrow of WT or *Batf3*$^{-/-}$ mice treated with saline or MRX-2843 for 6 days (treatment initiated at day 12 post B-ALL inoculation). Mean values and standard deviations from 2 independent cohorts are shown (n = 6).

2.3.4 Mertk knockout increases CADM1 and Cathepsin E expressing DCs

To investigate how MERTK inhibition promotes antigen-presentation and anti-tumor capacities in DCs, we determined differentially expressed genes (DEGs) in *Cd8*$^+$ DCs from *Mertk*$^{-/-}$ and WT mice and compared expression levels in all four genotypes. The top 2 DEGs *Cadm1* (CADM1) and *Ctse* (Cathepsin E) were significantly upregulated in *Mertk*$^{-/-}$ (*Cd8a*$^+$) DCs compared to all other genotypes (Fig. 2.9 *A*). The cell-adhesion molecule CADM1 (also known as synCAM, NECL2 or TSLC-1) is expressed in murine CD8$^+$ DCs and their human counterparts (288, 289) and binding to the receptor protein CRTAM on T-cells promotes cytokine production (289, 290) and retention

of CD8⁺ T-cells in draining lymph nodes (291). Cathepsin E processes antigens for the MHC-II pathway (292-294) and lack of *Ctse* reduced DC motility, adhesion to the extracellular matrix, and tissue-infiltration in a murine graft-versus-host-disease model (295). Of note, C57Bl/6 mice have naturally reduced Cathepsin E expression levels in DCs compared to other mouse strains, where DCs also have higher antigen processing capability (296). Flow cytometry confirmed significantly increased expression of CADM1 and cathepsin E on (CD8α⁺) DCs from naïve *Mertk*$^{-/-}$ mice compared to WT and *Tyro3*$^{-/-}$ (Fig. 2.9 *B*+*C*). Of note, the increase in CADM1 expression in *Mertk*$^{-/-}$ mice was significantly more pronounced on CD8α⁺ DCs compared to total DCs (Fig. 2.9 *B*). These data identify CADM1 and cathepsin E as potential mediators of improved DC function in *Mertk*$^{-/-}$ mice.

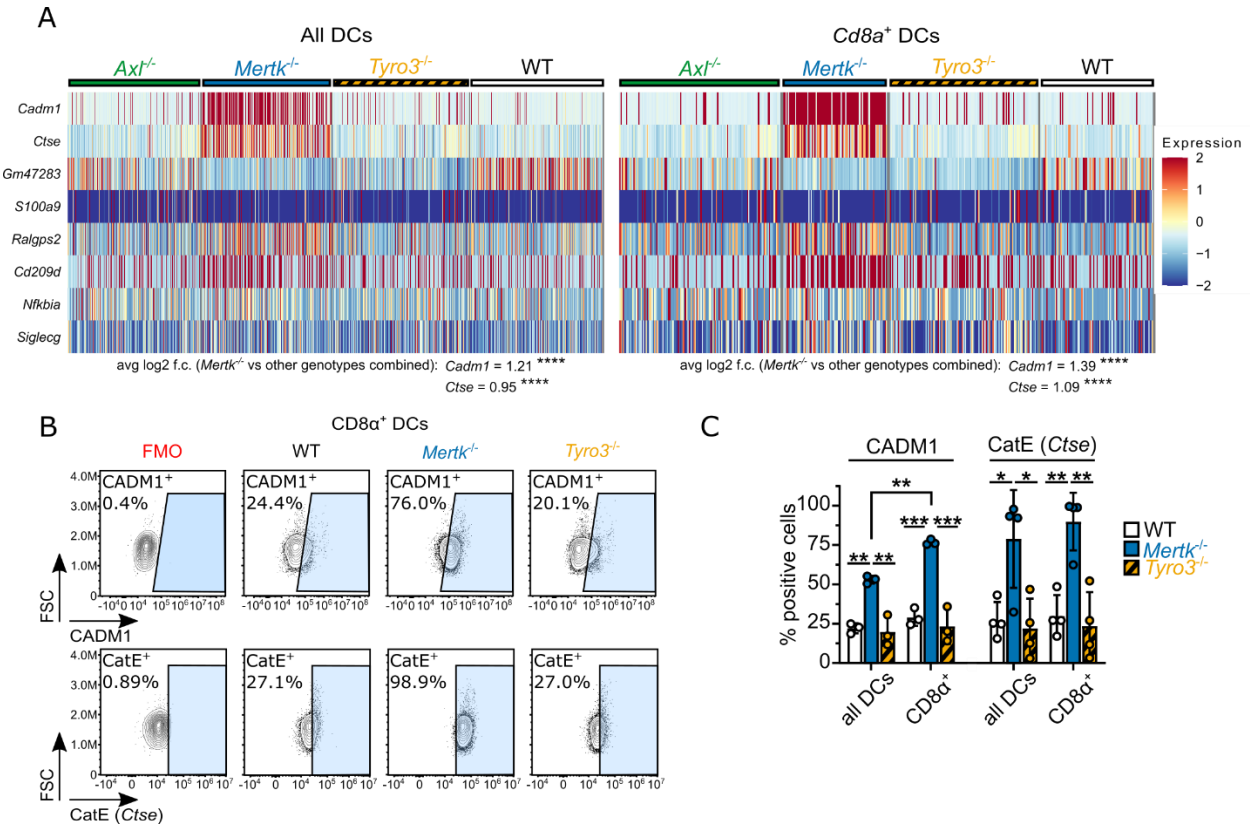

Fig. 2.9: *Mertk* knockout increases CADM1 and Cathepsin E expression by DCs.

A) Heat maps showing top 10 differentially expressed genes in dendritic cells (DCs) from *Mertk*$^{-/-}$ and WT mice compared to expression levels in *Axl*$^{-/-}$ and *Tyro3*$^{-/-}$ mice. DC clusters (#17 + 19) were selected from the combined object shown in Fig 3A. LEFT: Expression levels in all DCs.

RIGHT: Expression levels in *Cd8a*$^{+}$ DCs. avg log2 f.c. = average log2 fold change. **** adjusted $P < 0.0001$; Wilcoxon rank test.

B) Representative flow plots showing expression of CADM1 or Cathepsin E (CatE, *Ctse*) by CD8α^{+} DCs. FMO = Fluorescence Minus One control.

C) Percentage of all DCs (CD3^{-} CD19^{-} NK1.1^{-} CD11c^{+} MHC-II^{+}) or CD8α^{+} DCs (CD3^{-} CD19^{-} NK1.1^{-} CD11c^{+} CD8α^{+} MHC-II^{+}) expressing CADM1 or Cathepsin E (CatE, *Ctse*) in bone marrow from naïve WT, *Mertk*$^{-/-}$ and *Tyro3*$^{-/-}$ mice determined by flow cytometry. Mean values and standard deviations from 2-3 independent cohorts are shown (n = 3–4, $^{**}P < 0.01$, $^{***}P < 0.001$; 1-way ANOVA).

2.3.5 MRX-2843 reduces T-cell exhaustion markers in the leukemia microenvironment.

T, NK and NKT cells play essential roles in anti-cancer immunity and can directly kill tumor cells. To better understand the impact of MERTK inhibition in T-cells, the T/NK/NKT cell clusters from both scRNA-seq studies were subjected to unsupervised clustering, yielding 6 subclusters for the *MRX-2843 study* (Fig. 2.10 *A*) and 13 subclusters for the *KO study* (Fig. 2.10 *D*). These were annotated using canonical markers and genes implicated in activation or exhaustion (Fig. 2.11 *A* + Fig. 2.12 *A*). CD4^{+} and CD8^{+} T-cells decreased during leukemia progression (vehicle-treated mice) and during leukemia regression (MRX-2843-treated), without significant differences between treatment groups (Fig. 2.11 *B*+*C*). Similarly, TAM kinase deletion had no striking effect on CD4^{+} or CD8^{+} T-cell frequencies and this was confirmed by flow cytometry (Fig. 2.12 *B*-*D*). However, treatment with MRX-2843 decreased the percentage of CD8^{+} T-cells expressing high levels of *Tox*, a transcription factor required for induction of T-cell exhaustion (297), and flow cytometry confirmed decreased TOX expression after 6-day treatment (Fig. 2.10 *B*+*C*). *Tox*$^{[HIGH]}$ CD8^{+} T-cells also showed increased expression of other exhaustion markers compared to *Tox*$^{[LOW]}$ (Fig. 2.11 *E*). Thus, MRX-2843 decreases exhaustion markers on CD8^{+} T-cells in the B-ALL microenvironment, consistent with our previous findings demonstrating PD-1 reduction following long-term treatment (206). Interestingly, a trend towards decreased TOX expression

was also observed in *Batf3*$^{-/-}$ mice, suggesting that the CD8^{+} T-cell immune response may remain partially intact in cDC1-deficient mice (Fig. 2.10 *C*).

2.3.6 NK1.1^{+} cells are not required for anti-leukemia immunity in Mertk$^{-/-}$ mice.

TAM kinases suppress NK cell function (201), while MERTK likely has a pro-inflammatory role in NKT cells (166). In the *MRX-2843 study*, both NK and NKT cell subclusters increased in MRX-2843-treated mice compared to vehicle-treated controls (Fig. 2.10 *B*) and a trend towards increased NK cells was observed by flow cytometry (Fig. 2.11 *D*). In contrast, NKT cells were decreased in *Mertk*$^{-/-}$ mice compared to WT (Fig. 2.10 *E*) and a significant decrease was confirmed by flow cytometry in naïve mice (Fig. 2.10 *F*). Similarly, NK cells were only slightly increased in *Mertk*$^{-/-}$ mice compared to WT and *Tyro3*$^{-/-}$ (Fig. 2.10 *E*), while no differences were detected by flow cytometry (Fig. 2.10 *F*). These phenotypic differences could reflect mechanistic differences between pharmacologic and genetic MERTK inhibition and/or differences in the immune microenvironment in early versus late disease. Notably, NKT cells from *Tyro3*$^{-/-}$ mice were not decreased compared to WT, indicating a *Mertk*$^{-/-}$ specific effect. However, *in vivo* depletion experiments revealed no difference in survival in the absence of NK1.1^{+} cells. Thus, NK and NKT cells are not essential for anti-leukemia effects in *Mertk*$^{-/-}$ mice (Fig. 2.10 *G*), although they may play a role in the context of established disease (Fig. 2.10 *B*).

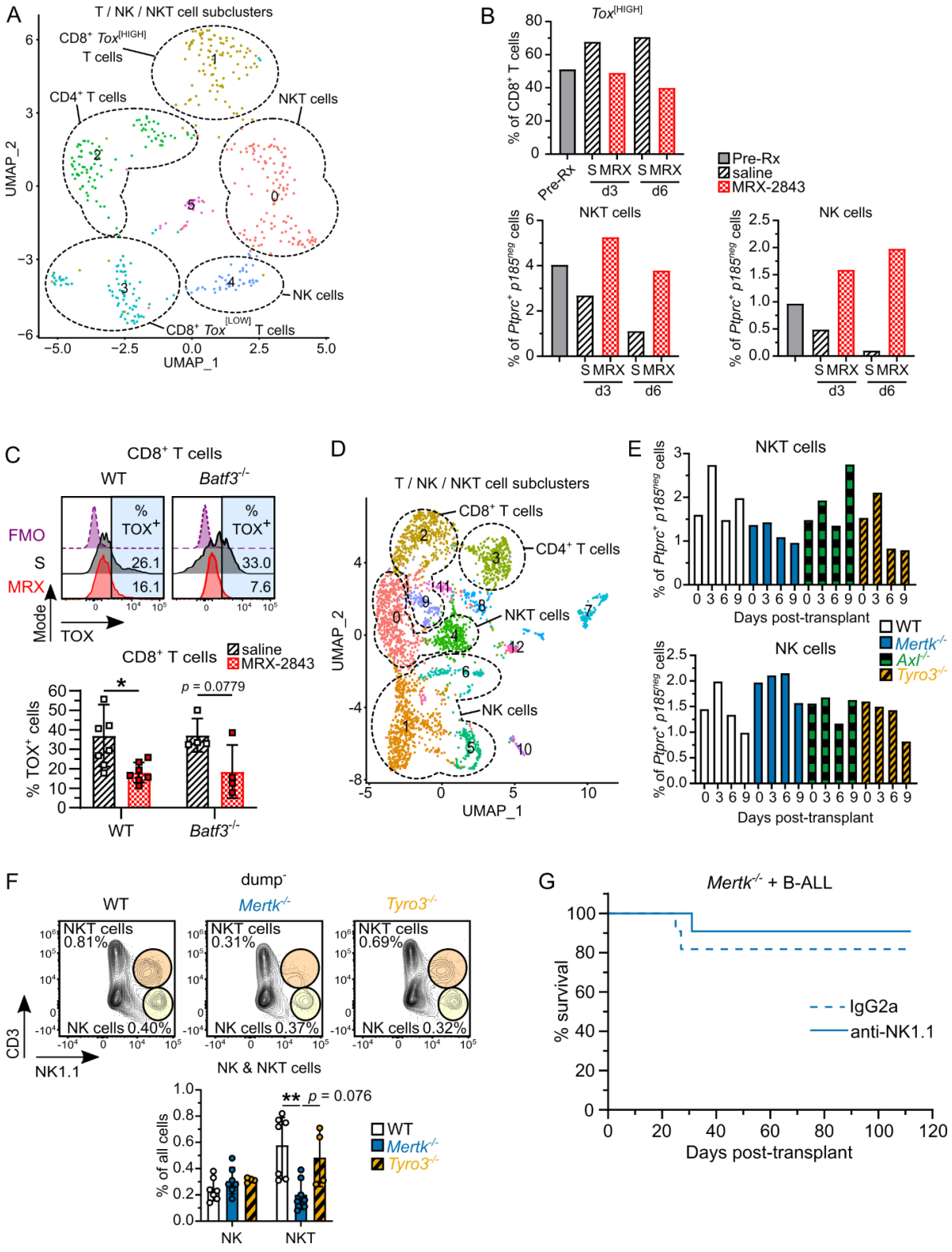

Fig. 2.10: MRX-2843 decreases T-cells expressing exhaustion markers and increases NK and NKT cells, but NK1.1⁺ cells are not required for anti-leukemia immunity in *Mertk*$^{-/-}$ mice.

A) UMAP visualization of unsupervised sub-clustering of cells from the main T/NK/NKT cell cluster from overall data in Fig 1B (*MRX-2843 study*) (476 individual cells combined from all conditions, 71 – 130 cells per condition).

B) Frequency of $CD8^+$ T-cells with high levels of *Tox* expression (top panel) and frequency of NKT and NK among non-leukemia immune cells ($Ptprc^+$ $p185^-$) (bottom panel) in leukemic bone marrow prior to treatment initiation (Pre-Rx) and after 3 or 6 days of treatment with saline (S) or 60 mg/Kg MRX-2843 (MRX).

C) TOX expression by bone marrow $CD8^+$ T-cells ($CD11c^-$ $CD11b^-$ $CD19^-$ $NK1.1^-$ $CD3^+$ $CD4^-$ $CD8^+$) from WT or $Batf3^{-/-}$ mice treated with saline or MRX-2843 for 6 days (treatment initiated at day 12 post B-ALL inoculation). TOP: Representative flow plots. BOTTOM: Quantification showing mean values and standard deviations from 3 independent cohorts (n = 7–8, 2-way ANOVA). FMO = Fluorescence Minus One control, Mode = normalized to mode.

D) UMAP visualization of unsupervised sub-clustering of cells from the main T/NK/NKT cell cluster from overall data in Fig 2D (*KO study*) (3 141 individual cells combined from all conditions, 100 – 305 cells per condition).

E) Frequency of NKT (top panel) and NK (bottom panel) cells among $Ptprc^+$ immune cells in bone marrow from mice without B-ALL (0) and 3, 6 or 9 days after inoculation of leukemia.

F) TOP: Representative flow plots showing frequency of NK or NKT cells. BOTTOM: Frequency of NK and NKT cells in bone marrow from naïve wild-type (WT), $Mertk^{-/-}$, or $Tyro3^{-/-}$mice determined by flow cytometry ($CD11c^-$ $CD11b^-$ $CD19^-$ $CD3^+$ $NK1.1^{+/-}$). Mean values and standard deviations from 1-3 independent cohorts are shown. (n = 4–7, $^{**}P < 0.01$; 1-way ANOVA).

G) Kaplan-Meier survival curves from $Mertk^{-/-}$ mice inoculated with syngeneic GFP-expressing $Arf^{-/-}$ $p185^+$ B-ALL cells and treated with anti-NK1.1 depleting antibody or an isotype control antibody (IgG2a) (n = 11 per group in 2 independent cohorts).

Pre-Rx = prior to treatment initiation, d = day S = saline, MRX = MRX-2843.

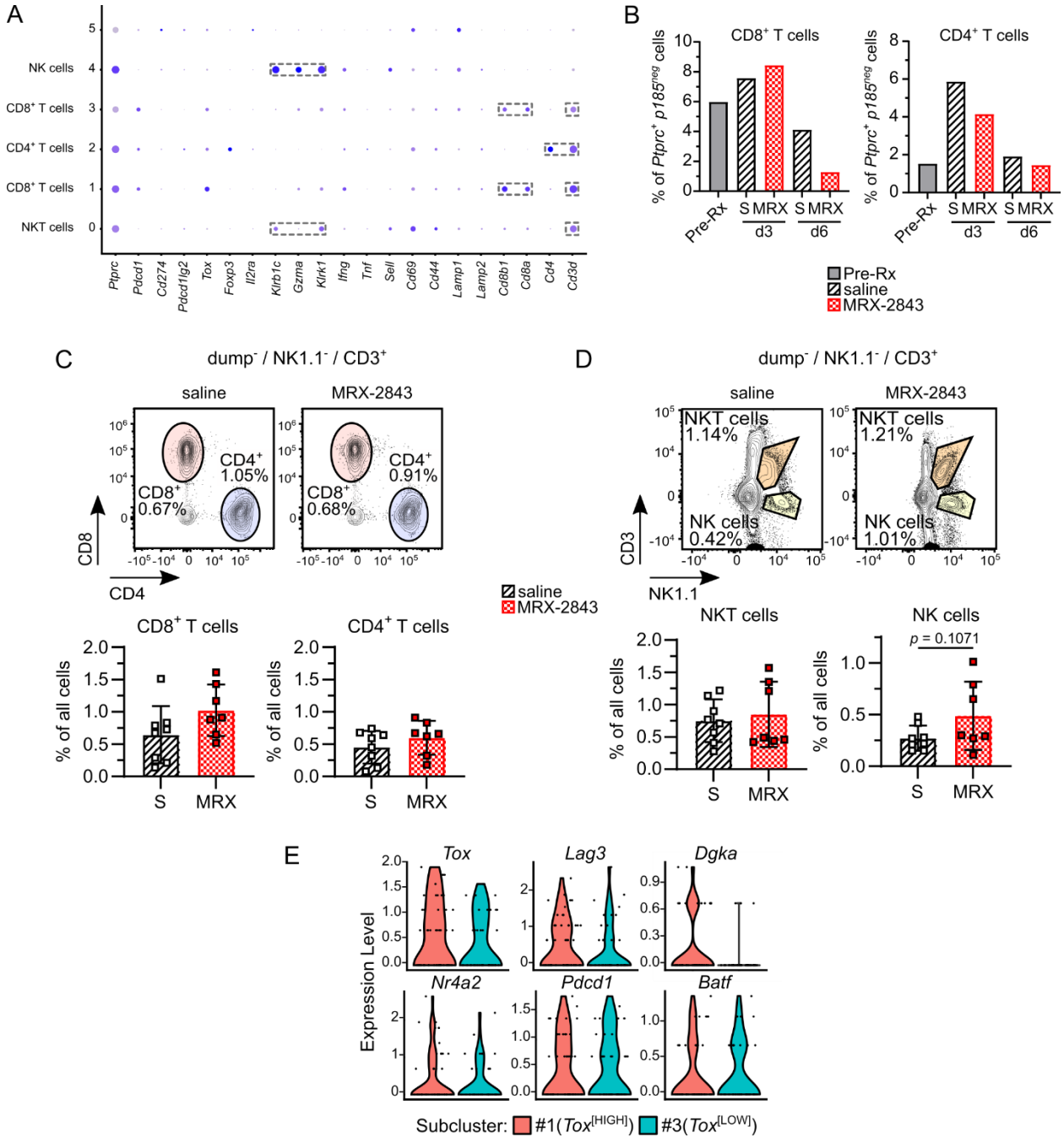

Fig. 2.11: Analysis of T / NK / NKT cells in MRX-2843-treated mice.

A) Dot plot of canonical gene markers used to identify T/NK/NKT cell subclusters from the *MRX-2843 study* (Fig 3A).

B) Frequency of CD8⁺ and CD4⁺ T-cells among non-B-ALL immune cells (*Ptprc*⁺ *p185*⁻) in leukemic bone marrow prior to treatment initiation (Pre-Rx) and after 3 or 6 days of treatment with saline (S) or 60 mg/Kg MRX-2843 (MRX).

C) Frequency of CD8⁺ and CD4⁺ T-cells (CD11c⁻ CD11b⁻ CD19⁻ NK1.1⁻ CD3⁺ CD4⁺/⁻ CD8⁺/⁻) in bone marrow from leukemic WT mice treated with saline or MRX-2843 for 6 days (treatment initiated at day 12 post B-ALL inoculation). TOP: Representative flow plots. BOTTOM: Quantification showing mean values and standard deviations from 3 independent cohorts (*n* = 7–8, 1-way ANOVA).

D) Frequency of NKT (CD11c⁻ CD11b⁻ CD19⁻ NK1.1⁺ CD3⁺) and NK (CD11c⁻ CD11b⁻ CD19⁻ NK1.1⁺ CD3⁻) cells in bone marrow from leukemic WT mice treated with saline or MRX-2843 for 6 days (treatment initiated at day 12 post inoculation). TOP: Representative flow plots. BOTTOM: Quantification showing mean values and standard deviations from 3 independent cohorts (*n* = 7–8, 1-way ANOVA).

E) Expression levels of T-cell exhaustion markers in CD8⁺ T-cell subclusters #1 (*Tox*[HIGH]) and #3 (*Tox*[LOW]) of scRNAseq object shown in Fig. 6A.

Pre-Rx = prior to treatment initiation, d = day S = saline, MRX / M = MRX-2843

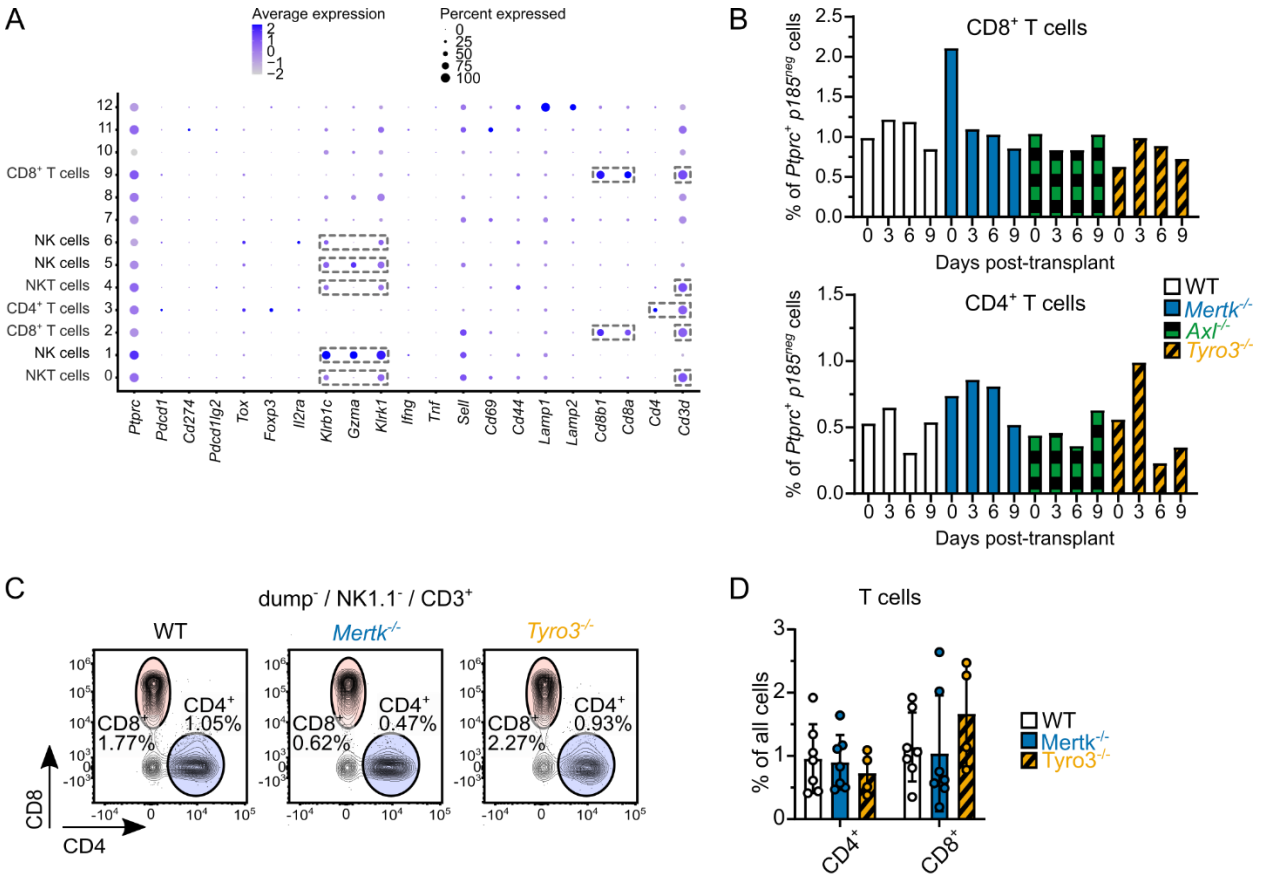

Fig. 2.12: Analysis of CD4⁺ and CD8⁺ T-cells in TAM knockout mice.

A) Dot plot of canonical gene markers used to identify T/NK/NKT cell subclusters from the *MRX-2843 study* (Fig 3A).

B) Frequency of CD8$^+$ and CD4$^+$ T-cells among non-B-ALL immune cells (*Ptprc*$^+$ *p185*$^-$) in leukemic bone marrow prior to treatment initiation (Pre-Rx) and after 3 or 6 days of treatment with saline (S) or 60 mg/Kg MRX-2843 (MRX).

C) Frequency of CD4$^+$ and CD8$^+$ T-cells among non-B-ALL immune cells (*Ptprc*$^+$ *p185*$^-$) in bone marrow from wild-type (WT), *Mertk*$^{-/-}$, or *Tyro3*$^{-/-}$ mice without leukemia (Day 0) and 3, 6 or 9 days after leukemia inoculation.

D) Quantification of CD4$^+$ and CD8$^+$ T-cell frequencies in bone marrow from naïve WT, *Mertk*$^{-/-}$, or *Tyro3*$^{-/-}$ mice. Mean values and standard deviations from 1-3 independent cohorts are shown. (n = 4–7, $^{**}P < 0.01$; 1-way ANOVA).

2.3.7 Combined depletion of CD8α$^+$ DCs and CD8$^+$ T-cells is required to abrogate anti-tumor immunity in Mertk$^{-/-}$ mice.

Depletion studies were conducted to evaluate roles for CD8α$^+$ DCs and CD8$^+$ T-cells in anti-B-ALL immunity in *Mertk*$^{-/-}$ mice. CD8$^+$ T-cells express CD8α/β heterodimers while CD8$^+$ DCs predominantly express CD8α/α homodimers (298, 299) Treatment with anti-CD8α antibody depleted 98% of bone marrow CD8$^+$ T-cells and 93% of CD8α$^+$ DCs (Fig. 2.13 *A*+*B*). In contrast, anti-CD8β antibody depleted 72% of CD8$^+$ T-cells, but did not decrease CD8α$^+$ DCs. Similar effects were observed in spleen samples, where anti-CD8β even increased the frequency of CD8α$^+$ DCs. (Fig. 2.14 *A*). As expected, WT and *Axl*$^{-/-}$ mice quickly succumbed to disease regardless of antibody treatment (Fig. 2.14 *B*+*C*). In *Mertk*$^{-/-}$ mice, selective depletion of CD8$^+$ T-cells reduced protection from B-ALL (median survival = 66.5 days), but survival was still prolonged relative to WT (combined IgG controls = 25 days; IgG1 = 25.5 days) (Fig. 2.13 *C* + Fig. 2.14 *D*). Thus, while a full complement of CD8$^+$ T-cells was required for complete protection, the anti-leukemia response remained partially intact when CD8$^+$T-cells were severely diminished, implicating an innate immune mechanism. Indeed, combined depletion of CD8$^+$ T-cells and CD8α$^+$ DCs in *Mertk*$^{-/-}$ mice led to more complete abrogation of anti-B-ALL immunity (median survival: 38 days). In contrast, selective depletion of CD8$^+$ T-cells was sufficient to completely abrogate

protection in *Tyro3*$^{-/-}$ mice (median survival = 27 days) (Fig. 2.13 *D*). Thus, the mechanisms of anti-leukemia immunity differ in *Mertk* and *Tyro3* knockout mice, with MERTK playing a more prominent role in innate anti-tumor immunity mediated by CD8^{+} DCs. In support of this, WT (CD8^{+}) DCs expressed MERTK but not TYRO3 (Fig. 2.13 *E*+*F*).

2.3.8 Low MERTK expression or high DC gene set expression are associated with improved survival in patients with high-risk pediatric ALL.

To explore the translational relevance of our findings, we analyzed the publicly available and relapse-enriched pediatric TARGET-P2 B-ALL patient dataset using the *Survival Genie* webtool (280). Low levels of *MERTK* were associated with significantly prolonged overall- (Fig. 2.13 *G*) and event-free (Fig. 2.15 *A*) survival in children with high-risk B-ALL. Since only ~30% of pediatric B-ALLs express MERTK (218), it is likely that *MERTK* expression in immune cells plays a considerable role in this observation. Strikingly, when stratified based on expression of a human DC gene set, B-ALL patients with high enrichment scores, suggestive of increased DCs, had significantly improved overall- (Fig. 2.13 *H*) and event-free (Fig. 2.15 *B*) survival. Additionally, high enrichment scores for gene sets representing common markers (300) for CD141^{+} DCs (corresponding to murine cDC1s), CD1c^{+} DCs (murine cDC2s), or human pDCs were associated with significantly improved overall survival (Fig. 2.15 *C*-*D*). These data are consistent with immunosuppressive roles for MERTK in DCs in the leukemia microenvironment and provide important evidence implicating MERTK as a translationally relevant-therapeutic target in pediatric patients with high-risk B-ALL.

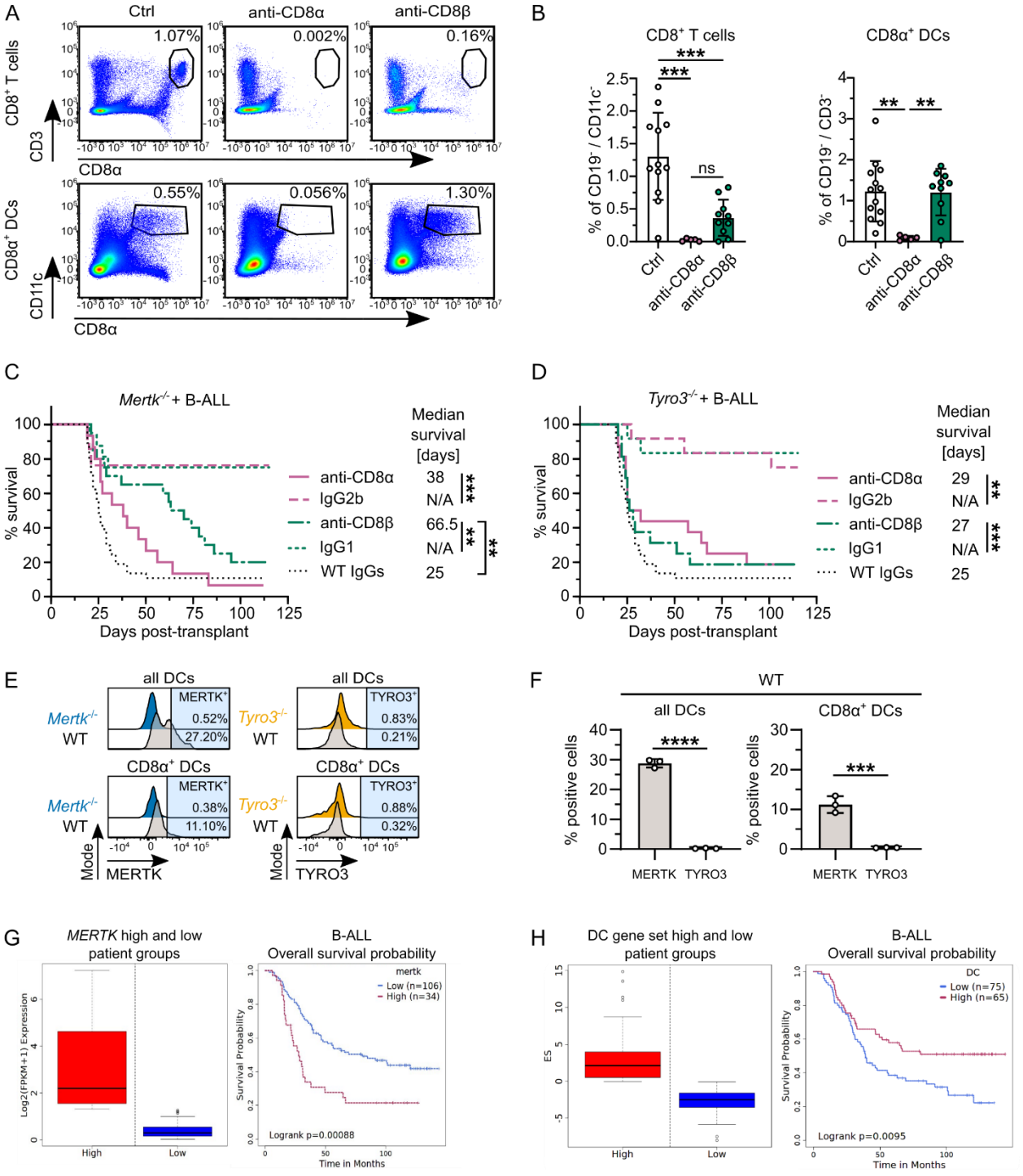

Fig. 2.13: Combined depletion of CD8α⁺ DCs and CD8⁺ T-cells is required to abrogate the survival advantage in *Mertk*$^{-/-}$ mice, while selective depletion of CD8⁺ T-cells is sufficient to block anti-leukemia immunity in *Tyro3*$^{-/-}$ mice.

A) Representative flow plots showing efficiency of $CD8^+$ T-cell depletion (top panels) and CD8α+ dendritic cells (DCs, bottom panels) in bone marrow from *Mertk*$^{-/-}$ mice treated with a single 200 μg dose of anti-CD8α or anti-CD8β depleting or isotype control (Ctrl, IgG1 or IgG2b) antibodies.

B) Percentage of $CD19^-/CD11c^-$ cells expressing CD8 ($CD8^+$ T-cells, left panel) or $CD19^-/CD3^-$ cells expressing CD8α ($CD8\alpha^+$ DCs, right panel) in bone marrow from mice treated with a single dose of control antibody (Ctrl, IgG1 or IgG2b), anti-CD8α depletion antibody, or anti-CD8β depletion antibody administered 3-6 days before sample collection. Data are pooled from wild-type (n=10), *Tyro3*$^{-/-}$ (n=10), *Axl*$^{-/-}$ (n=2) or *Mertk*$^{-/-}$ (n=8) mice. $^{**}P < 0.01$, $^{***}P < 0.001$; 1-way ANOVA.

C,D) Kaplan-Meier survival curves derived from *Mertk*$^{-/-}$ *(C) or Tyro3*$^{-/-}$ *(D)* mice inoculated with syngeneic GFP-expressing *Arf*$^{-/-}$ $p185^+$ B-ALL cells by tail vein injection and treated with 200 ug/mouse anti-CD8α depletion antibody, anti-CD8β depletion antibody or isotype control antibody (IgG1 for CD8α, IgG2b for CD8β) every 7 days starting the day before leukemia inoculation. (n=15-21 per group for *Mertk*$^{-/-}$ and 12-16 per group for *Tyro3*$^{-/-}$*;* 2-3 independent cohorts). Black dotted line = combined survival curve derived from wild-type mice inoculated with B-ALL and treated with IgG1 or IgG2b (see Fig S6B, n = 37 in 2-3 independent cohorts). Statistically significant differences were determined using Mantel-Cox log-rank test. $^{**}P < 0.01$, $^{***}P < 0.001$

E) Representative flow plots showing MERTK or TYRO3 expression on all dendritic cells (DCs) ($CD3^-CD19^-NK1.1^-CD11c^+$ MHC-II^+) and $CD8\alpha^+$ DCs ($CD3^-CD19^-NK1.1^-CD11c^+$ MHC-$II^+CD8\alpha^+$) from naïve bone marrow of WT mice compared to *Mertk*$^{-/-}$ or *Tyro3*$^{-/-}$. Mode = normalized to mode.

F) Percentage of MERTK or TYRO3 positive cells among all DCs (LEFT) and $CD8^+$ DCs (RIGHT) of naïve WT bone marrow (n = 3 in 1 cohort). 2-tailed t test: $^{***}P < 0.001$, $^{****}P < 0.0001$.

G) LEFT: Distribution of pediatric B-ALL patient groups with high (red) and low (blue) *MERTK* gene expression in the TARGET-ALL-P2-Bcell data set. Groups were defined using the Cutp (cutpoint) method within the *Survival Genie* webtool. RIGHT: Overall survival probability for *MERTK* high vs low patient groups in the TARGET-ALL-P2-Bcell data set.

H) LEFT: Distribution of pediatric B-ALL patient groups with high (red) or low (blue) enrichment score (ES) for a dendritic cell (DC) gene set in the TARGET-ALL-P2-Bcell data set. Groups were defined using the Cutp (cutpoint) method within the *Survival Genie* webtool. RIGHT: Overall survival probability for DC gene set high vs low patient groups in the TARGET-ALL-P2-Bcell data set.

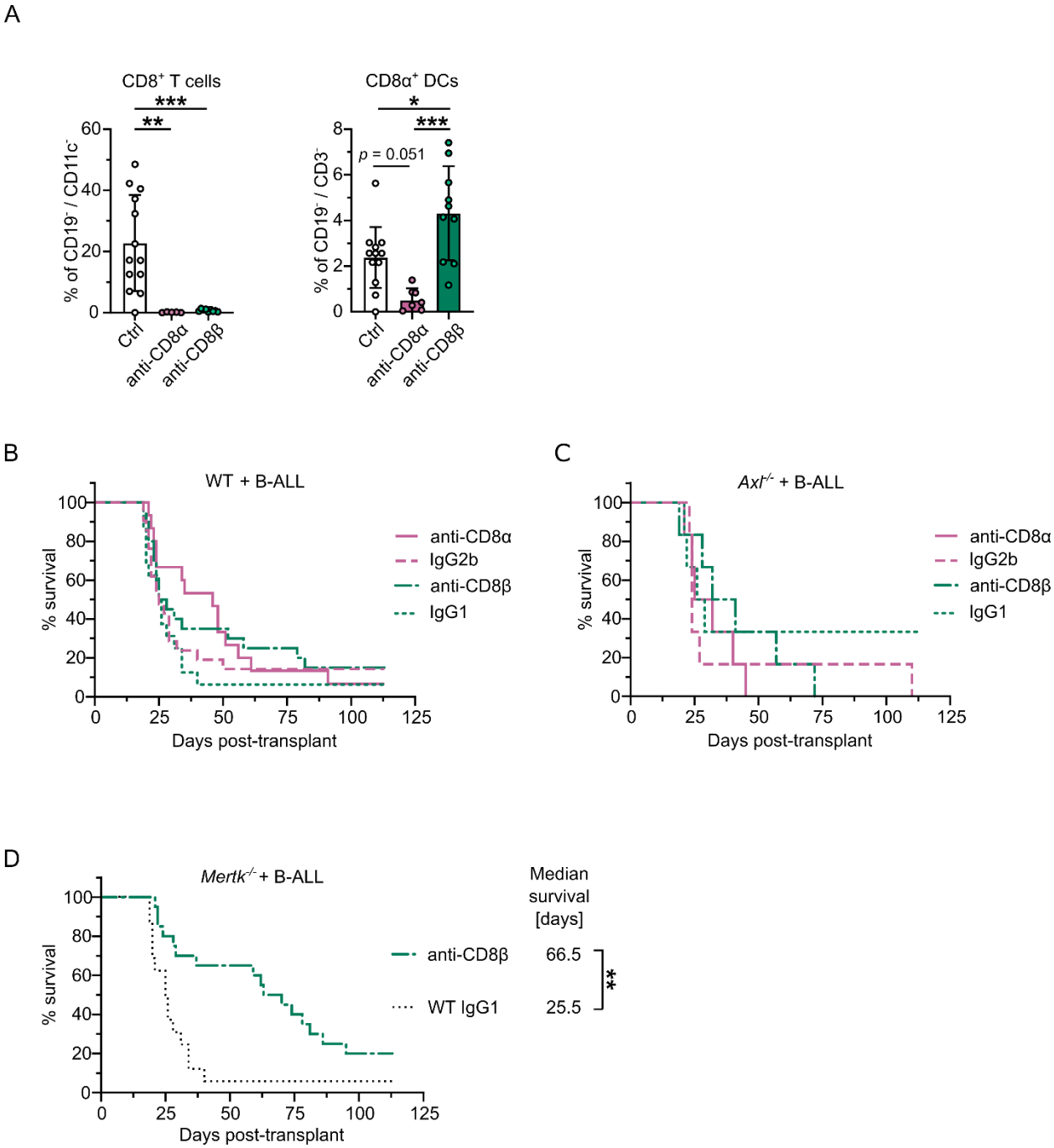

Fig. 2.14: Anti-CD8α antibody depletes CD8⁺ T-cells and DCs in the spleen, while anti-CD8β antibody depletes CD8⁺ T-cells more selectively.

A) Percentages of CD8⁺ T-cells among all CD19⁻/CD11c⁻ cells (LEFT) and CD8α⁺ dendritic cells (DCs) amongst all CD19⁻/CD3⁻ cells (RIGHT) in spleens from mice treated with a single dose of control antibody (Ctrl, IgG1 or IgG2b), anti-CD8α depletion antibody, or anti-CD8β depletion antibody administered 3-6 days before collection of samples. Data were pooled from wild-type (*WT, n*=10*), Tyro3*$^{-/-}$ *(n*=10*), Axl*$^{-/-}$ *(n*=2*)* and *Mertk*$^{-/-}$ *(n=8)* mice. $^{**}P < 0.05$, $^{**}P < 0.01$, $^{***}P < 0.001$; 1-way ANOVA.

B-D) Kaplan-Meier survival curves derived from WT (panel B, *n*=15-21 per group in 2-3 independent cohorts), *Axl*$^{-/-}$ (panel C, n=6 per group in 1 cohort), or *Mertk*$^{-/-}$ (panel D, n=18 per group in 2 independent cohorts) mice inoculated with syngeneic GFP-expressing *Arf*$^{-/-}$ p185^{+} B-ALL cells by tail vein injection and treated with 200 ug/mouse anti-CD8α or anti-CD8β depletion antibody or isotype control antibody (IgG1 for CD8α, IgG2b for CD8β) every 7 days starting the day before leukemia inoculation. Statistically significant differences were determined using Mantel-Cox log-rank test. *$P < 0.05$

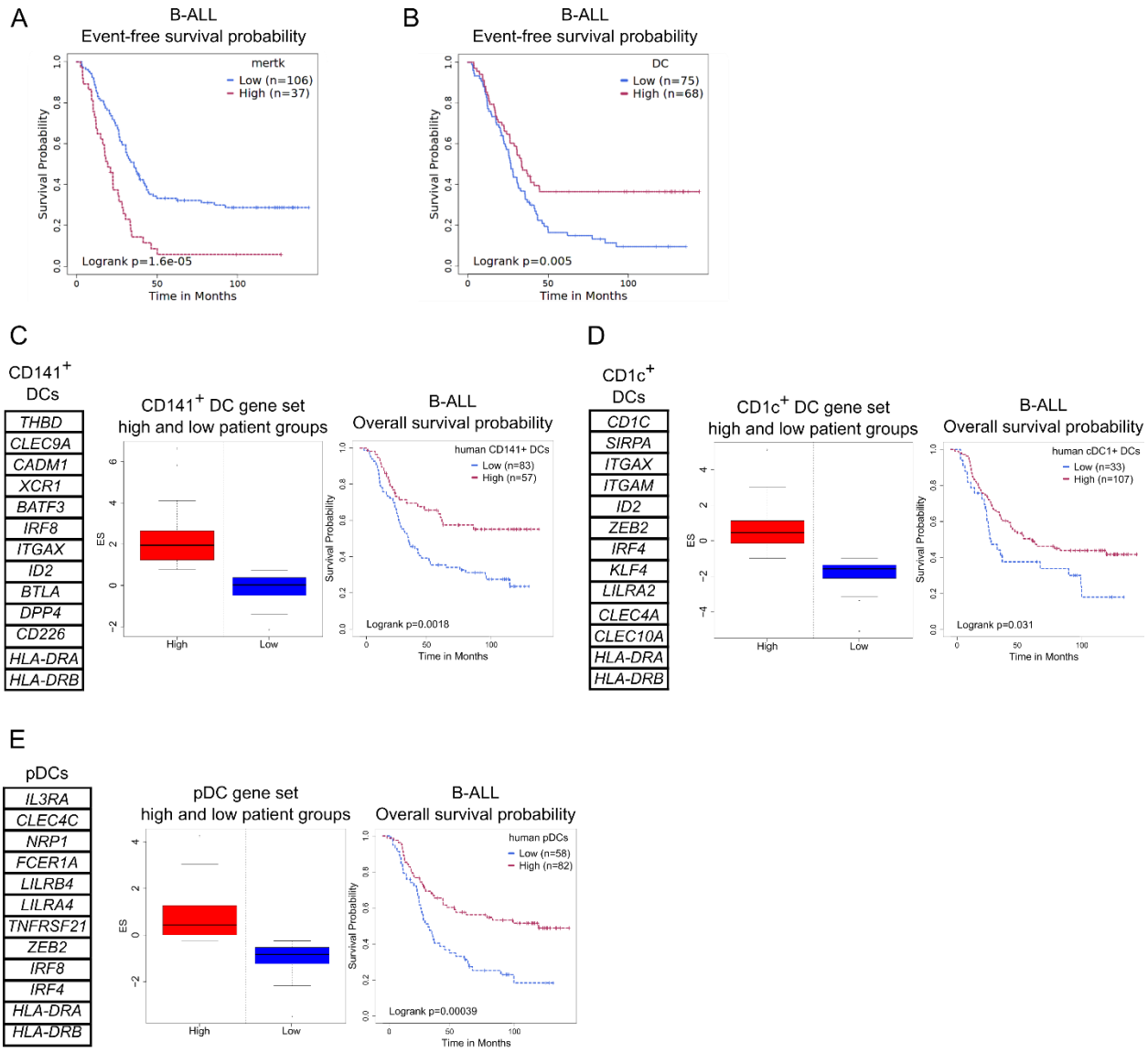

Fig. 2.15: Low level expression of *MERTK* or high-level expression of a human DC gene set are associated with improved survival in patients with high-risk pediatric ALL.

A) Probability of event-free survival in patients with B-ALL expressing high versus low levels of *MERTK* from the TARGET-ALL-P2-Bcell data set.

B) Probability of event-free survival in patients with B-ALL expressing high versus low levels of a DC gene set from the TARGET-ALL-P2-Bcell data set.

C) LEFT: $CD141^+$ DC gene set. CENTER: Distribution of pediatric B-ALL patient groups with high (red) or low (blue) ES for $CD141^+$ DC gene set in the TARGET-ALL-P2-Bcell data set. RIGHT: Overall survival probability for $CD141^+$ DC gene set high vs low patient groups in the same data set.

2.4 Discussion

We previously identified MERTK as a potential therapeutic target in the immune microenvironment in an aggressive B-ALL model (206). Here, we identify a $CD8^+$ DC – T-cell axis driving the anti-leukemia immune response. MERTK inhibition increased the incidence of bone marrow $CD8\alpha^+$ DCs with elevated antigen-presenting capacity and CD103 expression. Murine $CD8\alpha^+$ and/or $CD103^+$ DCs play crucial roles in anti-tumor immunity, including recruitment and priming of $CD8^+$ T-cells, cross-presentation of tumor antigens, and initiation of proinflammatory type 1 T helper cell (T_H1) responses (264, 265). $CD103^+$ DCs have also been associated with sensitivity to checkpoint inhibitors in cancer patients and mouse models (265, 301). Combined depletion of $CD8\alpha^+$ DCs and $CD8^+$ T-cells was required to abrogate protection against B-ALL in *Mertk*$^{-/-}$ mice, confirming that the immune response is at least partially driven by $CD8\alpha^+$ DCs. Increased CD103 expression was specific to cDC1s, but $CD8\alpha^+$ DCs also included cDC2-like and pDC-like subsets and all subsets might contribute to anti-B-ALL immunity. The exact dynamics of reduced exhaustion markers and T-cell activation in the bone marrow and other organs will be elucidated in future studies. Additional studies are also needed to elucidate how $CD8\alpha^+$ DCs contribute to tumor control independently of $CD8^+$ T-cells. While $NK1.1^+$ cells were not strictly required for anti-tumor immunity in *Mertk*$^{-/-}$ mice, they may play a role in the partial immunity mediated by $CD8\alpha^+$ DCs in the absence of $CD8^+$ T-cells. Consistent with this possibility, treatment with MRX-2843 increased NK and NKT cells in leukemic bone marrow. *"Th1 pathway"* and *Ifng* gene regulatory networks were also upregulated in *Cd8a*$^+$ DCs that were differentially increased with MERTK inhibition. Thus, $CD8\alpha^+$ DCs may also promote tumor control by inducing $CD4^+$ T_H1 T-cell responses and/or production of tumoricidal cytokines.

In a previous study using melanoma and brain cancer models, anti-tumor immunity in *Mertk*$^{-/-}$ mice was not solely mediated by MERTK ablation, but required additional genetic changes introduced during generation of the knockout line (302). The same *Mertk*$^{-/-}$ mice were used for

the studies reported here; however, both here and in previous studies (206) *Mertk*$^{-/-}$ and MRX-2843 had similar effects in our model. Additionally, MRX-2843 did not increase survival in immune-deficient mice inoculated with B-ALL (206), so direct leukemia cell killing does not contribute to therapeutic activity. Together these data provide strong evidence that MERTK inhibition is sufficient to elicit anti-tumor immunity in our current B-ALL model.

Tyro3 knockout also protected mice from B-ALL, implicating TYRO3 as a novel immunotherapeutic target in acute leukemia. In contrast to *Mertk*$^{-/-}$, host *Tyro3* deletion did not increase CD8α^{+} CD103^{+} DCs or CD8α^{+} DC antigen-presenting potential and CD8α^{+} DCs did not provide protection from leukemia in the absence of CD8^{+} T cells in *Tyro3*$^{-/-}$mice. Thus, anti-leukemia immunity was less dependent on CD8α^{+} DCs in *Tyro3*$^{-/-}$ mice. These data indicate a differential role for MERTK in CD8α^{+} DCs in the leukemia microenvironment. Other publications support a selective role for MERTK as an immunosuppressive regulator of DCs. Murine bone marrow-derived DCs only minimally express TYRO3 and upregulate MERTK in an immunosuppressive context (118), as do human monocytic DCs (209). While additional studies are needed to investigate the anti-B-ALL immune mechanism in *Tyro3*$^{-/-}$ mice, the differential mechanisms demonstrated here provide rationale for development of dual MERTK/TYRO3-targeted therapies with potential for combinatory effects.

Axl$^{-/-}$ did not protect against B-ALL in our model. These data contrast with previous studies demonstrating increased survival in mice with selective *Axl* knockout in cells expressing the colony stimulating factor 1 receptor (*Csf1r*$^{+}$, including monocytes, macrophages and DCs) inoculated with *Arf*$^{-/-}$ p185(*BCR-ABL*)$^{+}$ B-ALL cells (247). It is possible that *Axl* ablation in *Csf1r*-negative cells provides immunosuppressive effects that counteract the functions of *Csf1r*$^{+}$ *Axl*$^{-/-}$ cells, ultimately inhibiting the anti-B-ALL immune response in mice with ubiquitous *Axl* knock-down. The involvement of individual TAM family members may also depend on the ligands that tumor cells release or induce in the microenvironment and their affinity for each TAM kinase

(116). Additionally, continuous TAM kinase deletion might impact immune cell development, and the consequences might differ between ubiquitous- and *Csf1r*$^{+}$-specific *Axl* deletion. Additional studies are needed to better understand the differences between these two models. These data also highlight the importance of understanding the roles for individual TAM kinases in different cell types and disease contexts to determine their relevance as therapeutic targets.

In summary, the data shown here demonstrate critical roles for MERTK and TYRO3 as mediators of immunosuppression in the leukemia microenvironment in a B-ALL model and reveal a selective role for MERTK as a suppressor of antigen presenting CD8α^{+} DCs, which are critical mediators of efficient tumor antigen cross-presentation, anti-tumor immune activation, and sensitivity to immune checkpoint inhibitors. The associations between *MERTK* expression or DC cell enrichment in leukemia samples and survival outcomes in pediatric patients with high-risk B-ALL support the translational relevance of our findings and provide rationale for clinical development of MERTK inhibitors for treatment of pediatric leukemia. MRX-2843 is well-tolerated and therapeutically effective in murine leukemia models (206, 283) and is currently in phase-I/Ib clinical trials, including a trial in adolescent and adult patients with acute leukemia (NCT03510104, NCT04762199, NCT04872478). These studies may also inform co-development of biomarkers of sensitivity to MERTK versus TYRO3 and/or AXL inhibition, which will be essential for optimal application of MRX-2843 and other TAM kinase inhibitors as immuno-oncology agents.

Chapter 3. TAM RTKs have differential roles in suppressing anti-AML immunity depending on disease model

3.1 Introduction

AML is a heterogenous disease and various factors differ between subtypes, including genetic and epigenetic background, morphology and immunophenotype (13). While ALL is the most common leukemia in children, AML becomes more prevalent with age and is the most common form in adult patients (12). Unfortunately, AML survival outcomes remain poor - particularly in older individuals - and only about a quarter of AML patients survive longer than 5 years post-diagnosis., indicating a need for novel therapeutic strategies.

Immunotherapies may provide such novel treatment options, as suggested by successful graft-versus-leukemia responses following allogeneic stem cell transplantation in some patients (37). Antibody-based immunotherapies, including CAR-T cells and bispecific T cell engagers are in development, but the limit option of targets on AML cells poses a risk for adverse effects through ablation of non-malignant myeloid and/or hematopoietic cells (13). Moreover, clinical trials of immune checkpoint inhibitors revealed only limited efficacy in AML, even though patients might benefit from combining immune checkpoint inhibitors with other treatment modalities, such as chemotherapies, DNA hypomethylating agents, or targeted agents.

Given our findings that MERTK and TYRO3 are potential immunotherapeutic targets in B-ALL, we assessed the roles of TAM RTKs in the anti-AML immune response, using syngeneic models in wild-type (WT) and knockout mice.

3.2 Material and Methods

3.2.1 Cell culture

C1498 cells were cultured in RPMI 1640 medium (Gibco™ #11835030) with 10% FBS (Atlanta Biologicals #S11550), 1x penicillin/streptomycin (Gibco™ #15140122), and 0.55 µM 2-Mercaptoethanol (Gibco™ #21985023).

3.2.2 AML mouse models

Mertk$^{-/-}$ (B6;129-*Mertk*^{tm1Grl}/J) (152), *Axl*$^{-/-}$ and *Tyro3*$^{-/-}$ (277) mice were backcrossed with WT C57BL/6J mice (Jackson Laboratory #000664) for at least 10 generations (206). Male and female mice were used for experiments at 8-16 weeks of age (180).

C1498 cells were injected into the tail vain at a concentration of 5,000 cells / mouse.

A42-2A cells had previously been isolated from leukemic MLL-AF9 transgenic mouse (303), serial passaged several times in C57Bl/6 WT mice, and frozen for cryopreservation. Frozen cells were thawed immediately before tail vein injections at a concentration of 2×10^6 cells / mouse.

Mice with advanced leukemia (> 20% weight loss, tachypnea, hind-limb paralysis, minimal activity) were euthanized. Animal studies were conducted in accordance with relevant regulatory standards and approved by the Emory University IACUC (PROTO201700276).

3.2.3 Statistics

Statistical analyses were performed using GraphPad Prism software (version 9.3.1). Differences in survival were determined by log-rank test.) and P values < 0.05 were considered significant.

3.3 Results

3.3.1 Host ablation of all three TAM RTKs prolongs survival in MML-AF9 AML model, while only Mertk ablation *provides immunity in a second AML model.*

To determine the role of individual TAM RTKs in anti-AML immunity, we monitored survival of WT, *Tyro3*$^{-/-}$, *Axl*$^{-/-}$ or *Mertk*$^{-/-}$ mice in two different syngeneic models: C1498, or A42-2A. The latter is driven by expression of the *MLL-AF9* fusion gene, and leukemia patients with *MLL* (*KMT2A*) fusions often respond poorly to the current standard chemotherapies (20). WT mice succumbed quickly to disease in the first model (median survival = 28 days), whereas the A42-2A model only reached a penetrance of about 50% in these mice (Fig. 3.1 *A*+*B*). Similar to previous results (248), *Mertk*$^{-/-}$ let to significantly prolonged survival in both models, indicating that MERTK deletion in the TME also promotes anti-leukemia immunity against AML in addition to B-ALL. Interestingly, we found differential roles for TYRO3 and AXL in the anti-AML immunity depending on the model: While deletion of either RTK did not affect leukemogenesis in the C1498 model, both knockout mice were largely protected against AML in the A24-2A model.

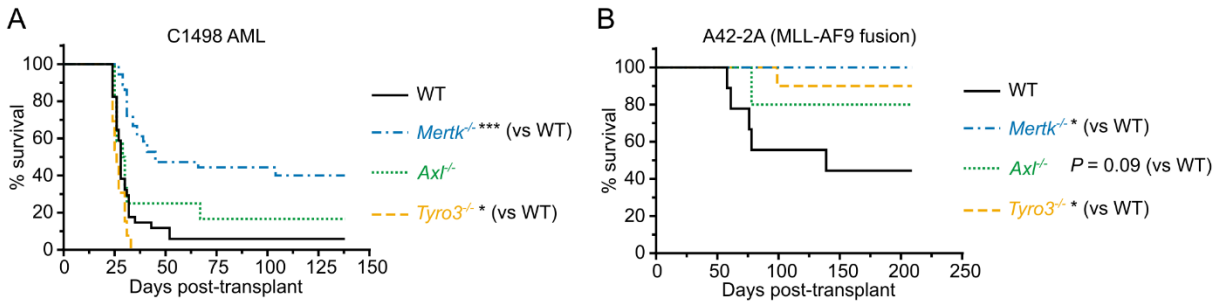

Fig. 3.1: Host ablation of all three TAM RTKs prolongs survival in MML-AF9 AML model, while only *Mertk* ablation provides immunity in a second AML model.

A) Kaplan-Meier survival curves derived from wild-type (WT), *Tyro3*$^{-/-}$, *Axl*$^{-/-}$ or *Mertk*$^{-/-}$mice inoculated with syngeneic C1498 AML cells by tail vein injection. Statistically significant differences were determined using Mantel-Cox log-rank test (WT *n*=22, *Tyro3*$^{-/-}$ *n=13, Axl*$^{-/-}$ *n=10, Mertk*$^{-/-}$ *n=23* in 1-2 independent cohorts, **P* < 0.05, ****P* < 0.0005).

B) Kaplan-Meier survival curves derived from WT, *Tyro3*$^{-/-}$, *Axl*$^{-/-}$ or *Mertk*$^{-/-}$mice inoculated with syngeneic A42-2A AML cells by tail vein injection. Statistically significant differences were determined using Mantel-Cox log-rank test (WT *n*=9, *Tyro3*$^{-/-}$ *n=10, Axl*$^{-/-}$ *n=10, Mertk*$^{-/-}$ *n=9* in 1 cohort, **P* < 0.05).

3.4 Discussion

Our results implicate MERTK as an immunotherapeutic target - not only in ALL - but also in AML. Moreover, they suggest that TYRO3 and AXL may represent targets in AML depending on the specific disease subtype, or cancer cell properties. Of note, previous studies in melanoma and brain cancer models found that the anti-tumor immune effects in *Mertk*$^{-/-}$ mice were not entirely mediated by MERTK deletion, but required additional genetic changes introduced during generation of the knockout line (302). The same *Mertk*$^{-/-}$ mice were used here, and the *Tyro3*$^{-/-}$ and *Axl*$^{-/-}$ mice were generated with similar methods. Hence, in future studies we will test whether these results repeat in knockout mice generated with more modern and "cleaner" methods, or in WT mice using TAM RTK inhibitors. Moreover, we only achieved about 50% penetrance in WT mice in the 42-2A model, warranting additional repeats and optimization. Nonetheless, the results presented here indicate a strong context-specificity regarding the role of individual TAM RTKs in suppressing anti-leukemia immunity. Their relevance as an immunotherapeutic target may be determined by several factors, including properties inherent to the leukemia cells, and the specific conditions they induce in the TME. TAM ligands have varying affinity for the individual RTKs (112, 116, 117, 119-125) and investigating their production by leukemias cells or cells of the TME may provide an initial insight into the mechanisms that determine the involvement of each kinase. Better understanding the role of individual TAM RTKs in different disease contexts will be essential for the development of TAM-targeting agents for the treatment of acute leukemia.

Chapter 4: Conclusions and closing remarks

4.1 Summary

Despite significant improvements in treatment outcomes, acute leukemia remains a leading cause of cancer-related death in pediatric patients, with particularly poor prognosis in children with relapsed disease. Additionally, survival outcomes strongly decrease with age and many elderly patients do not tolerate the current cytotoxic treatment options. Anti-leukemia immunotherapies may provide new and less toxic treatment options with the potential to improve outcomes, but more research is needed to identify targets and understand the underlying mechanisms.

Expanding on previous results by our laboratory, we here investigated the mechanism by which MERTK inhibition provides immunity in an aggressive *Arf*$^{-/-}$ BCR-ABL^{+} B-ALL model. Providing evidence for a DC – T cell axis, we found that that MERTK inhibition increased DC antigen-presentation capacity and reduced expression of CD8^{+} T cell exhaustion markers. Indeed, anti-leukemia immunity in *Mertk*$^{-/-}$ mice depended on CD8α^{+} DCs and CD8^{+} T-cells.

While host *Axl* deletion did not affect leukemogenesis, *Tyro3*$^{-/-}$ mice were also protected against B-ALL, albeit through a separate mechanism than MERTK inhibition. These data implicate TYRO3 as an additional immunotherapeutic target in acute leukemia. Moreover, host knockout of all three TAM RTKs prolonged survival in an *MML-AF9* AML model, while only *Mertk* ablation provided immunity in a second AML model.

In summary, this work provides rational for the development of TAM RTK-targeted anti-leukemia immunotherapies and highlights the importance of understanding the context-dependent roles of individual TAM RTKs in anti-leukemia immunity.

4.2 Differential roles for TAM RTKs in the acute leukemia microenvironment

Our data indicate a high context-specificity for the roles of individual TAM RTKs in acute leukemia immunity and this may have important implications for the clinical development of TAM inhibitors. We observed a selective survival advantage only with *Mertk*$^{-/-}$ in the C1498 AML model, while knockout of all three TAM RTKs prolonged survival in the A42-2A model (Fig. 3.1). Moreover, *Axl*$^{-/-}$ did not protect against B-ALL in our model, contrasting a previous publication showing that deletion of *Axl* in CSF1R^{+} cells promotes survival in AML and ALL models (247). As discussed above (chapter 2.4), it is possible that the anti-leukemia immune effects of inhibiting *Axl* specifically in CSF1R^{+} cells are counteracted by immunosuppressive effects stemming from *Axl* deletion in other cell types in our ubiquitous knockout mice. Hence, the relevance of an individual TAM RTK as immunotherapeutic target may to some extend depend on the immune cell types that are engaged in the tumor microenvironment and the specific roles that the kinase plays in these. Understanding these biological roles in different disease contexts will be critical to evaluate individual TAM RTKs as therapeutic targets in patients.

Our findings suggest that MERTK inhibition drives the anti-B-ALL immune response at least partially by increasing antigen-presentation and anti-tumor capabilities of CD8^{+} DCs. Several previous studies support an immunosuppressive MERTK role in DCs. For example, *Mertk*$^{-/-}$ increased the frequency and activation of pancreatic CD8α^{+} DCs in a murine diabetes model and increased *in vivo* CD4^{+} T cell proliferation and IFN-γ production in a DC-dependent manner (184). Similarly, pretreatment of *ex vivo*-matured DCs with a MERTK-blocking antibody increased naïve CD4^{+} T cell proliferation and cytokine production in a mixed lymphocyte reaction experiment (207). *Mertk*$^{-/-}$ mice were also more efficient than wild-type mice at activating OT-I T cells *in vivo* following intranasal injection of OVA protein (304). In human monocytic DCs, the TAM ligand PROS1 increased LPS-induced production of the immunosuppressive cytokine IL-10, particularly in MERTK$^{[HIGH]}$ DCs, and this was overcome by treatment with a MERTK inhibitor

(209). Our work also indicates that MERTK selectively regulates CD103 expression by DCs in the leukemia microenvironment and other publications support this notion: $CD103^{+}$ DCs from a murine melanoma model were MERTK negative, while the kinase was expressed on $CD103^{-}$ APCs (including DCs and macrophages) (305). Moreover, a recent study described a MERTK-expressing and -dependent DC population in murine lungs with intermediate CD103 expression, that is increased during early post-natal days (304). These $CD103^{[INT]}$ DCs were related to $CD103^{[HIGH]}$ cDC1s but were characterized by a tolerogenic and immunosuppressive gene signature and possessed inferior cross-presentation capacities compared to cDC1s.

In contrast to host *Mertk* deletion or MRX-2843 treatment, *Tyro3*$^{-/-}$ did not increase $CD8\alpha^{+}$ $CD103^{+}$ DCs or $CD8\alpha^{+}$ DC antigen-presenting potential. Moreover, the anti-B-ALL immune response was less dependent on $CD8\alpha^{+}$ DCs in *Tyro3*$^{-/-}$ mice compared to *Mertk*$^{-/-}$ mice. These data indicate a selective role for MERTK in $CD8\alpha^{+}$ DCs in the leukemia microenvironment. In support of this, freshly isolated ($CD8\alpha^{+}$) DCs from wild-type bone marrow expressed MERTK but not TYRO3, and the same had previously been reported for splenic DCs (170). Likewise, MERTK was shown to be the only TAM RTK expressed by *ex* vivo-differentiated human monocytic DCs (209) and expression is increased following treatment with immunosuppressive glucocorticoids, such as dexamethasone (207, 209). Nonetheless, TYRO3 may be expressed by certain DC subsets and play an immunosuppressive role in specific circumstances, such as type 2 inflammatory responses (169). As such, *Tyro3*$^{-/-}$ mice, but not *Axl*$^{-/-}$*Mertk*$^{-/-}$ double-knockout mice, showed a more pronounced response in an allergic asthma model compared to wild-type (169).

While our work focused on DCs and T cells, it is likely that other immune cell types also contribute to B-ALL immunity following MERTK inhibition. We observed substantial changes in the incidence of monocytes, macrophages, and B cells with MRX-2843 treatment (Fig. 2.2 *C*) and MERTK is known to have immunomodulatory functions in these cell types (107, 156, 211). Likewise, NK and NKT cells may play an important role, even though our $NK1.1^{+}$ depletion

experiment showed that they are not strictly required for the protective mechanism in *Mertk*$^{-/-}$ mice. Nonetheless, TAM kinase activation has been implicated in suppressing NK cell proliferation and activity (201) and it is possible that these cell types are engaged by CD8^{+} DCs in the absence of CD8^{+} T cells (anti-CD8β treatment). Moreover, MRX-2843 treatment increased the incidence of NK and NKT cells in fully established disease, indicating a more prominent role here. Notably, NK cells also play important roles in the recruitment of CD8^{+} DCs to the tumor microenvironment and promote their survival (64, 306). Further research will be needed to fully elucidate the contribution of other immune cell types to the anti-B-ALL immune response.

Interestingly, pharmacologic MERTK inhibition also decreased the frequency of CD8^{+} T cells expressing TOX, a transcription factor that is required for the induction of T cell exhaustion (297). This is consistent with our previously published data showing that *Mertk*$^{-/-}$ or MRX-2843 decreases PD-1 on T cells (206). Whether these changes are due to preventing exhaustion or due to increasing the recruitment of non-exhausted T cells to the bone marrow will have to be determined in future experiments. If MERTK inhibition prevents exhaustion, it will be of interest to study whether this is mediated by T cell-autonomous regulations or indirectly induced by other MERTK-expressing cell types, such as DCs and macrophages. While it was long believed that T cells do not express TAM RTKs, more recent publications indicate that certain subsets of human CD4^{+} and CD8^{+} T cells can upregulate MERTK following activation (207-209). Interestingly, expression of TYRO3 or AXL is not - or only minimally - induced on T cell subsets following activation (208, 209), suggesting that potential T cell-autonomous mechanism might be restricted to MERTK.

In summary, our findings indicate differential roles for individual TAM RTKs in the leukemia immune microenvironment, which may determine their potential as a therapeutic target, depending on the specific disease context.

4.3 Further implications for the development of TAM-targeted acute leukemia therapies

In addition to MERTK and AXL, our work identifies TYRO3 as a potential immunotherapeutic target in acute leukemia. Importantly, TAM RTKs also represent promising candidates for direct anti-leukemia targeted therapies, as they are frequently upregulated in acute leukemia cells, which they provide with crucial survival advantages (216, 218, 219, 307, 308). Genetic and/or pharmacologic inhibition of cancer cell-intrinsic TAM RTKs reduced viability, growth or chemo-resistance of leukemia cell lines (216, 218, 219, 309-312) and improved survival in acute leukemia xenograft models (206, 216, 218, 219, 312). Thus, TAM RTK-targeted therapeutics may provide patients with a dual therapeutic effect by directly targeting leukemia cells, while also boosting the anti-leukemia immune response (Fig 4.1).

MRX-2843 is a promising candidate for MERTK-targeted therapies in acute leukemia: Therapeutic doses of MRX-2843 (282, 283) are well tolerated, show direct anti-cancer cell, as well as immune-mediated efficiency in murine AML and/or ALL models (206, 283), and the compound is currently in phase-I/Ib clinical trials, including a trial in relapsed/refractory acute leukemia (clinicaltrials.gov: NCT03510104, NCT04762199, NCT04872478). Here we show that short-term treatment with MRX-2843 induces an immunotherapeutic response even in mice with high disease burden (Fig, 2.2 *A*). These data suggest that MERTK inhibition will benefit patients with robustly established leukemia and provide further rationale for advancing the development of MERTK-targeted therapies.

Additionally, our team is currently developing TYRO3 and dual MERTK/TYRO3-targeting agents. Future pre-clinical studies, as well as additional research into the *Tyro3*$^{-/-}$-mediated anti-B-ALL immune mechanism, may provide additional rational for the development of TYRO3 and/or dual MERTK/TYRO3 inhibitors for the clinic. Of note, we show here that *Mertk*$^{-/-}$ and *Tyro3*$^{-/-}$ mice are protected from B-ALL by differential underlying immune mechanisms, suggesting the

potential for combinatory anti-BALL immune effects with dual MERTK/TYRO3-targeted therapies.

As discussed above, the role of each TAM kinase and its relevance as a therapeutic target in acute leukemia patients will likely depend on several parameters, including patient's inflammatory and immune status, as well as cancer-cell intrinsic properties, such as overexpression of individual TAM RTKs and/or ligands. Hence, it will be crucial to better understand the role of individual TAM kinases in different disease contexts and to identify biomarkers, through additional studies in pre-clinical models, tumor and/or blood samples, as well as through correlative biology studies in clinical trials. As part of the ongoing MRX-2843 trial in adolescent and adult acute leukemia patients (NCT04872478), bone marrow and/or blood samples will be collected at baseline and 28 days post treatment initiation to be analyzed in biomarker and correlative assays. Assessment of blood cytokine levels of IFN-α, IFN-β, IL-6, IL-12, and IL-10 will help gain an insight into the degree of immune engagement following MRX-2843 treatment. Additionally, bone marrow and/or blood samples will be collected for scRNA-seq analysis. This may proof to be an excellent tool to analyze changes in the immune microenvironment and to correlate to the scRNA-seq studies presented in this thesis. Lastly, bone marrow samples will be frozen for analysis in PDX models or a 3D biomimicry bone marrow scaffold, potentially allowing for further testing of immunotherapeutic effects of MRX-2843. These systems may also help identifying biomarkers of sensitivity to MERTK versus TYRO3 and/or AXL inhibition.

Our findings also provide rationale for the development of combining MERTK-targeted agents with immune checkpoint inhibitors: enrichment of a gene signature representing $CD103^+$ DCs has been associated with better responsiveness to anti-PD1 checkpoint inhibitors in melanoma patients (306) and anti-tumor effects of PD-L1 inhibitors in a melanoma model depended on $CD103^+$ DCs (265). Future studies will elucidate whether combining MRX-2843 with checkpoint inhibitors improves treatment outcome compared to either single therapy in our B-ALL model.

In summary, our findings highlight several ways by which acute leukemia patients may benefit from the treatment of TAM RTK-targeted compounds, either as single agents or in combination with other therapies.

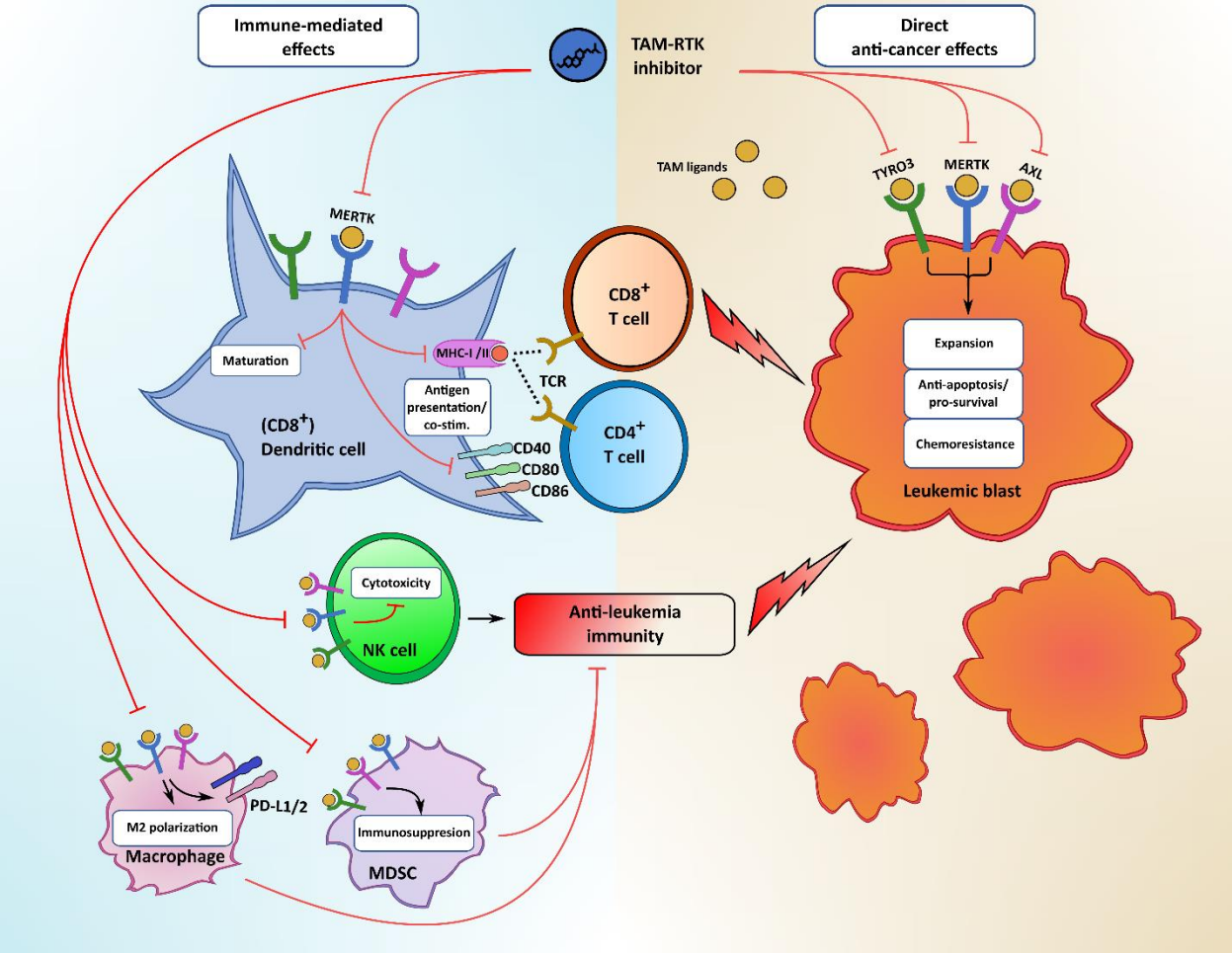

Fig. 4.1 Dual anti-leukemia effects of targeting TAM RTKs.

Targeting the TYRO3, AXL and MERTK (TAM) receptor tyrosine kinases (RTKs) may provide acute leukemia patients with a dual therapeutic effect through immune-mediated (LEFT) and direct anti-cancer (RIGHT) mechanisms.

The results of this work indicate that MERTK inhibition in the B cell acute lymphoblastic leukemia (B-ALL) microenvironment increases anti-cancer immunity by increasing ($CD8^+$) dendritic cell (DC) maturation, antigen-presentation capacities, and expression of co-stimulatory (co-stim.) proteins, leading to increased anti-leukemia $CD8^+$ T cell activity. While the other TAM RTKs likely also play immunosuppressive roles in DCs, our results suggest that anti-B-ALL immunity following TYRO3 inhibition is less dependent on $CD8^+$ DCs.

Anti-leukemia immunity may be further boosted by inhibiting TAM RTKs in macrophages (247, 248), thereby overcoming immunosuppressive M2 polarization (247, 248) and increased expression of programmed cell death 1 ligand 1/2 (PD-L1/2) (206, 248). Additionally, natural killer (NK) cells can be essential for anti-leukemia immunity following TAM inhibition (247), and TAM RTKs play immunosuppressive roles in these cells (200, 201). TAM RTKs also promote immunosuppressive functions of myeloid-derived suppressor cells (MDSCs) (238), which are increased in acute leukemia patients (86, 87).

TAM RTKs are frequently upregulated in leukemic blasts, which they provide with crucial survival advantages and pre-clinical studies found direct-anti cancer cell effects in acute leukemia cell lines and xenograft models (206, 216, 218, 219, 309-312). Hence, TAM RTK-targeted therapeutics may directly target leukemia cells, while also boosting the anti-leukemia immune response.

MHC-I/II = major histocompatibility complex - class I/II; TCR = T cell receptor.

4.4 Future directions

While our data provide important knowledge for the advancement of TAM-RTK-targeted therapies, more research is needed to assess the immunotherapeutic potential of inhibiting individual TAM RTKs in specific disease contexts.

Our results indicate TYRO3 as a novel immunotherapeutic target in acute leukemia. To further validate these findings, we plan to test TYRO3-targeted small molecule inhibitors, that are currently being developed by our team, in wild-type mice inoculated with the leukemia models used in this study. It will also be important to understand the mechanism underlying immunity in *Tyro3*$^{-/-}$ mice. Initially, we will perform flow cytometry analysis on bone marrow from WT and knockout mice to identify immune cell (sub)populations that express TYRO3 and therefore represent candidates for mediating the anti-leukemia immune response. Subsequent analysis of these populations in our B-ALL scRNAseq dataset may help gain an insight into the immune mechanism and inform additional experiments.

In addition to TYRO3-targeted agents, we are developing dual MERTK/TYRO3 inhibitors that will be used in the same models to test for potential combinatory effects suggested by the distinct

protective mechanisms in *Mertk*$^{-/-}$ and *Tyro3*$^{-/-}$ mice. In an alternative approach, leukemia cell doses high enough to overwhelm the immune system in single *Mertk* or *Tyro3* knockout mice, will be engrafted into dual *Mertk*$^{-/-}$*Tyro3*$^{-/-}$ mice, to test whether dual deletion can prolong survival under such conditions.

Furthermore, we will strive to gain an insight into the parameters that determine the relevance of individual TAM RTKs in different leukemia models. The requirement of individual TAM RTKs for immunosuppression could be dependent on the ligands (which have varying affinities to the RTKs) that are released by leukemia cells or induced in the microenvironment. Hence, we will test the expression of different TAM ligands within the leukemia cell lines by western blot, as well as their presence in cell culture supernatants or in samples of bone marrow, spleen, and blood from leukemic mice.

Our analysis of publicly available and relapse-enriched pediatric B-ALL patient data revealed that high *MERTK* or low DC gene expression were associated with poor prognosis and provides important translationally relevant evidence. Nonetheless, it will be crucial for the development of MERTK-targeted immunotherapies to generate additional human or patient-derived data. As discussed above, we are hoping to gain valuable information regarding immune engagement and/or biomarkers from analyzing patient samples collected from the MRX-2843 trial in adolescent and adult acute leukemia patients (NCT04872478). Additionally, we are planning to generate and establish colonies of humanized mice in our laboratory to test the immune-mediated effects of MRX-2843 on (MERTK-negativ) PDX models.

It is my sincere hope that the results of this thesis and the future studies outlined here will aid the development of novel therapeutic agents to advance survival outcomes, reduce side effects, and improve the quality of life for acute leukemia patients.

References

1. www.seer.cancer.gov. Surveillance, Epidemiology, and End Results (SEER) Program. SEER*Stat Database: Prevalence—SEER 12 Registries Research Data, 2019 Cancer Prevalence Data. National Cancer Institute, Division of Cancer Control and Population Sciences, Surveillance Research Program. 2022.
2. www.seer.cancer.gov. Surveillance, Epidemiology, and End Results (SEER) Program. SEER*Stat Database: U.S. Mortality—Data source: US Mortality Files, National Center for Health Statistics, CDC. National Cancer Institute, Division of Cancer Control and Population Sciences, Surveillance Research Program. 2022.
3. Miller KD, Nogueira L, Devasia T, Mariotto AB, Yabroff KR, Jemal A, et al. Cancer treatment and survivorship statistics, 2022. CA Cancer J Clin. 2022.
4. Kaspers GJ. Pediatric acute myeloid leukemia. Expert review of anticancer therapy. 2012;12(3):405-13.
5. Mulrooney DA, Dover DC, Li S, Yasui Y, Ness KK, Mertens AC, et al. Twenty years of follow-up among survivors of childhood and young adult acute myeloid leukemia: a report from the Childhood Cancer Survivor Study. Cancer. 2008;112(9):2071-9.
6. Tarlock K, Meshinchi S. Pediatric acute myeloid leukemia: biology and therapeutic implications of genomic variants. Pediatric clinics of North America. 2015;62(1):75-93.
7. Rasche M, Zimmermann M, Borschel L, Bourquin JP, Dworzak M, Klingebiel T, et al. Successes and challenges in the treatment of pediatric acute myeloid leukemia: a retrospective analysis of the AML-BFM trials from 1987 to 2012. Leukemia. 2018;32(10):2167-77.
8. www.seer.cancer.gov. Surveillance, Epidemiology, and End Results (SEER) Program. SEER*Stat Database: Survival—SEER 17 Registries Research Data. National Cancer Institute, Division of Cancer Control and Population Sciences, Surveillance Research Program. 2022.
9. Witkowski MT, Lasry A, Carroll WL, Aifantis I. Immune-Based Therapies in Acute Leukemia. Trends Cancer. 2019;5(10):604-18.
10. Tran TH, Hunger SP. The genomic landscape of pediatric acute lymphoblastic leukemia and precision medicine opportunities. Semin Cancer Biol. 2022;84:144-52.
11. de Rooij JD, Zwaan CM, van den Heuvel-Eibrink M. Pediatric AML: From Biology to Clinical Management. Journal of clinical medicine. 2015;4(1):127-49.
12. Shallis RM, Wang R, Davidoff A, Ma X, Zeidan AM. Epidemiology of acute myeloid leukemia: Recent progress and enduring challenges. Blood Rev. 2019;36:70-87.
13. Döhner H, Wei AH, Löwenberg B. Towards precision medicine for AML. Nat Rev Clin Oncol. 2021;18(9):577-90.
14. Bachireddy P, Burkhardt UE, Rajasagi M, Wu CJ. Haematological malignancies: at the forefront of immunotherapeutic innovation. Nat Rev Cancer. 2015;15(4):201-15.
15. Vardiman JW, Thiele J, Arber DA, Brunning RD, Borowitz MJ, Porwit A, et al. The 2008 revision of the World Health Organization (WHO) classification of myeloid neoplasms and acute leukemia: rationale and important changes. Blood. 2009;114(5):937-51.
16. Creutzig U, van den Heuvel-Eibrink MM, Gibson B, Dworzak MN, Adachi S, de Bont E, et al. Diagnosis and management of acute myeloid leukemia in children and adolescents: recommendations from an international expert panel. Blood. 2012;120(16):3187-205.

17. Paolini S, Gazzola A, Sabattini E, Bacci F, Pileri S, Piccaluga PP. Pathobiology of acute lymphoblastic leukemia. Semin Diagn Pathol. 2011;28(2):124-34.
18. Mullighan CG, Goorha S, Radtke I, Miller CB, Coustan-Smith E, Dalton JD, et al. Genome-wide analysis of genetic alterations in acute lymphoblastic leukaemia. Nature. 2007;446(7137):758-64.
19. Balgobind BV, Hollink IH, Arentsen-Peters ST, Zimmermann M, Harbott J, Beverloo HB, et al. Integrative analysis of type-I and type-II aberrations underscores the genetic heterogeneity of pediatric acute myeloid leukemia. Haematologica. 2011;96(10):1478-87.
20. Esposito MT, Zhao L, Fung TK, Rane JK, Wilson A, Martin N, et al. Synthetic lethal targeting of oncogenic transcription factors in acute leukemia by PARP inhibitors. Nature medicine. 2015;21(12):1481-90.
21. Pui CH, Yang JJ, Hunger SP, Pieters R, Schrappe M, Biondi A, et al. Childhood Acute Lymphoblastic Leukemia: Progress Through Collaboration. Journal of clinical oncology : official journal of the American Society of Clinical Oncology. 2015;33(27):2938-48.
22. Tomizawa D, Tsujimoto SI. Risk-Stratified Therapy for Pediatric Acute Myeloid Leukemia. Cancers (Basel). 2023;15(16).
23. Hunger SP, Mullighan CG. Acute Lymphoblastic Leukemia in Children. The New England journal of medicine. 2015;373(16):1541-52.
24. Kato M, Manabe A. Treatment and biology of pediatric acute lymphoblastic leukemia. Pediatr Int. 2018;60(1):4-12.
25. Siegel RL, Miller KD, Fuchs HE, Jemal A. Cancer statistics, 2022. CA Cancer J Clin. 2022;72(1):7-33.
26. Escherich G, Zimmermann M, Janka-Schaub G. Doxorubicin or daunorubicin given upfront in a therapeutic window are equally effective in children with newly diagnosed acute lymphoblastic leukemia. A randomized comparison in trial CoALL 07-03. Pediatr Blood Cancer. 2013;60(2):254-7.
27. Seibel NL, Steinherz PG, Sather HN, Nachman JB, Delaat C, Ettinger LJ, et al. Early postinduction intensification therapy improves survival for children and adolescents with high-risk acute lymphoblastic leukemia: a report from the Children's Oncology Group. Blood. 2008;111(5):2548-55.
28. Sauer MG, Lang PJ, Albert MH, Bader P, Creutzig U, Eyrich M, et al. Hematopoietic stem cell transplantation for children with acute myeloid leukemia-results of the AML SCT-BFM 2007 trial. Leukemia. 2020;34(2):613-24.
29. Matloub Y, Lindemulder S, Gaynon PS, Sather H, La M, Broxson E, et al. Intrathecal triple therapy decreases central nervous system relapse but fails to improve event-free survival when compared with intrathecal methotrexate: results of the Children's Cancer Group (CCG) 1952 study for standard-risk acute lymphoblastic leukemia, reported by the Children's Oncology Group. Blood. 2006;108(4):1165-73.
30. Pinnix CC, Yahalom J, Specht L, Dabaja BS. Radiation in Central Nervous System Leukemia: Guidelines From the International Lymphoma Radiation Oncology Group. Int J Radiat Oncol Biol Phys. 2018;102(1):53-8.
31. Rheingold SR, Ji L, Xu X, Devidas M, Brown PA, Gore L, et al.
32. Inaba H, Mullighan CG. Pediatric acute lymphoblastic leukemia. Haematologica. 2020;105(11):2524-39.
33. Nguyen K, Devidas M, Cheng SC, La M, Raetz EA, Carroll WL, et al. Factors influencing survival after relapse from acute lymphoblastic leukemia: a Children's Oncology Group study. Leukemia. 2008;22(12):2142-50.
34. Rasche M, Zimmermann M, Steidel E, Alonzo T, Aplenc R, Bourquin JP, et al. Survival Following Relapse in Children with Acute Myeloid Leukemia: A Report from AML-BFM and COG. Cancers (Basel). 2021;13(10).
35. Bhojwani D, Pui CH. Relapsed childhood acute lymphoblastic leukaemia. Lancet Oncol. 2013;14(6):e205-17.

36. Zarnegar-Lumley S, Caldwell KJ, Rubnitz JE. Relapsed acute myeloid leukemia in children and adolescents: current treatment options and future strategies. Leukemia. 2022;36(8):1951-60.
37. Toffalori C, Zito L, Gambacorta V, Riba M, Oliveira G, Bucci G, et al. Immune signature drives leukemia escape and relapse after hematopoietic cell transplantation. Nature medicine. 2019;25(4):603-11.
38. Krull KR, Cheung YT, Liu W, Fellah S, Reddick WE, Brinkman TM, et al. Chemotherapy Pharmacodynamics and Neuroimaging and Neurocognitive Outcomes in Long-Term Survivors of Childhood Acute Lymphoblastic Leukemia. Journal of clinical oncology : official journal of the American Society of Clinical Oncology. 2016;34(22):2644-53.
39. Schmiegelow K, Levinsen MF, Attarbaschi A, Baruchel A, Devidas M, Escherich G, et al. Second malignant neoplasms after treatment of childhood acute lymphoblastic leukemia. Journal of clinical oncology : official journal of the American Society of Clinical Oncology. 2013;31(19):2469-76.
40. Brackett J, Schafer ES, Leung DH, Bernhardt MB. Use of allopurinol in children with acute lymphoblastic leukemia to reduce skewed thiopurine metabolism. Pediatr Blood Cancer. 2014;61(6):1114-7.
41. Tay CG, Lee VWM, Ong LC, Goh KJ, Ariffin H, Fong CY. Vincristine-induced peripheral neuropathy in survivors of childhood acute lymphoblastic leukaemia. Pediatr Blood Cancer. 2017;64(8).
42. Kandula T, Farrar MA, Cohn RJ, Mizrahi D, Carey K, Johnston K, et al. Chemotherapy-Induced Peripheral Neuropathy in Long-term Survivors of Childhood Cancer: Clinical, Neurophysiological, Functional, and Patient-Reported Outcomes. JAMA Neurol. 2018;75(8):980-8.
43. Kızılocak H, Okcu F. Late Effects of Therapy in Childhood Acute Lymphoblastic Leukemia Survivors. Turk J Haematol. 2019;36(1):1-11.
44. Essig S, Li Q, Chen Y, Hitzler J, Leisenring W, Greenberg M, et al. Risk of late effects of treatment in children newly diagnosed with standard-risk acute lymphoblastic leukaemia: a report from the Childhood Cancer Survivor Study cohort. Lancet Oncol. 2014;15(8):841-51.
45. Oeffinger KC, Mertens AC, Sklar CA, Kawashima T, Hudson MM, Meadows AT, et al. Chronic health conditions in adult survivors of childhood cancer. The New England journal of medicine. 2006;355(15):1572-82.
46. Teachey DT, Pui CH. Comparative features and outcomes between paediatric T-cell and B-cell acute lymphoblastic leukaemia. Lancet Oncol. 2019;20(3):e142-e54.
47. Bhatt NS, Baassiri MJ, Liu W, Bhakta N, Chemaitilly W, Ehrhardt MJ, et al. Late outcomes in survivors of childhood acute myeloid leukemia: a report from the St. Jude Lifetime Cohort Study. Leukemia. 2021;35(8):2258-73.
48. Slats AM, Egeler RM, van der Does-van den Berg A, Korbijn C, Hählen K, Kamps WA, et al. Causes of death--other than progressive leukemia--in childhood acute lymphoblastic (ALL) and myeloid leukemia (AML): the Dutch Childhood Oncology Group experience. Leukemia. 2005;19(4):537-44.
49. Gökbuget N.
50. Abuelgasim KA, Albuhayri B, Munshi R, Mugairi AA, Alahmari B, Gmati G, et al. Impact of age and induction therapy on outcome of 180 adult patients with acute myeloid leukemia; retrospective analysis and literature review. Leuk Res Rep. 2020;14:100206.
51. Mocellin S, Lise M, Nitti D. Targeted therapy for colorectal cancer: mapping the way. Trends Mol Med. 2005;11(7):327-35.
52. Weisberg E, Manley PW, Cowan-Jacob SW, Hochhaus A, Griffin JD. Second generation inhibitors of BCR-ABL for the treatment of imatinib-resistant chronic myeloid leukaemia. Nat Rev Cancer. 2007;7(5):345-56.
53. Owattanapanich W, Rujirachun P, Ungprasert P, Buaboonnam J, Techavichit P. Prevalence and Clinical Outcome of Philadelphia-Like Acute Lymphoblastic Leukemia: Systematic Review and Meta-analysis. Clin Lymphoma Myeloma Leuk. 2020;20(1):e22-e9.

54. Madhusoodhan PP, Carroll WL, Bhatla T. Progress and Prospects in Pediatric Leukemia. Curr Probl Pediatr Adolesc Health Care. 2016;46(7):229-41.
55. Cordo V, van der Zwet JCG, Canté-Barrett K, Pieters R, Meijerink JPP. T-cell Acute Lymphoblastic Leukemia: A Roadmap to Targeted Therapies. Blood Cancer Discov. 2021;2(1):19-31.
56. Smith CC, Wang Q, Chin CS, Salerno S, Damon LE, Levis MJ, et al. Validation of ITD mutations in FLT3 as a therapeutic target in human acute myeloid leukaemia. Nature. 2012;485(7397):260-3.
57. Straube J, Lane SW, Vu T. Optimizing DNA hypomethylating therapy in acute myeloid leukemia and myelodysplastic syndromes. Bioessays. 2021;43(10):e2100125.
58. Pollyea DA, Amaya M, Strati P, Konopleva MY. Venetoclax for AML: changing the treatment paradigm. Blood Adv. 2019;3(24):4326-4335. Blood advances. 2020;4(6):1020.
59. Waldman AD, Fritz JM, Lenardo MJ. A guide to cancer immunotherapy: from T cell basic science to clinical practice. Nat Rev Immunol. 2020;20(11):651-68.
60. Curran EK, Godfrey J, Kline J. Mechanisms of Immune Tolerance in Leukemia and Lymphoma. Trends Immunol. 2017;38(7):513-25.
61. Lv M, Liu Y, Liu W, Xing Y, Zhang S. Immunotherapy for Pediatric Acute Lymphoblastic Leukemia: Recent Advances and Future Perspectives. Front Immunol. 2022;13:921894.
62. Abbott M, Ustoyev Y. Cancer and the Immune System: The History and Background of Immunotherapy. Semin Oncol Nurs. 2019;35(5):150923.
63. Swann JB, Smyth MJ. Immune surveillance of tumors. The Journal of clinical investigation. 2007;117(5):1137-46.
64. Böttcher JP, Bonavita E, Chakravarty P, Blees H, Cabeza-Cabrerizo M, Sammicheli S, et al. NK Cells Stimulate Recruitment of cDC1 into the Tumor Microenvironment Promoting Cancer Immune Control. Cell. 2018;172(5):1022-37.e14.
65. Masuda K, Hiraki A, Fujii N, Watanabe T, Tanaka M, Matsue K, et al. Loss or down-regulation of HLA class I expression at the allelic level in freshly isolated leukemic blasts. Cancer science. 2007;98(1):102-8.
66. Luczyński W, Stasiak-Barmuta A, Iłendo E, Kovalchuk O, Krawczuk-Rybak M, Malinowska I, et al. Low expression of costimulatory molecules and mRNA for cytokines are important mechanisms of immunosuppression in acute lymphoblastic leukemia in children? Neoplasma. 2006;53(4):301-4.
67. Rouce RH, Shaim H, Sekine T, Weber G, Ballard B, Ku S, et al. The TGF-β/SMAD pathway is an important mechanism for NK cell immune evasion in childhood B-acute lymphoblastic leukemia. Leukemia. 2016;30(4):800-11.
68. Iannello A, Thompson TW, Ardolino M, Marcus A, Raulet DH. Immunosurveillance and immunotherapy of tumors by innate immune cells. Current opinion in immunology. 2016;38:52-8.
69. Beyar-Katz O, Gill S. Novel Approaches to Acute Myeloid Leukemia Immunotherapy. Clinical cancer research : an official journal of the American Association for Cancer Research. 2018;24(22):5502-15.
70. Ishida Y, Agata Y, Shibahara K, Honjo T. Induced expression of PD-1, a novel member of the immunoglobulin gene superfamily, upon programmed cell death. The EMBO journal. 1992;11(11):3887-95.
71. Dong H, Strome SE, Salomao DR, Tamura H, Hirano F, Flies DB, et al. Tumor-associated B7-H1 promotes T-cell apoptosis: a potential mechanism of immune evasion. Nature medicine. 2002;8(8):793-800.
72. Blank C, Brown I, Peterson AC, Spiotto M, Iwai Y, Honjo T, et al. PD-L1/B7H-1 inhibits the effector phase of tumor rejection by T cell receptor (TCR) transgenic CD8+ T cells. Cancer research. 2004;64(3):1140-5.

73. Hashimoto M, Kamphorst AO, Im SJ, Kissick HT, Pillai RN, Ramalingam SS, et al. CD8 T Cell Exhaustion in Chronic Infection and Cancer: Opportunities for Interventions. Annu Rev Med. 2018;69:301-18.
74. Zajac AJ, Blattman JN, Murali-Krishna K, Sourdive DJ, Suresh M, Altman JD, et al. Viral immune evasion due to persistence of activated T cells without effector function. The Journal of experimental medicine. 1998;188(12):2205-13.
75. Li B, Chan HL, Chen P. Immune Checkpoint Inhibitors: Basics and Challenges. Curr Med Chem. 2019;26(17):3009-25.
76. Salih HR, Wintterle S, Krusch M, Kroner A, Huang YH, Chen L, et al. The role of leukemia-derived B7-H1 (PD-L1) in tumor-T-cell interactions in humans. Experimental hematology. 2006;34(7):888-94.
77. Chen X, Liu S, Wang L, Zhang W, Ji Y, Ma X. Clinical significance of B7-H1 (PD-L1) expression in human acute leukemia. Cancer biology & therapy. 2008;7(5):622-7.
78. Berthon C, Driss V, Liu J, Kuranda K, Leleu X, Jouy N, et al. In acute myeloid leukemia, B7-H1 (PD-L1) protection of blasts from cytotoxic T cells is induced by TLR ligands and interferon-gamma and can be reversed using MEK inhibitors. Cancer immunology, immunotherapy : CII. 2010;59(12):1839-49.
79. Kang SH, Hwang HJ, Yoo JW, Kim H, Choi ES, Hwang SH, et al. Expression of Immune Checkpoint Receptors on T-Cells and Their Ligands on Leukemia Blasts in Childhood Acute Leukemia. Anticancer Res. 2019;39(10):5531-9.
80. Simone R, Tenca C, Fais F, Luciani M, De Rossi G, Pesce G, et al. A soluble form of CTLA-4 is present in paediatric patients with acute lymphoblastic leukaemia and correlates with CD1d+ expression. PLoS One. 2012;7(9):e44654.
81. El-Maadawy EA, Elshal MF, Bakry RM, Moussa MM, El-Naby S, Talaat RM. Regulation of CD4(+)CD25(+)FOXP3(+) cells in Pediatric Acute Lymphoblastic Leukemia (ALL): Implication of cytokines and miRNAs. Molecular immunology. 2020;124:1-8.
82. Søegaard SH, Rostgaard K, Skogstrand K, Wiemels JL, Schmiegelow K, Hjalgrim H. Neonatal Inflammatory Markers Are Associated with Childhood B-cell Precursor Acute Lymphoblastic Leukemia. Cancer research. 2018;78(18):5458-63.
83. Zhang XL, Komada Y, Chipeta J, Li QS, Inaba H, Azuma E, et al. Intracellular cytokine profile of T cells from children with acute lymphoblastic leukemia. Cancer immunology, immunotherapy : CII. 2000;49(3):165-72.
84. Cloppenborg T, Stanulla M, Zimmermann M, Schrappe M, Welte K, Klein C. Immunosurveillance of childhood ALL: polymorphic interferon-gamma alleles are associated with age at diagnosis and clinical risk groups. Leukemia. 2005;19(1):44-8.
85. Wu S, Gessner R, von Stackelberg A, Kirchner R, Henze G, Seeger K. Cytokine/cytokine receptor gene expression in childhood acute lymphoblastic leukemia: correlation of expression and clinical outcome at first disease recurrence. Cancer. 2005;103(5):1054-63.
86. Salem ML, El-Shanshory MR, Abdou SH, Attia MS, Sobhy SM, Zidan MF, et al. Chemotherapy alters the increased numbers of myeloid-derived suppressor and regulatory T cells in children with acute lymphoblastic leukemia. Immunopharmacol Immunotoxicol. 2018;40(2):158-67.
87. Zahran AM, Shibl A, Rayan A, Mohamed M, Osman AMM, Saad K, et al. Increase in polymorphonuclear myeloid-derived suppressor cells and regulatory T-cells in children with B-cell acute lymphoblastic leukemia. Sci Rep. 2021;11(1):15039.
88. Veglia F, Perego M, Gabrilovich D. Myeloid-derived suppressor cells coming of age. Nature immunology. 2018;19(2):108-19.
89. Murray PJ. Macrophage Polarization. Annu Rev Physiol. 2017;79:541-66.
90. Komohara Y, Niino D, Saito Y, Ohnishi K, Horlad H, Ohshima K, et al. Clinical significance of $CD163^{+}$ tumor-associated macrophages in patients with adult T-cell leukemia/lymphoma. Cancer science. 2013;104(7):945-51.

91. Al-Matary YS, Botezatu L, Opalka B, Hönes JM, Lams RF, Thivakaran A, et al. Acute myeloid leukemia cells polarize macrophages towards a leukemia supporting state in a Growth factor independence 1 dependent manner. Haematologica. 2016;101(10):1216-27.
92. Alsaab HO, Sau S, Alzhrani R, Tatiparti K, Bhise K, Kashaw SK, et al. PD-1 and PD-L1 Checkpoint Signaling Inhibition for Cancer Immunotherapy: Mechanism, Combinations, and Clinical Outcome. Frontiers in pharmacology. 2017;8:561.
93. Inaba H, Pui CH. Advances in the Diagnosis and Treatment of Pediatric Acute Lymphoblastic Leukemia. Journal of clinical medicine. 2021;10(9).
94. Hystad ME, Myklebust JH, Bø TH, Sivertsen EA, Rian E, Forfang L, et al. Characterization of early stages of human B cell development by gene expression profiling. Journal of immunology (Baltimore, Md : 1950). 2007;179(6):3662-71.
95. Wilkins O, Keeler AM, Flotte TR. CAR T-Cell Therapy: Progress and Prospects. Hum Gene Ther Methods. 2017;28(2):61-6.
96. Si Lim SJ, Grupp SA, DiNofia AM. Tisagenlecleucel for treatment of children and young adults with relapsed/refractory B-cell acute lymphoblastic leukemia. Pediatr Blood Cancer. 2021;68(9):e29123.
97. Schultz LM, Eaton A, Baggott C, Rossoff J, Prabhu S, Keating AK, et al. Outcomes After Nonresponse and Relapse Post-Tisagenlecleucel in Children, Adolescents, and Young Adults With B-Cell Acute Lymphoblastic Leukemia. Journal of clinical oncology : official journal of the American Society of Clinical Oncology. 2023;41(2):354-63.
98. Nagorsen D, Baeuerle PA. Immunomodulatory therapy of cancer with T cell-engaging BiTE antibody blinatumomab. Exp Cell Res. 2011;317(9):1255-60.
99. Klinger M, Benjamin J, Kischel R, Stienen S, Zugmaier G. Harnessing T cells to fight cancer with BiTE® antibody constructs--past developments and future directions. Immunological reviews. 2016;270(1):193-208.
100. Brown PA, Ji L, Xu X, Devidas M, Hogan LE, Borowitz MJ, et al. Effect of Postreinduction Therapy Consolidation With Blinatumomab vs Chemotherapy on Disease-Free Survival in Children, Adolescents, and Young Adults With First Relapse of B-Cell Acute Lymphoblastic Leukemia: A Randomized Clinical Trial. Jama. 2021;325(9):833-42.
101. Locatelli F, Zugmaier G, Rizzari C, Morris JD, Gruhn B, Klingebiel T, et al. Effect of Blinatumomab vs Chemotherapy on Event-Free Survival Among Children With High-risk First-Relapse B-Cell Acute Lymphoblastic Leukemia: A Randomized Clinical Trial. Jama. 2021;325(9):843-54.
102. Brivio E, Locatelli F, Lopez-Yurda M, Malone A, Díaz-de-Heredia C, Bielorai B, et al. A phase 1 study of inotuzumab ozogamicin in pediatric relapsed/refractory acute lymphoblastic leukemia (ITCC-059 study). Blood. 2021;137(12):1582-90.
103. Willier S, Rothämel P, Hastreiter M, Wilhelm J, Stenger D, Blaeschke F, et al. CLEC12A and CD33 coexpression as a preferential target for pediatric AML combinatorial immunotherapy. Blood. 2021;137(8):1037-49.
104. De Moerloose B. CAR-T treatment of pediatric AML: a long and winding road. Blood. 2021;137(8):1004-6.
105. DeRyckere D, Huelse JM, Earp HS, Graham DK. TAM family kinases as therapeutic targets at the interface of cancer and immunity. Nat Rev Clin Oncol. 2023.
106. Graham DK, DeRyckere D, Davies KD, Earp HS. The TAM family: phosphatidylserine sensing receptor tyrosine kinases gone awry in cancer. Nat Rev Cancer. 2014;14(12):769-85.
107. Huelse JM, Fridlyand DM, Earp S, DeRyckere D, Graham DK. MERTK in cancer therapy: Targeting the receptor tyrosine kinase in tumor cells and the immune system. Pharmacol Ther. 2020;213:107577.
108. Graham DK, Dawson TL, Mullaney DL, Snodgrass HR, Earp HS. Cloning and mRNA expression analysis of a novel human protooncogene, c-mer. Cell Growth Differ. 1994;5(6):647-57.

109. Lai C, Gore M, Lemke G. Structure, expression, and activity of Tyro 3, a neural adhesion-related receptor tyrosine kinase. Oncogene. 1994;9(9):2567-78.
110. O'Bryan JP, Frye RA, Cogswell PC, Neubauer A, Kitch B, Prokop C, et al. axl, a transforming gene isolated from primary human myeloid leukemia cells, encodes a novel receptor tyrosine kinase. Mol Cell Biol. 1991;11(10):5016-31.
111. Lai C, Lemke G. An extended family of protein-tyrosine kinase genes differentially expressed in the vertebrate nervous system. Neuron. 1991;6(5):691-704.
112. Lew ED, Oh J, Burrola PG, Lax I, Zagorska A, Traves PG, et al. Differential TAM receptor-ligand-phospholipid interactions delimit differential TAM bioactivities. eLife. 2014;3.
113. Chen J, Carey K, Godowski PJ. Identification of Gas6 as a ligand for Mer, a neural cell adhesion molecule related receptor tyrosine kinase implicated in cellular transformation. Oncogene. 1997;14(17):2033-9.
114. Nagata K, Ohashi K, Nakano T, Arita H, Zong C, Hanafusa H, et al. Identification of the product of growth arrest-specific gene 6 as a common ligand for Axl, Sky, and Mer receptor tyrosine kinases. J Biol Chem. 1996;271(47):30022-7.
115. Prasad D, Rothlin CV, Burrola P, Burstyn-Cohen T, Lu Q, Garcia de Frutos P, et al. TAM receptor function in the retinal pigment epithelium. Molecular and cellular neurosciences. 2006;33(1):96-108.
116. Kasikara C, Kumar S, Kimani S, Tsou WI, Geng K, Davra V, et al. Phosphatidylserine Sensing by TAM Receptors Regulates AKT-Dependent Chemoresistance and PD-L1 Expression. Molecular cancer research : MCR. 2017;15(6):753-64.
117. Tsou WI, Nguyen KQ, Calarese DA, Garforth SJ, Antes AL, Smirnov SV, et al. Receptor tyrosine kinases, TYRO3, AXL, and MER, demonstrate distinct patterns and complex regulation of ligand-induced activation. J Biol Chem. 2014;289(37):25750-63.
118. Zagorska A, Traves PG, Lew ED, Dransfield I, Lemke G. Diversification of TAM receptor tyrosine kinase function. Nature immunology. 2014;15(10):920-8.
119. Stitt TN, Conn G, Gore M, Lai C, Bruno J, Radziejewski C, et al. The anticoagulation factor protein S and its relative, Gas6, are ligands for the Tyro 3/Axl family of receptor tyrosine kinases. Cell. 1995;80(4):661-70.
120. Caberoy NB, Zhou Y, Li W. Tubby and tubby-like protein 1 are new MerTK ligands for phagocytosis. The EMBO journal. 2010;29(23):3898-910.
121. Caberoy NB, Alvarado G, Li W. Tubby regulates microglial phagocytosis through MerTK. Journal of neuroimmunology. 2012;252(1-2):40-8.
122. Caberoy NB, Alvarado G, Bigcas JL, Li W. Galectin-3 is a new MerTK-specific eat-me signal. Journal of cellular physiology. 2012;227(2):401-7.
123. Sassan H, Nour AK. Galectin-3 activates the receptor tyrosine kinase Tyro3 and stimulates ERK signaling, cell survival and migration in human head and neck cancer cells [abstract]. Proceedings of the American Association for Cancer Research Annual Meeting 2019. 2019;2019 Mar 29-Apr 3; Atlanta, GA. Philadelphia (PA): AACR; Cancer Res 2019;79(13 Suppl):Abstract nr 2638.
124. Al Kafri N, Hafizi S. Galectin-3 Stimulates Tyro3 Receptor Tyrosine Kinase and Erk Signalling, Cell Survival and Migration in Human Cancer Cells. Biomolecules. 2020;10(7).
125. Nomura K, Vilalta A, Allendorf DH, Hornik TC, Brown GC. Activated Microglia Desialylate and Phagocytose Cells via Neuraminidase, Galectin-3, and Mer Tyrosine Kinase. Journal of immunology (Baltimore, Md : 1950). 2017;198(12):4792-801.
126. Sinha S, Boysen J, Nelson M, Secreto C, Warner SL, Bearss DJ, et al. Targeted Axl Inhibition Primes Chronic Lymphocytic Leukemia B Cells to Apoptosis and Shows Synergistic/Additive Effects in Combination with BTK Inhibitors. Clinical cancer research : an official journal of the American Association for Cancer Research. 2015;21(9):2115-26.

127. Brown JE, Krodel M, Pazos M, Lai C, Prieto AL. Cross-phosphorylation, signaling and proliferative functions of the Tyro3 and Axl receptors in Rat2 cells. PLoS One. 2012;7(5):e36800.
128. Elkabets M, Pazarentzos E, Juric D, Sheng Q, Pelossof RA, Brook S, et al. AXL mediates resistance to PI3Kα inhibition by activating the EGFR/PKC/mTOR axis in head and neck and esophageal squamous cell carcinomas. Cancer Cell. 2015;27(4):533-46.
129. Yan D, Parker RE, Wang X, Frye SV, Earp HS, 3rd, DeRyckere D, et al. MERTK Promotes Resistance to Irreversible EGFR Tyrosine Kinase Inhibitors in Non-small Cell Lung Cancers Expressing Wild-type EGFR Family Members. Clinical cancer research : an official journal of the American Association for Cancer Research. 2018;24(24):6523-35.
130. Yan D, Huelse J, Parker R, Tan Z, Wang X, Frye SV, et al. Abstract 1882: MERTK drives residual tumor growth in EGFR-mutated non-small cell lung cancer cells treated with osimertinib. Cancer research. 2020;80(16 Supplement):1882-.
131. Komurov K, Padron D, Cheng T, Roth M, Rosenblatt KP, White MA. Comprehensive mapping of the human kinome to epidermal growth factor receptor signaling. J Biol Chem. 2010;285(27):21134-42.
132. Meyer AS, Miller MA, Gertler FB, Lauffenburger DA. The receptor AXL diversifies EGFR signaling and limits the response to EGFR-targeted inhibitors in triple-negative breast cancer cells. Sci Signal. 2013;6(287):ra66.
133. Brand TM, Iida M, Stein AP, Corrigan KL, Braverman CM, Luthar N, et al. AXL Mediates Resistance to Cetuximab Therapy. Cancer research. 2014;74(18):5152-64.
134. Adam-Artigues A, Arenas EJ, Martínez-Sabadell A, Brasó-Maristany F, Cervera R, Tormo E, et al. Targeting HER2-AXL heterodimerization to overcome resistance to HER2 blockade in breast cancer. Sci Adv. 2022;8(20):eabk2746.
135. Ghosh AK, Secreto C, Boysen J, Sassoon T, Shanafelt TD, Mukhopadhyay D, et al. The novel receptor tyrosine kinase Axl is constitutively active in B-cell chronic lymphocytic leukemia and acts as a docking site of nonreceptor kinases: implications for therapy. Blood. 2011;117(6):1928-37.
136. Aldonza MBD, Reyes RDD, Kim YS, Ku J, Barsallo AM, Hong J-Y, et al. Chemotherapy confers a conserved secondary tolerance to EGFR inhibition via AXL-mediated signaling bypass. Scientific reports. 2021;11(1):8016-.
137. Tsai CL, Chang JS, Yu MC, Lee CH, Chen TC, Chuang WY, et al. Functional Genomics Identifies Hepatitis-Induced STAT3-TYRO3-STAT3 Signaling as a Potential Therapeutic Target of Hepatoma. Clinical cancer research : an official journal of the American Association for Cancer Research. 2020;26(5):1185-97.
138. Lee YJ, Lee SH, Youn YS, Choi JY, Song KS, Cho MS, et al. Preventing cleavage of Mer promotes efferocytosis and suppresses acute lung injury in bleomycin treated mice. Toxicology and applied pharmacology. 2012;263(1):61-72.
139. Thorp E, Vaisar T, Subramanian M, Mautner L, Blobel C, Tabas I. Shedding of the Mer tyrosine kinase receptor is mediated by ADAM17 protein through a pathway involving reactive oxygen species, protein kinase Cdelta, and p38 mitogen-activated protein kinase (MAPK). J Biol Chem. 2011;286(38):33335-44.
140. Zhang Y, Wang Y, Zhou D, Zhang LS, Deng FX, Shu S, et al. Angiotensin deteriorates advanced atherosclerosis by promoting MerTK cleavage and impairing efferocytosis through AT1R/ROS/p38MAPK/ADAM17 pathway. American journal of physiology Cell physiology. 2019.
141. Cai B, Dongiovanni P, Corey KE, Wang X, Shmarakov IO, Zheng Z, et al. Macrophage MerTK Promotes Liver Fibrosis in Nonalcoholic Steatohepatitis. Cell metabolism. 2019.
142. Miller MA, Oudin MJ, Sullivan RJ, Wang SJ, Meyer AS, Im H, et al. Reduced Proteolytic Shedding of Receptor Tyrosine Kinases Is a Post-Translational Mechanism of Kinase Inhibitor Resistance. Cancer Discovery. 2016;6(4):382-99.
143. Ekman C, Stenhoff J, Dahlbäck B. Gas6 is complexed to the soluble tyrosine kinase receptor Axl in human blood. Journal of thrombosis and haemostasis : JTH. 2010;8(4):838-44.

144. Sather S, Kenyon KD, Lefkowitz JB, Liang X, Varnum BC, Henson PM, et al. A soluble form of the Mer receptor tyrosine kinase inhibits macrophage clearance of apoptotic cells and platelet aggregation. Blood. 2007;109(3):1026-33.
145. Uehara S, Fukuzawa, Y. , Matuyama, T. and Gotoh, K. Role of Tyro3, Axl, and Mer Receptors and Their Ligands (Gas6, and Protein S) in Patients with Hepatocellular Carcinoma. Journal of Cancer Therapy. 2017;8:112-30.
146. O'Bryan JP, Fridell YW, Koski R, Varnum B, Liu ET. The transforming receptor tyrosine kinase, Axl, is post-translationally regulated by proteolytic cleavage. J Biol Chem. 1995;270(2):551-7.
147. Linger RM, Keating AK, Earp HS, Graham DK. TAM receptor tyrosine kinases: biologic functions, signaling, and potential therapeutic targeting in human cancer. Adv Cancer Res. 2008;100:35-83.
148. Biesecker LG, Giannola DM, Emerson SG. Identification of alternative exons, including a novel exon, in the tyrosine kinase receptor gene Etk2/tyro3 that explain differences in 5' cDNA sequences. Oncogene. 1995;10(11):2239-42.
149. Brea-Fernández AJ, Pomares E, Brión MJ, Marfany G, Blanco MJ, Sánchez-Salorio M, et al. Novel splice donor site mutation in MERTK gene associated with retinitis pigmentosa. The British journal of ophthalmology. 2008;92(10):1419-23.
150. Branchford BR, Sather S, Brodsky G, White-Adams TC, DeRyckere D, Neeves KB, et al. Imer Blocks Phosphorylation of the β3 Integrin, Decreasing Platelet Activation Responses and Protecting Mice From Arterial Thrombosis. Blood. 2011;118(21):189.
151. Mao Y, Finnemann SC. Regulation of phagocytosis by Rho GTPases. Small GTPases. 2015;6(2):89-99.
152. Camenisch TD, Koller BH, Earp HS, Matsushima GK. A novel receptor tyrosine kinase, Mer, inhibits TNF-alpha production and lipopolysaccharide-induced endotoxic shock. Journal of immunology (Baltimore, Md : 1950). 1999;162(6):3498-503.
153. Lu Q, Lemke G. Homeostatic regulation of the immune system by receptor tyrosine kinases of the Tyro 3 family. Science (New York, NY). 2001;293(5528):306-11.
154. Sun B, Qi N, Shang T, Wu H, Deng T, Han D. Sertoli cell-initiated testicular innate immune response through toll-like receptor-3 activation is negatively regulated by Tyro3, Axl, and mer receptors. Endocrinology. 2010;151(6):2886-97.
155. Sandahl M, Hunter DM, Strunk KE, Earp HS, Cook RS. Epithelial cell-directed efferocytosis in the post-partum mammary gland is necessary for tissue homeostasis and future lactation. BMC developmental biology. 2010;10:122.
156. Shao WH, Zhen Y, Rosenbaum J, Eisenberg RA, McGaha TL, Birkenbach M, et al. A protective role of Mer receptor tyrosine kinase in nephrotoxic serum-induced nephritis. Clinical immunology (Orlando, Fla). 2010;136(2):236-44.
157. Duncan JL, LaVail MM, Yasumura D, Matthes MT, Yang H, Trautmann N, et al. An RCS-like retinal dystrophy phenotype in mer knockout mice. Investigative ophthalmology & visual science. 2003;44(2):826-38.
158. Chung WS, Clarke LE, Wang GX, Stafford BK, Sher A, Chakraborty C, et al. Astrocytes mediate synapse elimination through MEGF10 and MERTK pathways. Nature. 2013;504(7480):394-400.
159. Fourgeaud L, Traves PG, Tufail Y, Leal-Bailey H, Lew ED, Burrola PG, et al. TAM receptors regulate multiple features of microglial physiology. Nature. 2016;532(7598):240-4.
160. Ji R, Tian S, Lu HJ, Lu Q, Zheng Y, Wang X, et al. TAM receptors affect adult brain neurogenesis by negative regulation of microglial cell activation. Journal of immunology (Baltimore, Md : 1950). 2013;191(12):6165-77.
161. Healy LM, Perron G, Won SY, Michell-Robinson MA, Rezk A, Ludwin SK, et al. MerTK Is a Functional Regulator of Myelin Phagocytosis by Human Myeloid Cells. Journal of immunology (Baltimore, Md : 1950). 2016;196(8):3375-84.

162. Angelillo-Scherrer A, de Frutos P, Aparicio C, Melis E, Savi P, Lupu F, et al. Deficiency or inhibition of Gas6 causes platelet dysfunction and protects mice against thrombosis. Nature medicine. 2001;7(2):215-21.
163. Angelillo-Scherrer A, Burnier L, Lambrechts D, Fish RJ, Tjwa M, Plaisance S, et al. Role of Gas6 in erythropoiesis and anemia in mice. The Journal of clinical investigation. 2008;118(2):583-96.
164. Branchford BR, Stalker TJ, Law L, Acevedo G, Sather S, Brzezinski C, et al. The small-molecule MERTK inhibitor UNC2025 decreases platelet activation and prevents thrombosis. Journal of thrombosis and haemostasis : JTH. 2018;16(2):352-63.
165. Chen C, Li Q, Darrow AL, Wang Y, Derian CK, Yang J, et al. Mer receptor tyrosine kinase signaling participates in platelet function. Arteriosclerosis, thrombosis, and vascular biology. 2004;24(6):1118-23.
166. Behrens EM, Gadue P, Gong SY, Garrett S, Stein PL, Cohen PL. The mer receptor tyrosine kinase: expression and function suggest a role in innate immunity. European journal of immunology. 2003;33(8):2160-7.
167. Rothlin CV, Carrera-Silva EA, Bosurgi L, Ghosh S. TAM receptor signaling in immune homeostasis. Annu Rev Immunol. 2015;33:355-91.
168. Carrera Silva EA, Chan PY, Joannas L, Errasti AE, Gagliani N, Bosurgi L, et al. T cell-derived protein S engages TAM receptor signaling in dendritic cells to control the magnitude of the immune response. Immunity. 2013;39(1):160-70.
169. Chan PY, Carrera Silva EA, De Kouchkovsky D, Joannas LD, Hao L, Hu D, et al. The TAM family receptor tyrosine kinase TYRO3 is a negative regulator of type 2 immunity. Science (New York, NY). 2016;352(6281):99-103.
170. Rothlin CV, Ghosh S, Zuniga EI, Oldstone MB, Lemke G. TAM receptors are pleiotropic inhibitors of the innate immune response. Cell. 2007;131(6):1124-36.
171. Zizzo G, Hilliard BA, Monestier M, Cohen PL. Efficient clearance of early apoptotic cells by human macrophages requires M2c polarization and MerTK induction. Journal of immunology (Baltimore, Md : 1950). 2012;189(7):3508-20.
172. Ubil E, Caskey L, Holtzhausen A, Hunter D, Story C, Earp HS. Tumor-secreted Pros1 inhibits macrophage M1 polarization to reduce antitumor immune response. The Journal of clinical investigation. 2018;128(6):2356-69.
173. Triantafyllou E, Pop OT, Possamai LA, Wilhelm A, Liaskou E, Singanayagam A, et al. MerTK expressing hepatic macrophages promote the resolution of inflammation in acute liver failure. Gut. 2018;67(2):333-47.
174. Qi N, Liu P, Zhang Y, Wu H, Chen Y, Han D. Development of a spontaneous liver disease resembling autoimmune hepatitis in mice lacking tyro3, axl and mer receptor tyrosine kinases. PLoS One. 2013;8(6):e66604.
175. Howangyin KY, Zlatanova I, Pinto C, Ngkelo A, Cochain C, Rouanet M, et al. Myeloid-Epithelial-Reproductive Receptor Tyrosine Kinase and Milk Fat Globule Epidermal Growth Factor 8 Coordinately Improve Remodeling After Myocardial Infarction via Local Delivery of Vascular Endothelial Growth Factor. Circulation. 2016;133(9):826-39.
176. Wan E, Yeap XY, Dehn S, Terry R, Novak M, Zhang S, et al. Enhanced efferocytosis of apoptotic cardiomyocytes through myeloid-epithelial-reproductive tyrosine kinase links acute inflammation resolution to cardiac repair after infarction. Circulation research. 2013;113(8):1004-12.
177. Ait-Oufella H, Pouresmail V, Simon T, Blanc-Brude O, Kinugawa K, Merval R, et al. Defective mer receptor tyrosine kinase signaling in bone marrow cells promotes apoptotic cell accumulation and accelerates atherosclerosis. Arteriosclerosis, thrombosis, and vascular biology. 2008;28(8):1429-31.
178. Li Q, Lu Q, Lu H, Tian S, Lu Q. Systemic autoimmunity in TAM triple knockout mice causes inflammatory brain damage and cell death. PLoS One. 2013;8(6):e64812.

179. Scott RS, McMahon EJ, Pop SM, Reap EA, Caricchio R, Cohen PL, et al. Phagocytosis and clearance of apoptotic cells is mediated by MER. Nature. 2001;411(6834):207-11.
180. Cohen PL, Caricchio R, Abraham V, Camenisch TD, Jennette JC, Roubey RA, et al. Delayed apoptotic cell clearance and lupus-like autoimmunity in mice lacking the c-mer membrane tyrosine kinase. The Journal of experimental medicine. 2002;196(1):135-40.
181. Williams JC, Wagner NJ, Earp HS, Vilen BJ, Matsushima GK. Increased hematopoietic cells in the mertk-/- mouse peritoneal cavity: a result of augmented migration. Journal of immunology (Baltimore, Md : 1950). 2010;184(12):6637-48.
182. Weinger JG, Brosnan CF, Loudig O, Goldberg MF, Macian F, Arnett HA, et al. Loss of the receptor tyrosine kinase Axl leads to enhanced inflammation in the CNS and delayed removal of myelin debris during experimental autoimmune encephalomyelitis. Journal of neuroinflammation. 2011;8:49.
183. Hoehn HJ, Kress Y, Sohn A, Brosnan CF, Bourdon S, Shafit-Zagardo B. Axl-/- mice have delayed recovery and prolonged axonal damage following cuprizone toxicity. Brain Res. 2008;1240:1-11.
184. Wallet MA, Sen P, Flores RR, Wang Y, Yi Z, Huang Y, et al. MerTK is required for apoptotic cell-induced T cell tolerance. The Journal of experimental medicine. 2008;205(1):219-32.
185. Lindsay RS, Whitesell JC, Dew KE, Rodriguez E, Sandor AM, Tracy D, et al. MERTK on mononuclear phagocytes regulates T cell antigen recognition at autoimmune and tumor sites. The Journal of experimental medicine. 2021;218(10).
186. Waterborg CEJ, Koenders MI, van Lent P, van der Kraan PM, van de Loo FAJ. Tyro3/Axl/Mertk-deficient mice develop bone marrow edema which is an early pathological marker in rheumatoid arthritis. PLoS One. 2018;13(10):e0205902.
187. Waterborg CEJ, Broeren MGA, Blaney Davidson EN, Koenders MI, van Lent P, van den Berg WB, et al. The level of synovial AXL expression determines the outcome of inflammatory arthritis, possibly depending on the upstream role of TGF-beta1. Rheumatology (Oxford). 2019;58(3):536-46.
188. Rahman ZS, Shao WH, Khan TN, Zhen Y, Cohen PL. Impaired apoptotic cell clearance in the germinal center by Mer-deficient tingible body macrophages leads to enhanced antibody-forming cell and germinal center responses. Journal of immunology (Baltimore, Md : 1950). 2010;185(10):5859-68.
189. Khan TN, Wong EB, Soni C, Rahman ZS. Prolonged apoptotic cell accumulation in germinal centers of Mer-deficient mice causes elevated B cell and CD4+ Th cell responses leading to autoantibody production. Journal of immunology (Baltimore, Md : 1950). 2013;190(4):1433-46.
190. Alciato F, Sainaghi PP, Sola D, Castello L, Avanzi GC. TNF-alpha, IL-6, and IL-1 expression is inhibited by GAS6 in monocytes/macrophages. Journal of leukocyte biology. 2010;87(5):869-75.
191. Eken C, Martin PJ, Sadallah S, Treves S, Schaller M, Schifferli JA. Ectosomes released by polymorphonuclear neutrophils induce a MerTK-dependent anti-inflammatory pathway in macrophages. J Biol Chem. 2010;285(51):39914-21.
192. Park HJ, Baen JY, Lee YJ, Choi YH, Kang JL. The TAM-family receptor Mer mediates production of HGF through the RhoA-dependent pathway in response to apoptotic cells. Molecular biology of the cell. 2012;23(16):3254-65.
193. Zhang L, DeBerge M, Wang J, Dangi A, Zhang X, Schroth S, et al. Receptor tyrosine kinase MerTK suppresses an allogenic type I IFN response to promote transplant tolerance. American journal of transplantation : official journal of the American Society of Transplantation and the American Society of Transplant Surgeons. 2019;19(3):674-85.
194. Filardy AA, Pires DR, Nunes MP, Takiya CM, Freire-de-Lima CG, Ribeiro-Gomes FL, et al. Proinflammatory clearance of apoptotic neutrophils induces an IL-12(low)IL-10(high) regulatory phenotype in macrophages. Journal of immunology (Baltimore, Md : 1950). 2010;185(4):2044-50.
195. Tibrewal N, Wu Y, D'Mello V, Akakura R, George TC, Varnum B, et al. Autophosphorylation docking site Tyr-867 in Mer receptor tyrosine kinase allows for dissociation of multiple signaling pathways for

phagocytosis of apoptotic cells and down-modulation of lipopolysaccharide-inducible NF-kappaB transcriptional activation. J Biol Chem. 2008;283(6):3618-27.
196. Fujimori T, Grabiec AM, Kaur M, Bell TJ, Fujino N, Cook PC, et al. The Axl receptor tyrosine kinase is a discriminator of macrophage function in the inflamed lung. Mucosal Immunol. 2015;8(5):1021-30.
197. Sharif MN, Sosic D, Rothlin CV, Kelly E, Lemke G, Olson EN, et al. Twist mediates suppression of inflammation by type I IFNs and Axl. The Journal of experimental medicine. 2006;203(8):1891-901.
198. Yi Z, Li L, Matsushima GK, Earp HS, Wang B, Tisch R. A novel role for c-Src and STAT3 in apoptotic cell-mediated MerTK-dependent immunoregulation of dendritic cells. Blood. 2009;114(15):3191-8.
199. Sen P, Wallet MA, Yi Z, Huang Y, Henderson M, Mathews CE, et al. Apoptotic cells induce Mer tyrosine kinase-dependent blockade of NF-kappaB activation in dendritic cells. Blood. 2007;109(2):653-60.
200. Chirino LM, Kumar S, Okumura M, Sterner DE, Mattern M, Butt TR, et al. TAM receptors attenuate murine NK cell responses via E3 ubiquitin ligase Cbl-b. European journal of immunology. 2019.
201. Paolino M, Choidas A, Wallner S, Pranjic B, Uribesalgo I, Loeser S, et al. The E3 ligase Cbl-b and TAM receptors regulate cancer metastasis via natural killer cells. Nature. 2014;507(7493):508-12.
202. Nguyen KQ, Tsou WI, Calarese DA, Kimani SG, Singh S, Hsieh S, et al. Overexpression of MERTK receptor tyrosine kinase in epithelial cancer cells drives efferocytosis in a gain-of-function capacity. J Biol Chem. 2014;289(37):25737-49.
203. Skinner HD, Giri U, Yang LP, Kumar M, Liu Y, Story MD, et al. Integrative Analysis Identifies a Novel AXL-PI3 Kinase-PD-L1 Signaling Axis Associated with Radiation Resistance in Head and Neck Cancer. Clinical cancer research : an official journal of the American Association for Cancer Research. 2017;23(11):2713-22.
204. Lin J, Xu A, Jin J, Zhang M, Lou J, Qian C, et al. MerTK-mediated efferocytosis promotes immune tolerance and tumor progression in osteosarcoma through enhancing M2 polarization and PD-L1 expression. Oncoimmunology. 2022;11(1):2024941.
205. Maier B, Leader AM, Chen ST, Tung N, Chang C, LeBerichel J, et al. A conserved dendritic-cell regulatory program limits antitumour immunity. Nature. 2020;580(7802):257-62.
206. Lee-Sherick AB, Jacobsen KM, Henry CJ, Huey MG, Parker RE, Page LS, et al. MERTK inhibition alters the PD-1 axis and promotes anti-leukemia immunity. JCI insight. 2018;3(21).
207. Cabezon R, Carrera-Silva EA, Florez-Grau G, Errasti AE, Calderon-Gomez E, Lozano JJ, et al. MERTK as negative regulator of human T cell activation. Journal of leukocyte biology. 2015;97(4):751-60.
208. Peeters MJW, Dulkeviciute D, Draghi A, Ritter C, Rahbech A, Skadborg SK, et al. MERTK Acts as a Costimulatory Receptor on Human CD8(+) T Cells. Cancer immunology research. 2019;7(9):1472-84.
209. Giroud P, Renaudineau S, Gudefin L, Calcei A, Menguy T, Rozan C, et al. Expression of TAM-R in Human Immune Cells and Unique Regulatory Function of MerTK in IL-10 Production by Tolerogenic DC. Front Immunol. 2020;11:564133.
210. Shao WH, Eisenberg RA, Cohen PL. The Mer receptor tyrosine kinase is required for the loss of B cell tolerance in the chronic graft-versus-host disease model of systemic lupus erythematosus. Journal of immunology (Baltimore, Md : 1950). 2008;180(11):7728-35.
211. Shao WH, Zhen Y, Finkelman FD, Cohen PL. The Mertk receptor tyrosine kinase promotes T-B interaction stimulated by IgD B-cell receptor cross-linking. J Autoimmun. 2014;53:78-84.
212. Heit B, Tasnim T, Le Lam A. MER Tyrosine Kinase Mediates Efferocytosis Through a Novel β₂ Integrin-Activating Signalling Pathway. The Journal of Immunology. 2021;206(1 Supplement):97.04-97.04.
213. Kim SY, Lim EJ, Yoon YS, Ahn YH, Park EM, Kim HS, et al. Liver X receptor and STAT1 cooperate downstream of Gas6/Mer to induce anti-inflammatory arginase 2 expression in macrophages. Sci Rep. 2016;6:29673.

214. Scutera S, Fraone T, Musso T, Cappello P, Rossi S, Pierobon D, et al. Survival and migration of human dendritic cells are regulated by an IFN-alpha-inducible Axl/Gas6 pathway. Journal of immunology (Baltimore, Md : 1950). 2009;183(5):3004-13.
215. Ben-Batalla I, Schultze A, Wroblewski M, Erdmann R, Heuser M, Waizenegger JS, et al. Axl, a prognostic and therapeutic target in acute myeloid leukemia mediates paracrine crosstalk of leukemia cells with bone marrow stroma. Blood. 2013;122(14):2443-52.
216. Lee-Sherick AB, Eisenman KM, Sather S, McGranahan A, Armistead PM, McGary CS, et al. Aberrant Mer receptor tyrosine kinase expression contributes to leukemogenesis in acute myeloid leukemia. Oncogene. 2013;32(46):5359-68.
217. Whitman SP, Kohlschmidt J, Maharry K, Volinia S, Mrózek K, Nicolet D, et al. GAS6 expression identifies high-risk adult AML patients: potential implications for therapy. Leukemia. 2014;28(6):1252-8.
218. Linger RM, Lee-Sherick AB, DeRyckere D, Cohen RA, Jacobsen KM, McGranahan A, et al. Mer receptor tyrosine kinase is a therapeutic target in pre-B-cell acute lymphoblastic leukemia. Blood. 2013;122(9):1599-609.
219. Brandao LN, Winges A, Christoph S, Sather S, Migdall-Wilson J, Schlegel J, et al. Inhibition of MerTK increases chemosensitivity and decreases oncogenic potential in T-cell acute lymphoblastic leukemia. Blood Cancer J. 2013;3:e101.
220. Waizenegger JS, Ben-Batalla I, Weinhold N, Meissner T, Wroblewski M, Janning M, et al. Role of Growth arrest-specific gene 6-Mer axis in multiple myeloma. Leukemia. 2015;29(3):696-704.
221. Shi C, Li X, Wang X, Ding N, Ping L, Shi Y, et al. The proto-oncogene Mer tyrosine kinase is a novel therapeutic target in mantle cell lymphoma. J Hematol Oncol. 2018;11(1):43.
222. Wong JP, Stuhlmiller TJ, Giffin LC, Lin C, Bigi R, Zhao J, et al. Kinome profiling of non-Hodgkin lymphoma identifies Tyro3 as a therapeutic target in primary effusion lymphoma. Proceedings of the National Academy of Sciences of the United States of America. 2019;116(33):16541-50.
223. Cheng P, Phillips E, Kim SH, Taylor D, Hielscher T, Puccio L, et al. Kinome-wide shRNA screen identifies the receptor tyrosine kinase AXL as a key regulator for mesenchymal glioblastoma stem-like cells. Stem Cell Reports. 2015;4(5):899-913.
224. Song W, Wang H, Lu M, Ni X, Bahri N, Zhu S, et al. AXL Inactivation Inhibits Mesothelioma Growth and Migration via Regulation of p53 Expression. Cancers (Basel). 2020;12(10).
225. Migdall-Wilson J, Bates C, Schlegel J, Brandão L, Linger RM, DeRyckere D, et al. Prolonged exposure to a Mer ligand in leukemia: Gas6 favors expression of a partial Mer glycoform and reveals a novel role for Mer in the nucleus. PLoS One. 2012;7(2):e31635.
226. Liu Y, Lan L, Li Y, Lu J, He L, Deng Y, et al. N-glycosylation stabilizes MerTK and promotes hepatocellular carcinoma tumor growth. Redox Biol. 2022;54:102366.
227. Merilahti JAM, Ojala VK, Knittle AM, Pulliainen AT, Elenius K. Genome-wide screen of gamma-secretase-mediated intramembrane cleavage of receptor tyrosine kinases. Molecular biology of the cell. 2017;28(22):3123-31.
228. Lu Y, Wan J, Yang Z, Lei X, Niu Q, Jiang L, et al. Regulated intramembrane proteolysis of the AXL receptor kinase generates an intracellular domain that localizes in the nucleus of cancer cells. The FASEB Journal. 2017;31(4):1382-97.
229. Zhu S, Wurdak H, Wang Y, Galkin A, Tao H, Li J, et al. A genomic screen identifies TYRO3 as a MITF regulator in melanoma. Proceedings of the National Academy of Sciences of the United States of America. 2009;106(40):17025-30.
230. Dufour F, Silina L, Neyret-Kahn H, Moreno-Vega A, Krucker C, Karboul N, et al. TYRO3 as a molecular target for growth inhibition and apoptosis induction in bladder cancer. Br J Cancer. 2019;120(5):555-64.
231. Park M, Kim JW, Kim KM, Kang S, Kim W, Kim JK, et al. Circulating Small Extracellular Vesicles Activate TYRO3 to Drive Cancer Metastasis and Chemoresistance. Cancer research. 2021;81(13):3539-53.

232. Avilla E, Guarino V, Visciano C, Liotti F, Svelto M, Krishnamoorthy G, et al. Activation of TYRO3/AXL tyrosine kinase receptors in thyroid cancer. Cancer research. 2011;71(5):1792-804.
233. Chien CW, Hou PC, Wu HC, Chang YL, Lin SC, Lin SC, et al. Targeting TYRO3 inhibits epithelial-mesenchymal transition and increases drug sensitivity in colon cancer. Oncogene. 2016;35(45):5872-81.
234. Janssen JW, Schulz AS, Steenvoorden AC, Schmidberger M, Strehl S, Ambros PF, et al. A novel putative tyrosine kinase receptor with oncogenic potential. Oncogene. 1991;6(11):2113-20.
235. Georgescu MM, Kirsch KH, Shishido T, Zong C, Hanafusa H. Biological effects of c-Mer receptor tyrosine kinase in hematopoietic cells depend on the Grb2 binding site in the receptor and activation of NF-kappaB. Mol Cell Biol. 1999;19(2):1171-81.
236. Keating AK, Salzberg DB, Sather S, Liang X, Nickoloff S, Anwar A, et al. Lymphoblastic leukemia/lymphoma in mice overexpressing the Mer (MerTK) receptor tyrosine kinase. Oncogene. 2006;25(45):6092-100.
237. Du W, Phinney NZ, Huang H, Wang Z, Westcott J, Toombs JE, et al. AXL Is a Key Factor for Cell Plasticity and Promotes Metastasis in Pancreatic Cancer. Molecular cancer research : MCR. 2021;19(8):1412-21.
238. Holtzhausen A, Harris W, Ubil E, Hunter DM, Zhao J, Zhang Y, et al. TAM Family Receptor Kinase Inhibition Reverses MDSC-Mediated Suppression and Augments Anti-PD-1 Therapy in Melanoma. Cancer immunology research. 2019.
239. Cook RS, Jacobsen KM, Wofford AM, DeRyckere D, Stanford J, Prieto AL, et al. MerTK inhibition in tumor leukocytes decreases tumor growth and metastasis. The Journal of clinical investigation. 2013;123(8):3231-42.
240. Davra V, Kumar S, Geng K, Calianese D, Mehta D, Gadiyar V, et al. Axl and Mertk Receptors Cooperate to Promote Breast Cancer Progression by Combined Oncogenic Signaling and Evasion of Host Antitumor Immunity. Cancer research. 2021;81(3):698-712.
241. Novitskiy SV, Zaynagetdinov R, Vasiukov G, Gutor S, Han W, Serezani A, et al. Gas6/MerTK signaling is negatively regulated by NF-kappaB and supports lung carcinogenesis. Oncotarget. 2019;10(66):7031-42.
242. Guo Z, Li Y, Zhang D, Ma J. Axl inhibition induces the antitumor immune response which can be further potentiated by PD-1 blockade in the mouse cancer models. Oncotarget. 2017;8(52):89761-74.
243. Yokoyama Y, Lew ED, Seelige R, Tindall EA, Walsh C, Fagan PC, et al. Immuno-oncological Efficacy of RXDX-106, a Novel TAM (TYRO3, AXL, MER) Family Small-Molecule Kinase Inhibitor. Cancer research. 2019;79(8):1996-2008.
244. Rios-Doria J, Favata M, Lasky K, Feldman P, Lo Y, Yang G, et al. A Potent and Selective Dual Inhibitor of AXL and MERTK Possesses Both Immunomodulatory and Tumor-Targeted Activity. Front Oncol. 2020;10:598477.
245. Synn CB, Kim SE, Lee HK, Kim MH, Kim JH, Lee JM, et al. SKI-G-801, an AXL kinase inhibitor, blocks metastasis through inducing anti-tumor immune responses and potentiates anti-PD-1 therapy in mouse cancer models. Clin Transl Immunology. 2022;11(1):e1364.
246. Zhou Y, Fei M, Zhang G, Liang WC, Lin W, Wu Y, et al. Blockade of the Phagocytic Receptor MerTK on Tumor-Associated Macrophages Enhances P2X7R-Dependent STING Activation by Tumor-Derived cGAMP. Immunity. 2020;52(2):357-73.e9.
247. Tirado-Gonzalez I, Descot A, Soetopo D, Nevmerzhitskaya A, Schäffer A, Kur IM, et al. AXL Inhibition in Macrophages Stimulates Host-versus-Leukemia Immunity and Eradicates Naïve and Treatment-Resistant Leukemia. Cancer Discov. 2021.
248. Cruz Cruz J, Allison KC, Page LS, Jenkins AJ, Wang X, Earp HS, et al. Inhibiting efferocytosis reverses macrophage-mediated immunosuppression in the leukemia microenvironment. Front Immunol. 2023;14:1146721.

249. Loges S, Schmidt T, Tjwa M, van Geyte K, Lievens D, Lutgens E, et al. Malignant cells fuel tumor growth by educating infiltrating leukocytes to produce the mitogen Gas6. Blood. 2010;115(11):2264-73.
250. Dirks W, Rome D, Ringel F, Jäger K, MacLeod RA, Drexler HG. Expression of the growth arrest-specific gene 6 (GAS6) in leukemia and lymphoma cell lines. Leukemia research. 1999;23(7):643-51.
251. Abe A, Emi N, Kato H, Adachi K, Murate T, Saga S, et al. Establishment and characterization of an immature human megakaryoblastic cell line, MEG-A2. Leukemia. 1995;9(2):341-9.
252. Fei F, Abdel-Azim H, Lim M, Arutyunyan A, von Itzstein M, Groffen J, et al. Galectin-3 in pre-B acute lymphoblastic leukemia. Leukemia. 2013;27(12):2385-8.
253. Whitman SP, Kohlschmidt J, Maharry K, Volinia S, Mrózek K, Nicolet D, et al. GAS6 expression identifies high-risk adult AML patients: potential implications for therapy. 2013.
254. Cheng CL, Hou HA, Lee MC, Liu CY, Jhuang JY, Lai YJ, et al. Higher bone marrow LGALS3 expression is an independent unfavorable prognostic factor for overall survival in patients with acute myeloid leukemia. Blood. 2013;121(16):3172-80.
255. Sharma R, Huang X, Brekken RA, Schroit AJ. Detection of phosphatidylserine-positive exosomes for the diagnosis of early-stage malignancies. Br J Cancer. 2017;117(4):545-52.
256. Ran S, Downes A, Thorpe PE. Increased exposure of anionic phospholipids on the surface of tumor blood vessels. Cancer research. 2002;62(21):6132-40.
257. Cendrowicz E, Sas Z, Bremer E, Rygiel TP. The Role of Macrophages in Cancer Development and Therapy. Cancers (Basel). 2021;13(8).
258. Stanford JC, Young C, Hicks D, Owens P, Williams A, Vaught DB, et al. Efferocytosis produces a prometastatic landscape during postpartum mammary gland involution. The Journal of clinical investigation. 2014;124(11):4737-52.
259. Aguilera TA, Rafat M, Castellini L, Shehade H, Kariolis MS, Hui AB, et al. Reprogramming the immunological microenvironment through radiation and targeting Axl. Nature communications. 2016;7:13898.
260. Jeon Y, Kang H, Yang Y, Park D, Choi B, Kim J, et al. A Novel Selective Axl/Mer/CSF1R Kinase Inhibitor as a Cancer Immunotherapeutic Agent Targeting Both Immune and Tumor Cells in the Tumor Microenvironment. Cancers (Basel). 2022;14(19).
261. Novitskiy SV, Zaynagetdinov R, Vasiukov G, Gutor S, Han W, Serezani A, et al. Gas6/MerTK signaling is negatively regulated by NF-κB and supports lung carcinogenesis. Oncotarget. 2019;10(66):7031-42.
262. Ludwig KF, Du W, Sorrelle NB, Wnuk-Lipinska K, Topalovski M, Toombs JE, et al. Small-Molecule Inhibition of Axl Targets Tumor Immune Suppression and Enhances Chemotherapy in Pancreatic Cancer. Cancer research. 2018;78(1):246-55.
263. Kasikara C, Davra V, Calianese D, Geng K, Spires TE, Quigley M, et al. Pan-TAM tyrosine kinase inhibitor BMS-777607 enhances anti-PD-1 mAb efficacy in a murine model of triple-negative breast cancer. Cancer research. 2019.
264. Wculek SK, Cueto FJ, Mujal AM, Melero I, Krummel MF, Sancho D. Dendritic cells in cancer immunology and immunotherapy. Nature Reviews Immunology. 2020;20(1):7-24.
265. Salmon H, Idoyaga J, Rahman A, Leboeuf M, Remark R, Jordan S, et al. Expansion and Activation of CD103(+) Dendritic Cell Progenitors at the Tumor Site Enhances Tumor Responses to Therapeutic PD-L1 and BRAF Inhibition. Immunity. 2016;44(4):924-38.
266. Tsukita Y, Fujino N, Miyauchi E, Saito R, Fujishima F, Itakura K, et al. Axl kinase drives immune checkpoint and chemokine signalling pathways in lung adenocarcinomas. Molecular cancer. 2019;18(1):24.
267. Terry S, Dalban C, Rioux-Leclercq N, Adam J, Meylan M, Buart S, et al. Association of AXL and PD-L1 Expression with Clinical Outcomes in Patients with Advanced Renal Cell Carcinoma Treated with PD-1

Blockade. Clinical cancer research : an official journal of the American Association for Cancer Research. 2021;27(24):6749-60.
268. Jiang Z, Lim SO, Yan M, Hsu JL, Yao J, Wei Y, et al. TYRO3 induces anti-PD-1/PD-L1 therapy resistance by limiting innate immunity and tumoral ferroptosis. The Journal of clinical investigation. 2021;131(8).
269. Gray MJ, Gong J, Hatch MM, Nguyen V, Hughes CC, Hutchins JT, et al. Phosphatidylserine-targeting antibodies augment the anti-tumorigenic activity of anti-PD-1 therapy by enhancing immune activation and downregulating pro-oncogenic factors induced by T-cell checkpoint inhibition in murine triple-negative breast cancers. Breast cancer research : BCR. 2016;18(1):50.
270. Freimark BD, Gong J, Ye D, Gray MJ, Nguyen V, Yin S, et al. Antibody-Mediated Phosphatidylserine Blockade Enhances the Antitumor Responses to CTLA-4 and PD-1 Antibodies in Melanoma. Cancer immunology research. 2016;4(6):531-40.
271. Lee W, Kim DK, Synn CB, Lee HK, Park S, Jung DS, et al. Incorporation of SKI-G-801, a Novel AXL Inhibitor, With Anti-PD-1 Plus Chemotherapy Improves Anti-Tumor Activity and Survival by Enhancing T Cell Immunity. Front Oncol. 2022;12:821391.
272. Li H, Liu Z, Liu L, Zhang H, Han C, Girard L, et al. AXL targeting restores PD-1 blockade sensitivity of STK11/LKB1 mutant NSCLC through expansion of TCF1(+) CD8 T cells. Cell Rep Med. 2022;3(3):100554.
273. Boshuizen J, Pencheva N, Krijgsman O, Altimari DD, Castro PG, de Bruijn B, et al. Cooperative Targeting of Immunotherapy-Resistant Melanoma and Lung Cancer by an AXL-Targeting Antibody-Drug Conjugate and Immune Checkpoint Blockade. Cancer research. 2021;81(7):1775-87.
274. Caetano MS, Younes AI, Barsoumian HB, Quigley M, Menon H, Gao C, et al. Triple Therapy with MerTK and PD1 Inhibition plus Radiotherapy Promotes Abscopal Antitumor Immune Responses. Clinical cancer research : an official journal of the American Association for Cancer Research. 2019.
275. Zhao GJ, Zheng JY, Bian JL, Chen LW, Dong N, Yu Y, et al. Growth Arrest-Specific 6 Enhances the Suppressive Function of CD4(+)CD25(+) Regulatory T Cells Mainly through Axl Receptor. Mediators of inflammation. 2017;2017:6848430.
276. Williams RT, den Besten W, Sherr CJ. Cytokine-dependent imatinib resistance in mouse BCR-ABL+, Arf-null lymphoblastic leukemia. Genes & development. 2007;21(18):2283-7.
277. Lu Q, Gore M, Zhang Q, Camenisch T, Boast S, Casagranda F, et al. Tyro-3 family receptors are essential regulators of mammalian spermatogenesis. Nature. 1999;398(6729):723-8.
278. Butler A, Hoffman P, Smibert P, Papalexi E, Satija R. Integrating single-cell transcriptomic data across different conditions, technologies, and species. Nat Biotechnol. 2018;36(5):411-20.
279. Becht E, McInnes L, Healy J, Dutertre CA, Kwok IWH, Ng LG, et al. Dimensionality reduction for visualizing single-cell data using UMAP. Nat Biotechnol. 2018.
280. Dwivedi B, Mumme H, Satpathy S, Bhasin SS, Bhasin M. Survival Genie, a web platform for survival analysis across pediatric and adult cancers. Sci Rep. 2022;12(1):3069.
281. Shreedhar V, Moodycliffe AM, Ullrich SE, Bucana C, Kripke ML, Flores-Romo L. Dendritic cells require T cells for functional maturation in vivo. Immunity. 1999;11(5):625-36.
282. Zhang W, DeRyckere D, Hunter D, Liu J, Stashko MA, Minson KA, et al. UNC2025, a potent and orally bioavailable MER/FLT3 dual inhibitor. Journal of medicinal chemistry. 2014;57(16):7031-41.
283. Minson KA, Smith CC, DeRyckere D, Libbrecht C, Lee-Sherick AB, Huey MG, et al. The MERTK/FLT3 inhibitor MRX-2843 overcomes resistance-conferring FLT3 mutations in acute myeloid leukemia. JCI insight. 2016;1(3):e85630.
284. Devaiah BN, Singer DS. CIITA and Its Dual Roles in MHC Gene Transcription. Front Immunol. 2013;4:476.
285. Brown AS, Bourges D, Ang DK, Hartland EL, van Driel IR. CD8 subunit expression by plasmacytoid dendritic cells is variable, and does not define stable subsets. Mucosal Immunol. 2014;7(1):200-1.

286. Morón G, Rueda P, Casal I, Leclerc C. CD8alpha- CD11b+ dendritic cells present exogenous virus-like particles to CD8+ T cells and subsequently express CD8alpha and CD205 molecules. The Journal of experimental medicine. 2002;195(10):1233-45.
287. Hildner K, Edelson BT, Purtha WE, Diamond M, Matsushita H, Kohyama M, et al. Batf3 deficiency reveals a critical role for CD8alpha+ dendritic cells in cytotoxic T cell immunity. Science (New York, NY). 2008;322(5904):1097-100.
288. Minoda Y, Virshup I, Leal Rojas I, Haigh O, Wong Y, Miles JJ, et al. Human CD141+ Dendritic Cell and CD1c+ Dendritic Cell Undergo Concordant Early Genetic Programming after Activation in Humanized Mice In Vivo. Frontiers in Immunology. 2017;8.
289. Galibert L, Diemer GS, Liu Z, Johnson RS, Smith JL, Walzer T, et al. Nectin-like Protein 2 Defines a Subset of T-cell Zone Dendritic Cells and Is a Ligand for Class-I-restricted T-cell-associated Molecule *&#x2666. Journal of Biological Chemistry. 2005;280(23):21955-64.
290. Yeh J-H, Sidhu SS, Chan AC. Regulation of a Late Phase of T Cell Polarity and Effector Functions by Crtam. Cell. 2008;132(5):846-59.
291. Takeuchi A, Itoh Y, Takumi A, Ishihara C, Arase N, Yokosuka T, et al. CRTAM Confers Late-Stage Activation of CD8+ T Cells to Regulate Retention within Lymph Node1. The Journal of Immunology. 2009;183(7):4220-8.
292. Chain BM, Free P, Medd P, Swetman C, Tabor AB, Terrazzini N. The expression and function of cathepsin E in dendritic cells. Journal of immunology (Baltimore, Md : 1950). 2005;174(4):1791-800.
293. Bennett K, Levine T, Ellis JS, Peanasky RJ, Samloff IM, Kay J, et al. Antigen processing for presentation by class II major histocompatibility complex requires cleavage by cathepsin E. European journal of immunology. 1992;22(6):1519-24.
294. Nishioku T, Hashimoto K, Yamashita K, Liou SY, Kagamiishi Y, Maegawa H, et al. Involvement of cathepsin E in exogenous antigen processing in primary cultured murine microglia. J Biol Chem. 2002;277(7):4816-22.
295. Mengwasser J, Babes L, Cordes S, Mertlitz S, Riesner K, Shi Y, et al. Cathepsin E Deficiency Ameliorates Graft-versus-Host Disease and Modifies Dendritic Cell Motility. Front Immunol. 2017;8:203.
296. Tulone C, Tsang J, Prokopowicz Z, Grosvenor N, Chain B. Natural cathepsin E deficiency in the immune system of C57BL/6J mice. Immunogenetics. 2007;59(12):927-35.
297. Khan O, Giles JR, McDonald S, Manne S, Ngiow SF, Patel KP, et al. TOX transcriptionally and epigenetically programs CD8(+) T cell exhaustion. Nature. 2019;571(7764):211-8.
298. Ahmed KA, Wang L, Munegowda MA, Mulligan SJ, Gordon JR, Griebel P, et al. Direct in vivo evidence of CD4+ T cell requirement for CTL response and memory via pMHC-I targeting and CD40L signaling. Journal of leukocyte biology. 2012;92(2):289-300.
299. Lombardi V, Speak AO, Kerzerho J, Szely N, Akbari O. CD8$\alpha^+\beta^-$ and CD8$\alpha^+\beta^+$ plasmacytoid dendritic cells induce Foxp3$^+$ regulatory T cells and prevent the induction of airway hyper-reactivity. Mucosal Immunol. 2012;5(4):432-43.
300. Collin M, Bigley V. Human dendritic cell subsets: an update. Immunology. 2018;154(1):3-20.
301. Bottcher JP, Reis e Sousa C. The Role of Type 1 Conventional Dendritic Cells in Cancer Immunity. Trends Cancer. 2018;4(11):784-92.
302. Akalu YT, Mercau ME, Ansems M, Hughes LD, Nevin J, Alberto EJ, et al. Tissue-specific modifier alleles determine Mertk loss-of-function traits. eLife. 2022;11.
303. Johnson JJ, Chen W, Hudson W, Yao Q, Taylor M, Rabbitts TH, et al. Prenatal and postnatal myeloid cells demonstrate stepwise progression in the pathogenesis of MLL fusion gene leukemia. Blood. 2003;101(8):3229-35.
304. Silva-Sanchez A, Meza-Perez S, Liu M, Stone SL, Flores-Romo L, Ubil E, et al. Activation of regulatory dendritic cells by Mertk coincides with a temporal wave of apoptosis in neonatal lungs. Sci Immunol. 2023;8(84):eadc9081.

305. Broz ML, Binnewies M, Boldajipour B, Nelson AE, Pollack JL, Erle DJ, et al. Dissecting the tumor myeloid compartment reveals rare activating antigen-presenting cells critical for T cell immunity. Cancer Cell. 2014;26(5):638-52.
306. Barry KC, Hsu J, Broz ML, Cueto FJ, Binnewies M, Combes AJ, et al. A natural killer–dendritic cell axis defines checkpoint therapy–responsive tumor microenvironments. Nature medicine. 2018;24(8):1178-91.
307. Crosier PS, Hall LR, Vitas MR, Lewis PM, Crosier KE. Identification of a novel receptor tyrosine kinase expressed in acute myeloid leukemic blasts. Leukemia & lymphoma. 1995;18(5-6):443-9.
308. Shiozawa Y, Pedersen EA, Taichman RS. GAS6/Mer axis regulates the homing and survival of the E2A/PBX1-positive B-cell precursor acute lymphoblastic leukemia in the bone marrow niche. Experimental hematology. 2010;38(2):132-40.
309. Eryildiz F, Tyner JW. Abstract 1265: Dysregulated tyrosine kinase Tyro3 signaling in acute myeloid leukemia. Cancer research. 2016;76(14 Supplement):1265-.
310. Saito T, Itoh M, Tohda S. TYRO3 Knockdown Suppresses the Growth of Myeloid Leukaemia Cells. Anticancer Res. 2022;42(4):1757-61.
311. Koda Y, Itoh M, Tohda S. Effects of MERTK Inhibitors UNC569 and UNC1062 on the Growth of Acute Myeloid Leukaemia Cells. Anticancer Res. 2018;38(1):199-204.
312. DeRyckere D, Lee-Sherick AB, Huey MG, Hill AA, Tyner JW, Jacobsen KM, et al. UNC2025, a MERTK Small-Molecule Inhibitor, Is Therapeutically Effective Alone and in Combination with Methotrexate in Leukemia Models. Clinical cancer research : an official journal of the American Association for Cancer Research. 2017;23(6):1481-92.